WATER QUALITY MAPPING ON LAKE TEXOMA, USA

Jeffrey A. Mabe, B.S.

Thesis Prepared for the Degree of

MASTER OF SCIENCE

UNIVERSITY OF NORTH TEXAS

December 2002

APPROVED:

Samuel F. Atkinson, Major Professor
Kenneth R. Dickson, Committee Member
Minhe Ji, Committee Member
Thomas W. LaPoint, Director of the Institute of Applied Sciences
Earl Zimmerman, Chair of the Department of Biological Sciences
C. Neal Tate, Dean of the Robert B. Toulouse School of Graduate Studies

Mabe, Jeffrey A. Water Quality Mapping on Lake Texoma USA. Master of Science (Environmental Science), December 2002, 130 pages, 14 tables, 20 figures, 40 references. The primary objective of this study was to develop and evaluate a system capable of rapid, continuous collection of water quality and locational data on Lake Texoma. Secondary objectives included developing monthly distribution maps for chlorophyll-*a*, turbidity, and specific conductivity in Lake Texoma and investigating the spatial and temporal relationships between these common water quality indicators. A modified YSI multiprobe was used to develop a system capable of surveying the lake within 4 days with samples at 330 to 400 meter intervals. Data generated with this system compared favorably with previous studies of Lake Texoma. Two sets of raster format maps were developed for the monthly distributions of chlorophyll-*a*, turbidity, and specific conductivity across the lake. Spatial and temporal relationships generally took the form of decreasing gradients running from the lake arms towards the Main Lake Zone in the case of chlorophyll-*a* and turbidity or, in the case of specific conductivity, a decreasing gradient from the Red River arm to the Washita River arm. All three water quality indicators were strongly influenced by river discharge levels.

ACKNOWLEDGMENTS

We wish to thank the United States Army Corps of Engineers, Tulsa District, for their financial support of this project, and the University of Oklahoma Biological Station for providing logistical support. We also wish to acknowledge Bruce Hunter and the University of North Texas' Center for Spatial Analysis and Mapping for their invaluable support and advice.

TABLE OF CONTENTS

LIST OF TABLES

LIST OF FIGURES

CHAPTER 1

INTRODUCTION

1.1 Background

Lake Texoma, a 36,000 ha reservoir situated on the Texas - Oklahoma border, is naturally brackish due to ancient salt deposits in the Red River Basin, its primary watershed. The highly mineralized water - dominated by ions of chloride, sulfate, sodium, and calcium - poses problems for municipal, industrial, and agricultural uses of the reservoir. In response to this situation the U. S. Army Corps of Engineers has initiated a series of projects designed to reduce salt inputs into the Red River and Lake Texoma. Control measures are concentrated around sources of salt contamination in the Red River Basin and include a variety of mechanisms including ring dikes, low-flow collection dams, deep-well injection, and pipeline transfer to man-made brine lakes. Projected results include reducing concentrations of chloride and sodium by an estimated 45% and concentrations of calcium and sulfate by approximately 5 % (Toro et al., 1996). The U. S. Army Corps of Engineers estimates salt content measurements at Lake Texoma, post-control measures, will meet the U.S. Environmental Protection Agency's municipal water supply standard for dissolved salts (250 mg/L) 94% of the time as apposed to only 3% for pre-control (U.S. ACE, 1994).

Some concerns have been voiced about possible effects of the chloride control project on the quality of Lake Texoma's waters and the economically important striped

bass fishery it supports. Laboratory and field evidence suggests that salinity levels can affect the settling rates of suspended clay particles. Gade et al. (1992) cited three studies in Oklahoma where oil field brines were found to reduce clay turbidity when added to streams and ponds (Keeton, 1959; Mathis, 1965; and Harrel, 1966). Salinity levels affected settling and deposition of clays in Lake Pontchartrain and Lake Maurepas in Louisiana (Brooks and Ferrell, 1970). Toro et al. (1996) investigated the relationship between total dissolved solids (TDS) and turbidity in the waters of Lake Texoma itself. They concluded that a reduction in TDS would contribute to a decrease in the lake's sedimentation rate and, in turn, a decrease in the percentage of non-algal turbidity removed.

The physical model that explains how the ionic strength of water affects the sedimentation rate of colloidal clay particles is referred to as VODL theory after its progenitors Verwey, Overbeek, Derjagin, and Landau (Stumm and Morgan, 1970). Toro et al. (1996) summarized the pertinent aspects of VODL theory in their paper:

> Particles gain stability primarily by electrical forces due to charges on their surface or by hydration forces that provide a hydrophilic surface. TDS reduce the electrical forces by compressing the electrical double layer and the distance that electrical repulsion forces effectively act; this allows for more frequent collisions between particles that result in coagulation. Then, as coagulation proceeds, the size of the particle flocs grow until they are large enough to settle and overcome Brownian motion. In addition, TDS reduce the hydration forces by competing with the particles for water. The thickness of

the adsorbed water on the particles and the affinity of the particle for water are reduced, permitting easier aggregation of particles.

A reduction in the dissolved chloride concentration of Lake Texoma could contribute to a decrease in the sedimentation rates of suspended clays and an increase in turbidity. Higher turbidity could, in turn, have a negative effect on the productivity, recreational value, and environmental quality of the lake.

To address these concerns the Tulsa District of the US Army Corps of Engineers contracted with the Institute of Applied Sciences (IAS) at the University of North Texas to develop baseline water quality information for assistance in evaluating potential changes associated with the chloride control project. Sampling in the IAS study was linked to historical data by dividing the lake into 5 zones and utilizing two historical fixed sampling stations per zone (Atkinson et al., 1999). One additional random station per zone was sampled to provide additional data. This sampling scheme is adequate to assess the general water quality of Lake Texoma, but it does leave large areas between stations unexplored. Areas important to juvenile stripped bass such as littoral zones and stream arms (McCabe, 1989) are not sampled. In addition, Lake Texoma is a large and diverse system and it is not known how well these points represent the overall character of the lake or how well they detect patterns and changes. A rapid method for surveying and mapping important physical, biological, and chemical variables would aid in understanding the complex nature of Lake Texoma and assessing any changes due to chloride reductions.

This study was designed to supplement the IAS water quality survey and address spatial and temporal relationships between chemical, physical, and biological parameters on Lake Texoma.

1.2 Objectives

The objectives of this study were to:

1. Develop a system capable of rapid, continuous collection of water quality and locational data on Lake Texoma.
2. Use the system to collect monthly water quality data on Lake Texoma over the course of a year.
3. Develop monthly distribution maps for chlorophyll-*a*, turbidity, and specific conductivity.
4. Evaluate system performance and compare results to the IAS study.
5. Investigate the spatial and temporal relationships between chlorophyll-*a*, conductivity, and turbidity on Lake Texoma.

1.3 Mapping

Attempts to characterize the distribution of phytoplankton and other variables in the aquatic environment are common in the scientific literature. However, most studies on lakes utilized discrete sampling techniques where the boat is stopped at each station (Berman 1972; George and Heaney 1978; Stauffer 1988;). Continuous techniques are more common in the marine environment and rely primarily on the *in vivo* fluorescence

technique developed by Lorenzen (1966). Two different approaches are used to sample transects. Some researchers pump water from depth up to instruments on board a moving ship (Kiefer, 1973a; Hulse, 1975; Setser et al., 1983; Alpine et al., 1988; Madden and Day, 1992) while others place instrument packages on a submersible vehicle that is towed through the water (Herman and Denman, 1977). Pumping is a relatively slow process (Madden and Day, 1992) and not strictly an *in situ* measurement because some mixing of water samples occurs (Herman and Denman, 1977). While towed vehicles provide more speed relative to pumping, they present their own challenges when operating in shallow waters. Large scale towed vehicles such as those used in the ocean are too large for most lake applications. Fortunately, newer generations of environmental monitoring sondes are being equipped to work as small towed vehicles (Sieburth and Kester, 1999). These instruments are capable of carrying an array of sensors in a compact package suitable for lake studies.

1.4 Chlorophyll-*a* and Chloride

Measurements of chlorophyll-*a* concentrations are often used as a surrogate to estimate phytoplankton standing crop and productivity (Likens, 1975; Fee, 1976; Marshall and Peters, 1989; LaBaugh, 1995). This approach is advantageous for two reasons: (1) the relative abundance of chlorophyll-*a* has been found to be a good estimator of phytoplankton productive capacity and (2) it can be measured by several independent methods. The method of *in vivo* fluorometry, which measures chlorophyll-*a* within intact living cells, has been shown to be highly efficient (Lorenzen, 1966; Herman

and Denman, 1977) and relatively accurate when corrected by extraction methods (Alpine et al., 1988; Taylor and Yost, 1989). The *in vivo* fluorometric method relies on the fact that photosynthetic pigments fluoresce when excited by light of specific wavelengths. Most commercial fluorometers utilize a light emitting diode (LED) with a peak wavelength of 470 nm (YSI, 1999). Light of this wavelength appears blue to the eye and results in a peak fluorescence emission from chlorophyll-*a* of 650-700nm in whole cells. Fluorescence emitted by an excited water sample is detected by a photomultiplier with a filter to block backscattered light from the excitation source. Recent advances in instrumentation have resulted in fluormeters compact enough to be mounted on multiparameter data sondes. This configuration allows for the simultaneous collection of chlorophyll-*a* data along with other water quality parameters *in situ.*

Ideally fluorescence alone would be used to determine chlorophyll-*a* concentration. Unfortunately, many researchers have reported large variations in the ratio of fluorescence intensity and extractable chlorophyll-*a* yield (Heaney, 1978). Contributing factors include phytoplankton species present (Strickland, 1968 and Flemer, 1969) and their physiological condition (Keifer, 1973b and Harris, 1980). In addition, research by Carlson and Shapiro (1981) demonstrated that a large percentage of detectable fluorescence in lake water might be due to dissolved humic substances. This was especially true under low chlorophyll conditions. Therefore, correction of fluorescence measurements with results from more accurate extractive procedures is necessary to ensure reliability.

Marine evaporite salt (sodium chloride) deposits in the Red River Basin strongly influence the ionic composition of Lake Texoma (Ground and Groeger 1994) and make chloride the predominate anion (Atkinson et al., 1999). A report from the IAS comprehensive water quality survey showed a strong linear relationship between chloride concentration and specific conductance (µS/cm) with an R^2 = 95.51 % (Atkinson et al., 1999). This relationship allows for the indirect measurement of the general chloride concentration trends through measurement of specific conductance.

CHAPTER 2

MATERIALS AND METHODS

2.1 Sonde

The platform for our array of water sensors was a model 6600 data sonde from Yellow Springs Instruments (YSI) (Yellow Springs, OH). The 6600 sonde was outfitted with YSI's model 6300 Horizontal Deployment Apparatus (HDA) consisting of a wing, tail fin, and nose cone assembly bolted onto the data sonde allowing it to function as a towed submersible probe (Figure 1).

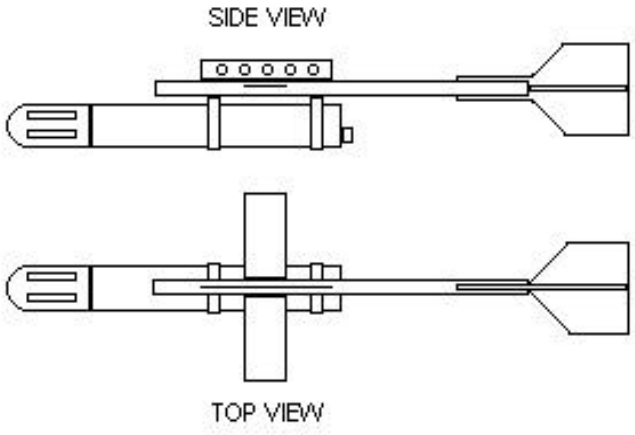

Figure 1. Diagram of the YSI 6600 series data sonde outfitted with the horizontal deployment apparatus that allows the unit to function as a small towed vehicle. Approximate length 1 meter.

The sonde carried a fixed wavelength fluorescence probe as well as probes for reading turbidity (nephelometric turbidity units, NTUs), specific conductance, pH, dissolved oxygen, temperature and depth. All sensors were standard YSI equipment and were housed within the nose cone assembly.

Chlorophyll estimates were made utilizing the fluorescence probe. A light emitting diode (LED) with a peak wavelength of 470nm provided the excitation light and a high sensitivity photodiode detected the resulting fluorescence. To reduce interference caused by turbidity, the detector was screened with an optical filter designed to restrict detection of 470 nm excitation light backscattered off of suspended particles in the water. It is important to note, however, that this instrument reads the fluorescence of everything in the water that emits above 630 nm when irradiated with 470 nm light. It cannot differentiate the separate forms of chlorophyll nor can it distinguish between chlorophyll and other fluorescing species.

The unitless fluorescence values were converted to µg/L of total chlorophyll by an algorithm in the sonde's software. Total chlorophyll was later converted to chlorophyll-*a* using regression equations developed from extracted grab samples. A data filter processed sensor readings to eliminate spikes and provide better estimates of the average total chlorophyll concentration.

Water quality data and position information were recording with YSI's 6200 Data Collection Platform (DCP). With this arrangement the towed sonde communicates via cable to a data collection unit that communicates with a laptop computer running YSI's EcoWatch DCP™ software (YSI Inc., Yellow Springs, OH). A Tremble Acutis™ Global

Positioning System (GPS) antenna (Trimble, Sunnyvale, CA) integrated into the data collection unit provides location information for each sonde reading. The EcoWatch software enables the 6200 DCP to collect data from the sonde and the GPS unit simultaneously. GPS data and sonde data were stored in two separate files and linked by a corresponding time stamp. The 6200 DCP was capable of collecting and storing data independent of the computer, however, because there is no data readout on the collection unit, attachment of the laptop computer was necessary for real time monitoring of incoming data.

2.2 Deployment System

A removable mast and boom system was designed to deploy the 6600 unit from a small boat (Figure 2). The system was fitted to an early model 17 foot boat with a 3/16 inch thick aluminum hull. The mast and boom are made from heavy wall 3 1/2-inch diameter 6061T-6 aluminum pipe. This material was originally designed for use as radar mast on larger vessels and is coated with a waterproof urethane coating. The 12 foot mast is attached to the boat deck using a compatible mounting plate bolted to the deck. An aluminum plate was welded to the floor of the boat to provide strength and enough material for the bolts to gain purchase. This was the only major boat modification required for installation of the mast and boom system. The mast was stabilized using three detachable guy wires with turnbuckles and attachments to the port sidewall. The 8 foot boom was attached perpendicular to the mast using an adapter and mounting plate held together with a cotter pin. Three detachable guy wires with turnbuckles, one secured

to the mast and two secured to the boat's port sidewall, stabilize the boom. An aluminum track ran the length of the boom and carried a traveler car that was used to adjust the position of the sonde. Attached to the traveler was a snatch-block pulley that carried the communications and tow cables. A custom designed control box was fitted between the mast and the boat's port sidewall. The control box holds the 600 lb. wench used for raising and lowering the 6600, cleats for attachment and control of the communications cable, and the mounting plate that assists in stabilizing the mast.

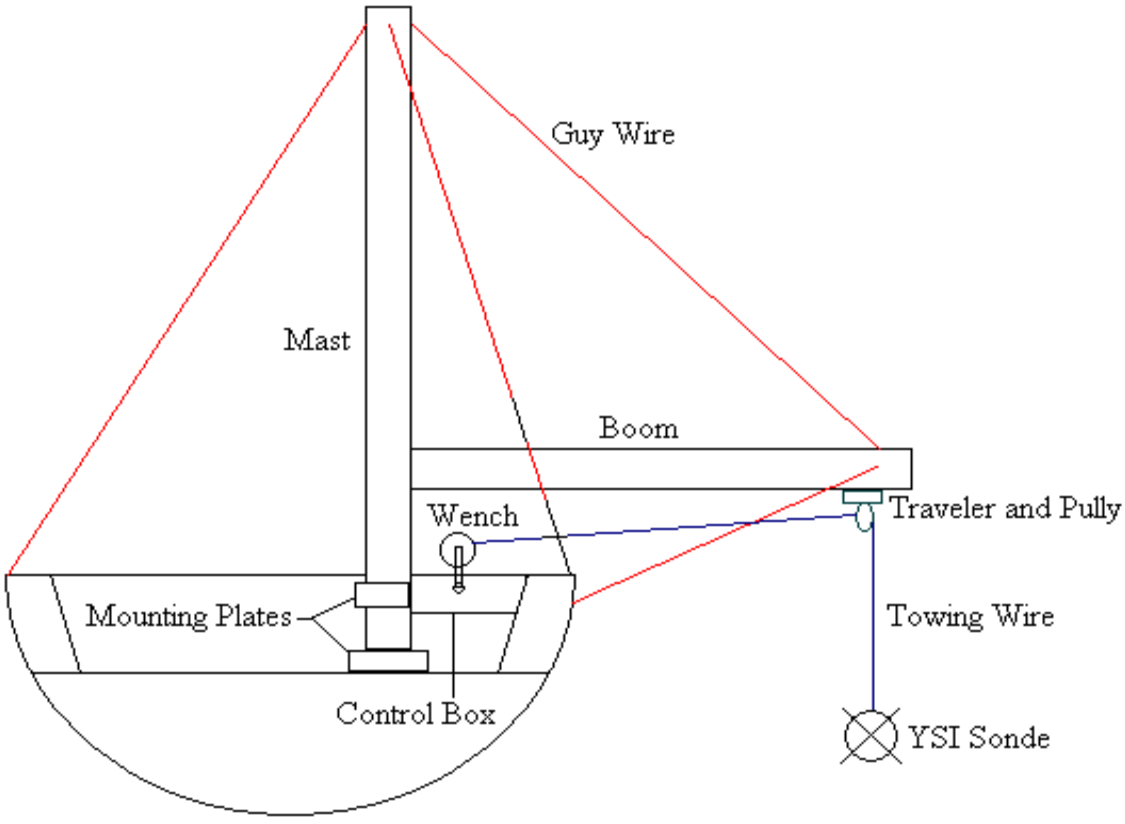

Figure 2. Diagram of the deployment system with the major components identified. The sonde's communication cable, the track for the traveler, and the control lines for the traveler are not shown for clarity.

2.3 Calibration

The probes on the 6600 unit were calibrated one to two days prior to sampling trips and, with the exception of the chlorophyll probe, all were calibrated with standard procedures each trip. Calibration of the conductivity probe was accomplished with a 2000 µS/cm standard produced by dilution of a 10,000 µS/cm traceable conductivity standard. Prepared conductivity standards were checked using an independent YSI model 33 conductivity probe. The turbidity probe was calibrated at 0 NTU, 10 NTU, and 100 NTU. Serial dilution of a 4,000 NTU formazin standard produced the 10 and 100 NTU turbidity standards while the 0 NTU standard was deionized water. The membrane on the dissolved oxygen probe was inspected and replaced if damaged and then the probe was calibrated using the saturated air method described in YSI's *Environmental Systems Operations Manual* (YSI, 1999). A two-point calibration was performed on the pH probe using pH 7 and pH 10 standards from Fisher Scientific.

Two methods of calibration were utilized for the chlorophyll probe during the course of the study. The first method involved collecting three water samples from Lake Texoma no more than 2 days prior to the mapping trip. The samples were divided and one half was stored in an opaque plastic bottle at 4° C while the other half was extracted with 90% acetone and stored at 4° C for approximately 24 hours. Extracted samples were analyzed for chlorophyll content as described in *Standard Methods for the Examination of Water and Wastewater 19th Edition* (American Public Health Association, 1995) using a Beckman DU-64 spectrophotometer (Beckman Instruments Inc., Fullerton, CA). The chlorophyll probe was then calibrated with the second half of the water sample having the

highest chlorophyll content and using DI water for the zero reading. This calibration approach was used for the months of July and August only.

Acridine orange hydrochloride hydrate emits detectable fluorescence within the optical constraints of the chlorophyll probe and can be used to produce a reliable standard for calibration (YSI, 1999). To reduce the amount of work needed to prepare the chlorophyll probe for the mapping trips the dye standard method was adopted for the remainder of the study. Standards were prepared as described in YSI's *Environmental Systems Operations Manual* (YSI, 1999).

2.4 Sonde Sampling

A total of 39 transects were used to cover all the major zones of Lake Texoma and most of the larger arms as well (Figure 3). Sampling trips occurred at the end of each month and often overlapped the beginning of the next month. Sonde sampling design involved dividing the reservoir into four zones and running transects for each zone over the course of a single day.

At the start of each transect the communications cable was attached to the 6200 data collection unit and the sonde was lowered into the water to a depth of 1 meter. The boat was stationary until the sonde was operational and the readings from the unit stabilized. The boat was navigated along the transect and at the end the sonde was removed from the water and disconnected from the 6200 collection unit. Disconnecting the sonde between transects makes it easier to identify individual transects during later inspection of the data.

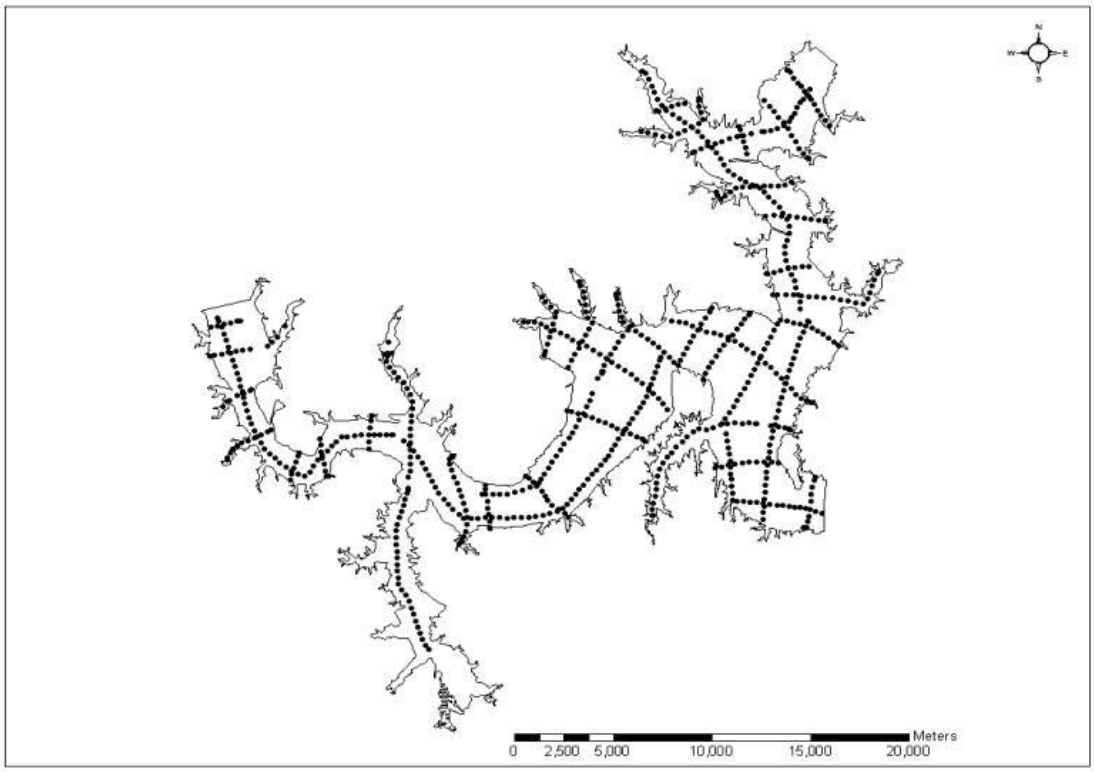

Figure 3. Map of transect layout. Transects pictured here are from October 2000 and are representative of the study as a whole. Gaps in some transects are the result of deletion of bad data points or locations where water depth was too shallow to take readings.

2.5 Chlorophyll Grab Sampling

Water samples were taken for chlorophyll extraction during each sampling period and compared to corresponding YSI chlorophyll readings. Three replicates were taken for all water samples and YSI readings. Extracted chlorophyll samples were used to adjust fluorometric readings from the sonde; thus water sampling was not done randomly but focused instead on obtaining a complete coverage of the range of YSI chlorophyll values observed during the sampling trip. The same procedure was used for all water samples and is detailed below:

1. Stop the boat, set the anchor and wait for the boat to stabilize.
2. Adjust the 6600 unit until it is ½ meter out from the side of the boat and at a depth as close to 1 meter as possible depending on conditions. Maintaining the unit at a specific depth in heavy waves is difficult thus the use of coves and sheltered areas is recommended for water sampling where possible.
3. After the boat has stabilized and the unit is at the desired depth record the times for the next three readings.
4. A Van Dorn water sampler was then lowered to one meter in the immediate vicinity of the 6600 unit and recovered three times to produce three separate water samples.
5. Water samples were immediately placed on ice in a cooler.
6. Water samples were filtered as soon as possible on the day of collection using a Gelman type A/E 47 mm glass fiber filter (Gelman Sciences, Ann Arbor, MI) and then frozen until they could be analyzed. The amount of water filtered for each sample varied with the amount of suspended particulate matter: 1000 ml for clear samples and 500 ml for turbid samples.
7. Samples were processed within three weeks using the chlorophyll extraction method from *Standard Methods for the Examination of Water and Wastewater 19th Edition* (APHA, 1995) and a Beckman DU-64 spectrophotometer.
8. Sample results from the spectrophotometer analysis were used to determine the chlorophyll-*a* concentrations in µg/L using the equation found in *Standard Methods*:

$$\text{Chlorophyll-}a \text{ mg/m}^3 = \frac{26.7(^{A}664 - {}^{A}665)V_1}{V_2 \, L}$$

Where:

V_1 = volume of extract, L.

V_2 = volume of filtered sample, m^3.

L = light path length of cuvette, cm.

A = light absorption in nm.

YSI and spectrophotometer (spec) results were analyzed using SAS Institute's SAS System for Windows version 8.2 software (SAS Institute, Cary, NC). Mean spec chlorophyll-*a* values were regressed against mean YSI total chlorophyll values to develop an equation for adjusting the sonde chlorophyll readings. Transect readings of total chlorophyll from the YSI sonde were then corrected to approximate spec chlorophyll-*a* with the regression equation.

2.6 Data Analysis and Mapping

Sonde and GPS data were downloaded as separate text files and converted to DBF format using Microsoft Excel (Microsoft Corporation, Seattle, WA). During the course of the study it was noted that the sonde occasionally surfaced during turns, in rough conditions, or when the boat speed was too high. Surfacing resulted in erroneous readings from the chlorophyll probe that could be on the order of 5 times as high as the readings just before and just after. Raw data were analyzed for these errors and they were

discarded. DBF files were imported into Environmental Systems Research Institute's (ESRI) ArcView™ software (Environmental Systems Research Institute Inc., Redlands.CA) to facilitate performing calculations and to prepare shapefiles for use in ESRI's Arc/INFO™ software (ESRI Inc., Redlands, CA).

Two calculations were used to adjust the sonde total chlorophyll readings. The first adjustment was for interference from suspended solids. Despite the fluorometer's optical backscatter filter, suspended solids can increase total chlorophyll estimates by a factor of approximately 0.03 µg/L per NTU (YSI, 1999). Multiplying this factor, termed the turbidity adjustment value, by the individual turbidity readings and then subtracting from the corresponding chlorophyll reading removed this effect.

The second calculation utilized the regression equation determined with SAS to adjust sonde readings to more accurately reflect extracted chlorophyll-*a* results. These were the final chlorophyll numbers used for the mapping process. All other mapped parameters were used without adjustment.

GPS files and sonde data files were merged within ArcView using the corresponding time stamps. The merged files were first converted to shapefiles and then to ArcInfo point coverages. All parameter maps were developed from point coverages utilizing ArcGrid™ software (ESRI Inc., Redlands, CA) and inverse distance weighted interpolation. Grid cell size was set at 150 meters for all maps and all cell values were interpolated using the values of the 12 closest points. Grid interpolations were made for the total area encompassed by the point coverage and then clipped to the lake boundary using a polygon coverage of Lake Texoma. One complete set of maps was imported

directly into ArcMap™ software (ESRI Inc., Redlands, CA) and displayed with a color ramp using the interpolated cell values. The cell values for a second complete set of maps were reclassified, using ArcGrid, into 10 categories covering the entire range of parameter values seen during the study period. The second set was then displayed in ArcMap using a color ramp and the 10 reclassified categories. The regression equations were used to transform YSI total chlorophyll into spectrophotometer chlorophyll-*a*; thus all chlorophyll final results were reported as chlorophyll-*a*.

Statistical investigations of chlorophyll-*a*, turbidity, and specific conductivity data were performed to supplement the maps and to facilitate comparisons to the IAS study. Analyses were divided by month and the 5 lake zones outlined in the IAS study. The lake zones were designated as: the Red River zone, the Red River transition zone, the Main Lake Zone, the Washita River transition zone, and the Washita River zone.

The IAS study (Atkinson et al. 1999) focused on the limnetic zone of the lake and did not sample in stream arms or up major tributaries as this study did. Therefore, to achieve a proper comparison to the IAS study, readings from stream arms were eliminated from the data set before statistical analyses were performed. All data sets were analyzed using SAS version 8.0. One-way parametric ANOVA and nonparametric Kruskal-Wallis tests were utilized to acquire basic statistics and assess variation within zones and across months. A Student-Newman-Keuls multiple range test and Tukey's multiple comparison test were performed to assess differences between months and zones. Relationships between variables were investigated with parametric and non-parametric correlation tests and linear regressions.

CHAPTER 3

RESULTS

3.1 Data Collection System

The design of the deployment system proved to be very strong and withstood high wind conditions quite well. Overall the system was stable and allowed the sonde to maintain its orientation and depth in all but the most extreme conditions. Rapid turning of the boat, however, either toward or away from the sonde, would cause the unit to swing in or out and rise to the surface

Proper placement of the tow-line and data cable were the major factors dictating the stability of the sonde in the water at speed. The tow-line must attach to the sonde through the center hole in the attachment plate at the top of the Horizontal Deployment Apparatus (HDA). Placement of the data cable was somewhat problematic and required experimentation to achieve the right setup. What ultimately dictated the sonde's tracking stability was the amount of data cable played out and the tension it placed on the sonde. Generally, the best performance in smooth conditions occurred when the data cable was placed on the outside of the HDA's tail system and looped upward before encountering the tail fins (Figure 4A). In rough conditions it was sometimes advantageous to allow the data cable to run out behind the sonde (Figure 4B). This setup appeared to produce more drag on the system and keep the sonde stable in choppy water. The top speed achieved as

measured by the Global Positioning System (GPS), with the sonde at 1 meter, was 7 mph (6 knots) – higher speeds tended to destabilize the system and cause the sonde to rise. Minimum sampling interval was restricted to 2 minutes due to the data collection unit's communications protocol (described below). The system's top speed was sufficient to allow mapping of the entire lake, with samples 330 to 400 meters apart, in 4 days.

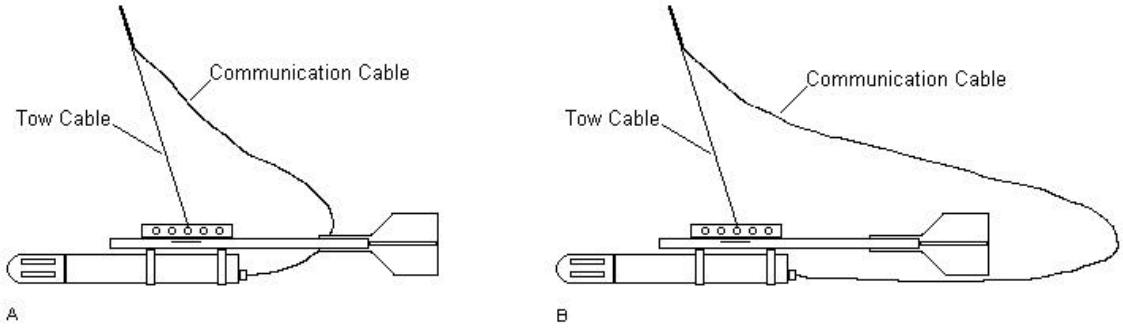

Figure 4. Configurations of the towing and communications cables for optimum stability under smooth water conditions (A) and rough water conditions (B).

The 4-day goal was reached in only 5 out of 8 sampling trips due to weather conditions and technical problems and only two trips were accomplished in 4 consecutive days. Thunderstorms with abundant lightning are common on Lake Texoma in the spring and fall and were responsible for most of the weather related delays.

One serious technical problem was encountered during the course of this study. A communication problem caused the Data Collection Platform (DCP) to report all sonde data as -1,000,000. What appeared to be a minor inconvenience turned into a major problem at the end of the study. Through consultation with the technical staff at Yellow Springs Instruments (YSI) it was determined that the problem was in the EcoWatch

DCP™ software (YSI Inc., Yellow Springs, OH). Sampling with the sonde and the GPS unit requires the DCP to communicate with two separate devices. When performing rapid sampling it is imperative that the communication configuration be given enough time to communicate with both devices without interference. The EcoWatch software creates a log file, designated Ecoww.log, which is accessed every time the DCP performs an operation. If this file becomes very large and the sampling interval is short the time needed to access it begins to interfere with the communications process. Accessing the software and renaming the .log file can correct the problem. A new empty .log file is then created by the system. The updated version of the EcoWatch software now renames this file automatically when it reaches a certain size. Although renaming the .log file restored operation of the system there continued to be occasional instances where the sonde needed to be rebooted manually. Thus it is important that the system setup include a laptop computer to monitor the real-time output for system problems.

3.2 Chlorophyll-*a* Calculations

All regression equations for adjusting YSI chlorophyll readings, with the exception of December, had R^2 values of 0.9 or greater (Figure 5). The data for December contained a single outlier that reduced the R^2 to 0.76. Elimination of this point increased the R^2 value to above 0.9. Deviation from a strict linear relationship between YSI chlorophyll and spectrophotometer measurements usually involved YSI readings that indicated a higher concentration of chlorophyll than what was actually present. Often these readings were taken in relatively turbid situations, but not always. Increased

fluorescence at these sites and the lack of an obvious correlation with turbidity suggests the presence of other fluorescing substances in the water. Deviations from linearity where the YSI instrument suggests a lower chlorophyll concentration than actual were less frequent and may indicate a heterogenic distribution for other fluorescing species. Low chlorophyll-*a* concentrations in the winter months resulted in some regression equations with negative y-intercept values.

Turbidity adjustments applied to the YSI total chlorophyll readings prior to developing the regression equations equaled (0.03 µg/L)turbidity for the months of July, August, September, October, and March. November and December required an adjustment of (0.07µg/L)turbidity and February needed a value of (0.05µg/L)turbidity. Turbidity adjustments were applied to all raw total chlorophyll readings with the exception of February. In February chlorophyll grab sampling fell slightly below the lowest YSI readings. As a result the regression equation developed during that month produced negative concentrations from a few of the lowest YSI chlorophyll readings. To eliminate this effect turbidity adjustments were applied only to chlorophyll readings with turbidity values over 12.0 nephelometric turbidity units (NTUs). The 12.0 NTU cutoff value for turbidity adjustments had no real biological bases and was selected only because it eliminated most of the negative chlorophyll-*a* conversion results. Turbidity adjustments were often negligible when overall water turbidity was low, but proved to be vital to developing regression equations when turbidity was high.

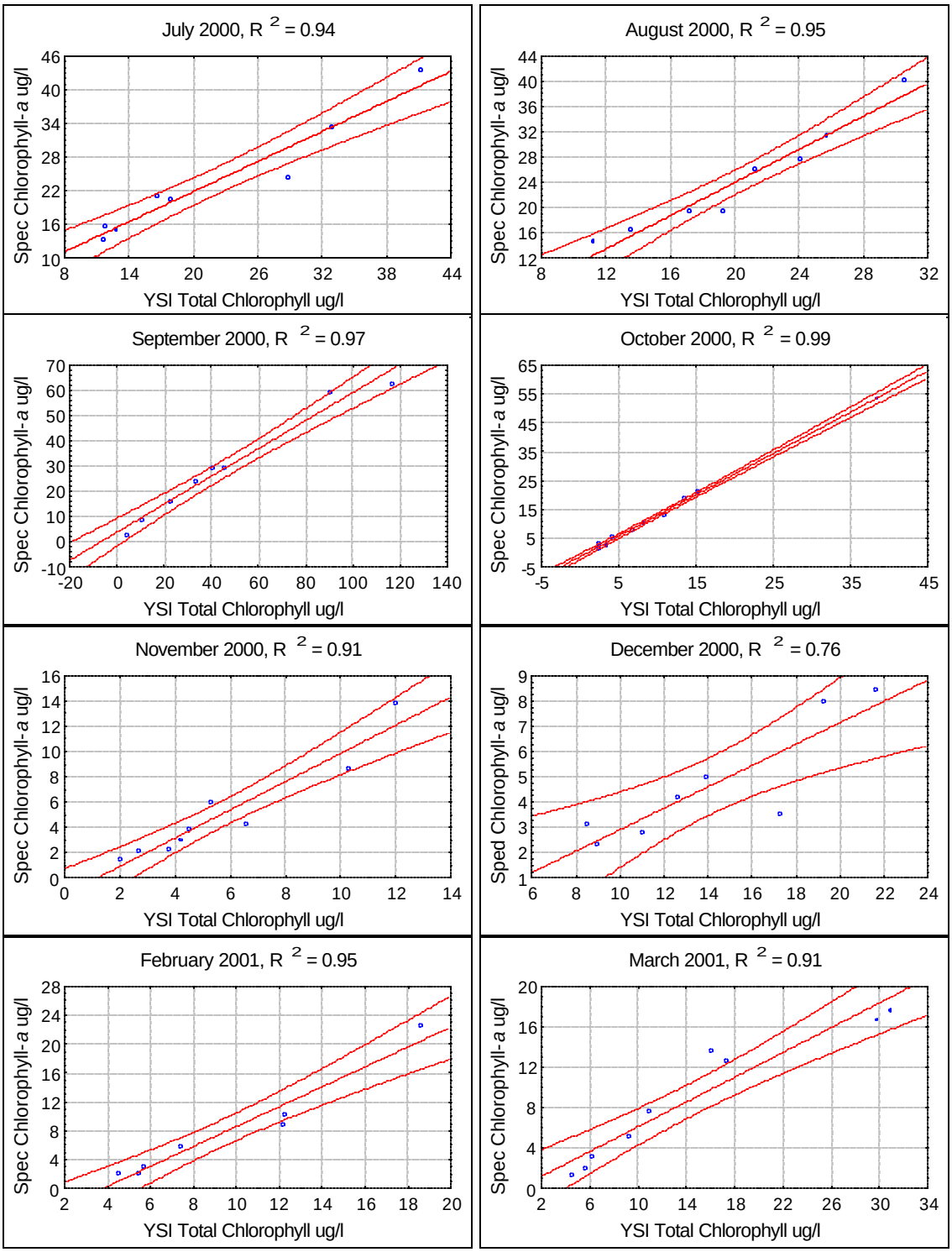

Figure 5. Regression plots of mean spectrophotometer determined chlorophyll-*a* regressed against mean YSI total chlorophyll from the data sonde for each month. The centerline represents the best-fit model and the curved outside lines are the 95% confidence belts for the best-fit line.

3.3 Maps

A total of eight sampling trips were completed between July 2000 and March 2001. Two sets of raster format maps were developed for three parameters: chlorophyll-*a*, turbidity, and specific conductivity. Map set 1 was designed to show maximum detail for the individual month using 10 categories - the categories do not have fixed values and cover only the range of values for the month. Map set 1 was categorized from actual cell values thus categories are not equal and do not necessarily break on whole numbers. Map set 2 compares values across months using 10 fixed categories that cover the combined range of all months. Map set 2 was produced from reclassified cells and has equal categories that break on whole numbers or whole fractions. The first map set places the chlorophyll-*a*, turbidity, and specific conductivity maps for a given month together for cross parameter comparisons within the month. The second map set places all the maps for a given parameter together to facilitate comparisons of a single parameter through time.

The interpolation process used to create the maps involves estimating values between known points; therefore the maps created should be understood as estimates of parameter distributions. The maps presented here were created using Inverse Distance Weighted interpolation (IDW). IDW gives values to unknown cells by weighting the value of neighboring cells by the distance they are from the analysis cell and then averaging the values. The interpolation cell size used to create the maps was designed to eliminate influences from cells that were close in space but unrelated. However, no attempt to quantify the amount of uncertainty in the mapping process was made.

The July chlorophyll-*a* map from set 1 is shown in Figure 6. The legend gives the chlorophyll-*a* concentrations, in µg/L, that are contained within the individual categories. The low end of the first category and the high end of the last category indicate the chlorophyll-*a* range for the month. The set number (visible in the upper left underneath the title) indicates the method used to develop this map (first number) and its position in the set series (second number). Complete copies of map sets 1 and 2 are located in Appendix A and Appendix B respectively.

Chlorophyll-*a* maps generated for the summer months tended to show the zonation characteristic of Lake Texoma (Maps 2:1, 2:2, and 2:3). Chlorophyll-*a* was generally higher in the river zones and decreased in the direction of the Main Lake Zone. The Washita branch of the lake displayed a variation to this pattern in September when the lower end of the Washita River Transition Zone recorded higher chlorophyll-*a* readings than the Washita River Zone (Map 1:7). Stream arms also tended to display falling concentration gradients going from the heads of the arms to the lake proper. This pattern was also true of the Big Mineral Arm (Maps 1:7, 1:10).

The maps recorded a dramatic shift in the chlorophyll-*a* distribution that occurred during the month of October and continued into November (Maps 2:4, 2:5). Chlorophyll-*a* concentrations for all zones decreased and the zoning of the lake underwent a shift. The zone of highest chlorophyll moved from the Red River Zone in September to the Red River Transition Zone in October and finally to the Main Lake Zone in November. This zonal shift followed immediately after a period of strong thunderstorms across Lake Texoma's watershed. Chlorophyll-*a* in the Big Mineral Arm showed a delayed reaction;

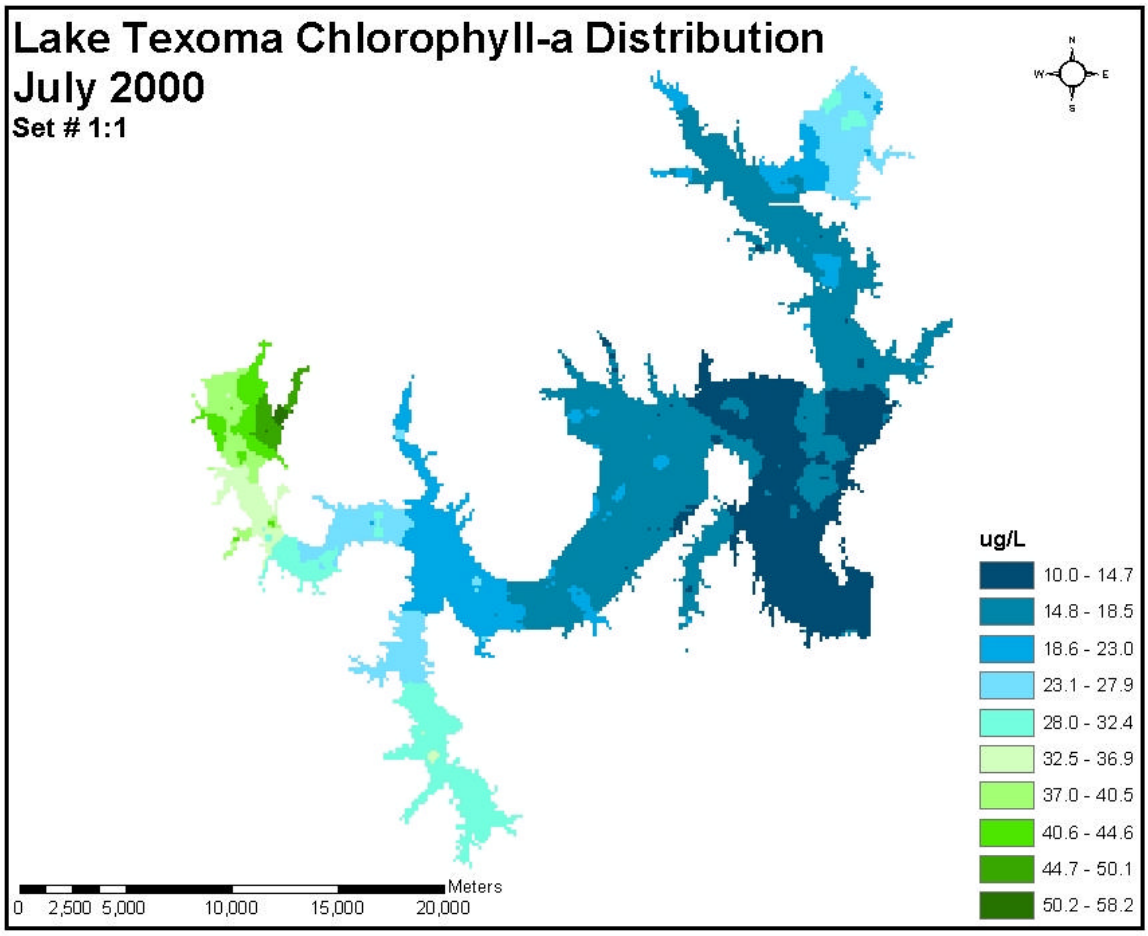

Figure 6. Map 1.1, Chlorophyll-*a* concentration distribution for July 2000.

it fell dramatically in November, but actually recorded its highest concentrations during October. A zonal pattern similar to the summer maps returned in December, was less pronounced in February, and strong again in March.

Specific Conductivity maps also displayed zonation in the summer although with a different pattern. There was a distinct falling concentration gradient running from the Red River Zone through the Main Lake Zone and to the Washita River Zone (Maps 2:17, 2:18, 2:19). This gradient was also overturned in October and November when conductivity dropped sharply in the river arms. Median specific conductivity in the Red

River Zone declined from 2589 µS/cm in September to 622 µS/cm in October. The general declining gradient from the Red River Zone to the Washita River Zone returned in December, but the zonation in the Red River branch was not the same as the summer months. During the months of December and February the specific conductivity was higher in the Main Lake Zone than the Red River Transition Zone. Overall specific conductivity declined throughout the lake during the winter months and only started to increase again in March. Specific conductivity in the Big Mineral Arm appeared to be tied more closely to the rest of the lake than chlorophyll-*a* and fluctuated with changes in the lake proper. Map 1:12 demonstrates a strong gradient set up in the Big Mineral Arm during October that apparently indicates a pulse of fresher water moving up the arm from the Red River Transition Zone.

Maps of turbidity were the most dynamic of the study and displayed the effects of the fall weather quite well. Turbidity was highly variable, but consistently showed a falling concentration gradient moving from the river arms to the main lake body. The storms in October, which had overturned the chlorophyll and conductivity distributions, only served to reinforce the turbidity gradient and move suspended sediments down-lake from the river arms. Median turbidity in the Red River Zone increased from 9.8 to 218.7 NTU between the September and October sampling trips. The Red River Transition Zone and the Washita River Zone recorded similar increases, while the Washita River Transition Zone and the Main Lake Zone increased to a lesser degree. The latter two zones appeared to resist large changes in their turbidity values. Turbidity in the Big

Mineral Arm appeared to be tied to changes in the lake proper, but not as closely as specific conductivity.

3.4 Statistical Analyses

Shapiro-Wilkes normality tests conducted on chlorophyll-*a*, turbidity, and specific conductivity data indicated that these parameters were not normally distributed thus the general statistical description of these parameters will involve the basic five number summary (minimum, 25^{th} percentile, median, 75^{th} percentile, and the maximum). Means and standard deviations will sometimes be used to facilitate comparisons to the IAS study, which primarily reported results using parametric statistics.

3.4.1 Chlorophyll-*a*

The 1999 IAS study delineated five zones in Lake Texoma. We felt that the Big Mineral Arm may constitute a separate zone and thus we delineated 6 zones. However, for the sake of comparison we will discuss our results from the five primary zones described in the IAS study. Results for the Big Mineral Arm will be given separately, but will not be included in the statistical ranking.

Both the IAS study and ours ranked the Red River Zone highest in chlorophyll-*a* concentration and variability (Atkinson et al. 1999) (Figure 7). From July through September median chlorophyll-*a* was highest in the river arms. The fall flushing event caused the median chlorophyll-*a* concentrations to fall dramatically across the lake (Figure 8). The zone of maximum chlorophyll-*a* moved down lake from the Red River

Zone to the Red River Transition Zone and eventually to the Main Lake Body in November. The zonal hierarchy in the Washita River branch displayed the same pattern. After November the river zones again became the zones of highest chlorophyll-*a*, but the pattern of chlorophyll-*a* zonation was not as clear as it was in the summer (Table 1).

Overall the Main Lake Zone was ranked last in chlorophyll-*a* concentration and variability. Again, this corresponds to the IAS findings. Outside of the fall flushing event the Main Lake Zone generally displayed the lowest chlorophyll-*a* concentrations. In the month of August, however, the Washita River Transition Zone had a median chlorophyll-*a* concentration 1 µg/L less than the Main Lake Zone. Interestingly, the lowest median

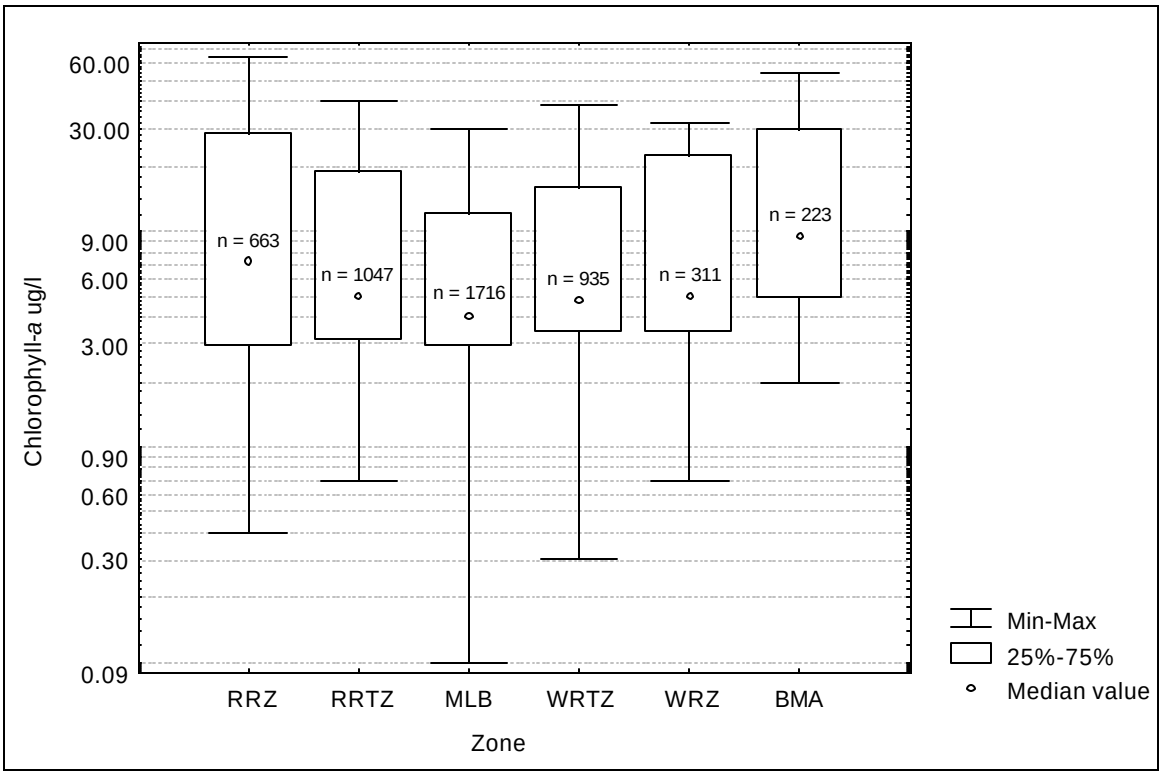

Figure 7. Five number summary of chlorophyll-*a* at 1-meter depth from July 2000 to March 2001 for the five zones delineated by the IAS study and the Big Mineral Arm.

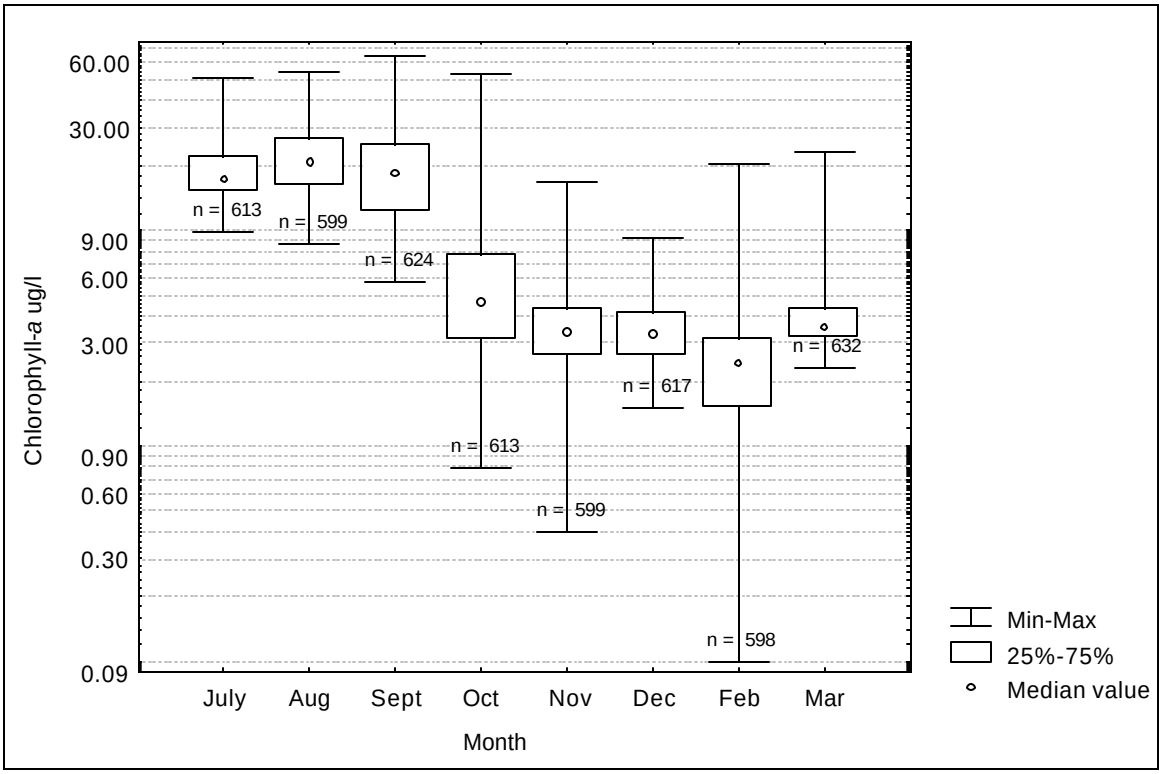

Figure 8. Five number summary of chlorophyll-*a* by month from July 2000 to March 2001 at 1-meter depth.

chlorophyll-*a* concentration seen was in the Red River Zone in November at 1.6 µg/L (Table 1). At this time the Main Lake Zone was the zone with the highest median chlorophyll-*a* concentration.

The IAS study located one fixed sampling station in the Big Mineral Arm that was sampled regularly and two random sites that were sampled once. The data from these stations were included in their calculations for the Red River Transition Zone. Data analysis for this study was conducted with the assumption that the Big Mineral Arm should not be included in the Red River Transition Zone. Chlorophyll-*a* concentrations in the Big Mineral Arm were quite different from those seen in the Red River Transition

Table 1. Medians for chlorophyll-*a* in µg/L at 1-meter depth by zone and month from July 2000 to March 2001.

	July	Aug	Sept	Oct	Nov	Dec	Feb	Mar
RRZ	33.4	36.5	27.9	2.5	1.6	6.7	4.2	7
RRTZ	18.4	24.7	19.6	9	2.7	3.4	2.1	3.9
MLB	14.6	16.8	9.5	3.6	4.2	2.5	2.1	3.1
WRTZ	16.8	15.8	18.7	6	3.8	3.5	2.4	3.6
WRZ	24.4	24.3	23.3	5.6	2.5	3.5	2.9	4.2
BMA	25.6	33.5	28.8	18.9	7.4	5.4	2.9	4.8

Zone and often exceeded those found in the Red River Zone (Figure 7). Minimum, 25th percentile, median, and 75th percentile measures over the course of the entire study were highest in the Big Mineral Arm (Table 2). In addition, parametric analysis ranked the Big Mineral Arm slightly higher in variation than the Red River Zone.

Table 2. Summary of chlorophyll-*a* in µg/L at 1-meter depth by zone from July 2000 to March 2001.

Zone	Min	Max	Median	Mean	SD	N
RRZ	0.4	63.9	7.2	15.5	14.4	663
RRTZ	0.7	40.3	5.0	10.7	8.9	1047
MLZ	0.1	30.0	4.1	7.4	6.1	1716
WRTZ	0.3	38.4	4.8	9.2	7.3	935
WRZ	0.7	31.9	5.0	11.9	10.0	311
BMA	2.0	54.4	9.5	17.5	14.9	223

Kruskal-Wallis non-parametric ANOVAs were performed on the chlorophyll-*a* data for each month as well as the entire data set. The data were then ranked and Tukey's multiple comparison tests were performed to assess similarities between zones. Results of the Tukey's tests are given in Table 3.

The Tukey's tests generally agreed with the zones described in the IAS study. During the peak-growing season (July through September) zones found to be statistically

similar were usually not spatially connected. The one exception occurred in August when the Main Lake Zone and the Washita River Transition Zone were not significantly different. Historically, the Washita River Transition Zone was not recognized in Lake Texoma. Preliminary investigations by Atkinson et al. (1996) led to the hypothesis of a transitional zone within the Washita River branch. Testing of the complete data set ranked the Washita River Zone with the Washita River Transition Zone. However, peak season results found these zones to be different.

The Big Mineral Arm was grouped with the Red River Transition Zone only in the month of October. Median chlorophyll-*a* in the Big Mineral Arm during the summer was 26% to 32% higher than the Red River Transition Zone.

Table 3. Tukey's multiple comparison ranks for chlorophyll-*a* at 1-meter depth. Zones followed by the same letter were not significantly different at an alpha level of 0.05. Statistically different classes are labeled in alphabetical order with class A representing the highest concentration and class E the lowest.

July	RRZ(A)	BMA(AB)	WRZ(B)	RRTZ(C)	WRTZ(D)	MLZ(E)
August	RRZ(A)	BMA(A)	RRTZ(B)	WRZ(B)	MLZ(C)	WRTZ(C)
September	BMA(A)	RRZ(A)	WRZ(B)	RRTZ(C)	WRTZ(C)	MLZ(D)
October	BMA(A)	RRTZ(A)	WRZ(B)	WRTZ(B)	MLZ(C)	RRZ(D)
November	BMA(A)	MLZ(AB)	WRTZ(B)	RRTZ(C)	WRZ(C)	RRZ(D)
December	RRZ(A)	BMA(A)	WRZ(B)	WRTZ(B)	RRTZ(B)	MLZ(C)
February	RRZ(A)	WRZ(AB)	BMA(AB)	WRTZ(BC)	RRTZ(C)	MLZ(C)
March	RRZ(A)	BMA(AB)	WRZ(B)	RRTZ(C)	WRTZ(D)	MLZ(E)
All Data	BMA(A)	RRZ(B)	WRZ(BC)	RRTZ(C)	WRTZ(C)	MLZ(D)

3.4.2 Turbidity

Median turbidity and turbidity variability were highest in the river arms and lowest in the Main Lake Body (Figure 9). The highest overall average turbidity was found in the

Red River Zone while the Washita River Zone was ranked second (Table 5). The IAS study found a similar relationship for turbidity, but reported the Washita River Zone as having the highest overall average turbidity. When the data covering the fall flushing event is removed and only the summer season is considered, our data agreed with the IAS results (Table 6).

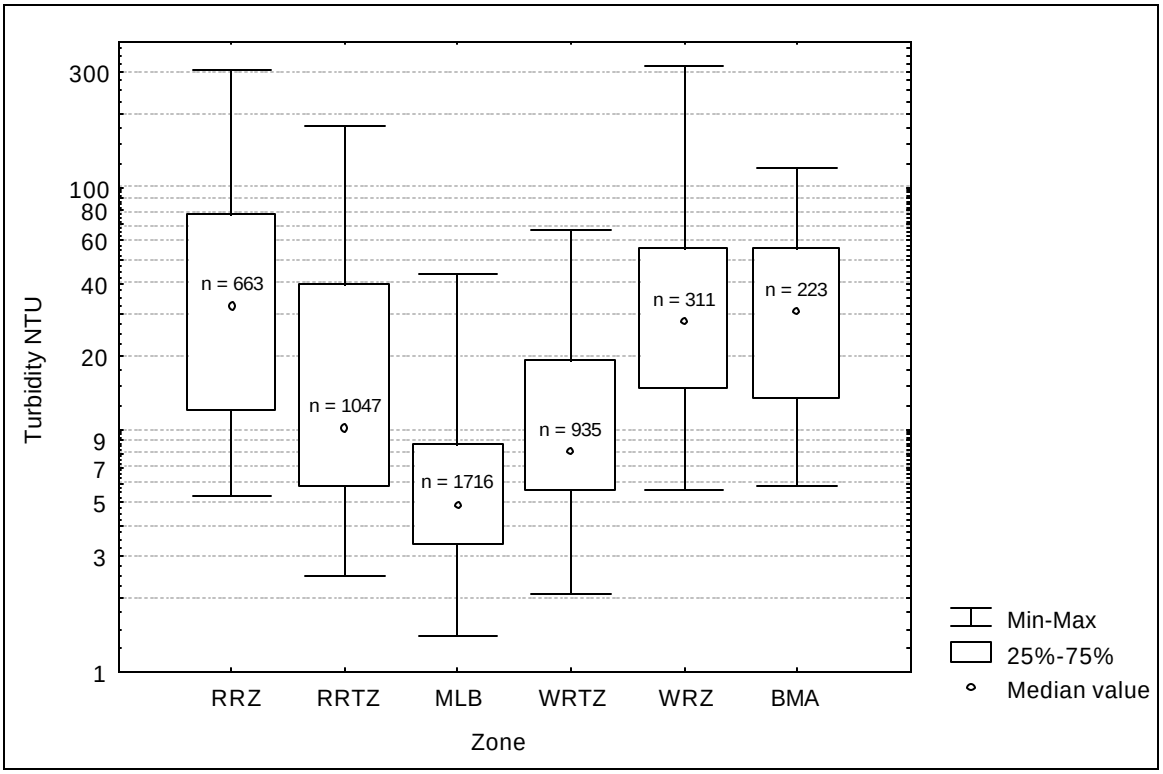

Figure 9. Five number summary of turbidity at 1-meter depth from July 2000 to March 2001 for the five zones delineated by the IAS study and the Big Mineral Arm.

Average turbidity values for the Red and Washita River Zones were 89% and 85% higher than the Main Lake Zone respectively. Atkinson et al. (1999) reported average values that were 74% and 82% higher than the Main Lake Zone. Average turbidities for the Red

River Transition Zone and the Washita River Transition Zone were 73.6% and 55.8% higher than the Main Lake Zone respectively.

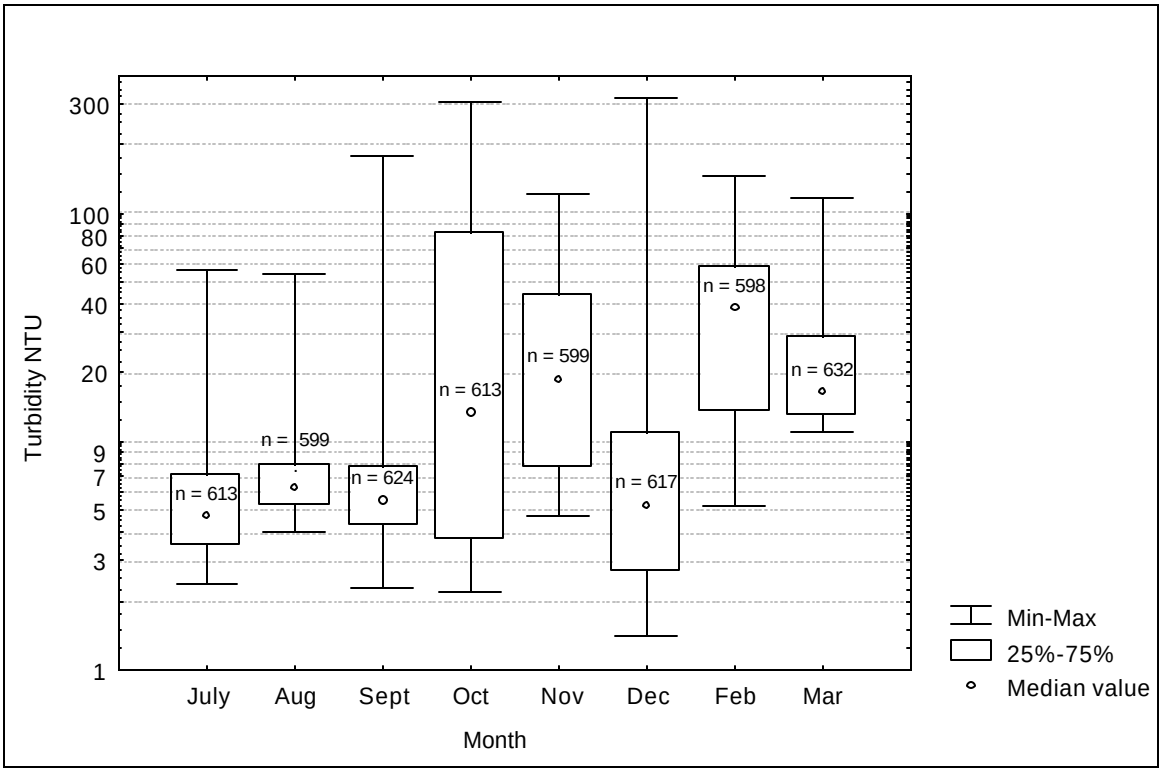

Figure 10. Five number summary of whole lake turbidity by month from July 2000 to March 2001 at 1-meter depth.

These data differ somewhat from the IAS study, which found the transition zones to be similar in average turbidity and 50% greater than the Main Lake Zone. Differences in average turbidity and turbidity variability between this study and the IAS study most likely stem from the much larger spatial distribution of samples associated with our work. The use of the towed data sonde allowed us to investigate entire zones and incorporate shallow water areas that are inherently more turbid. Also, we found turbidity to be higher

and more variable during periods of increased river discharge. This is in agreement with the IAS study, however we were able to thoroughly investigate the spatial dynamics of these increased turbidity periods and therefore found and recorded higher turbidity values during these events.

Median turbidity in the Big Mineral Arm was similar to The Red River Zone and 67.3% greater than the Red River Transition Zone. Turbidity variability, however, was similar to the Red River Transition Zone.

From July through September median turbidity was relatively low in all zones and higher readings appeared to be tied to water depths (Figure 10). The river zones are highly variable in terms of depth, and thus appeared to be highly variable in terms of turbidity too (Table 5). Variability in the Main Lake Zone was relatively low.

Table 4. Medians for turbidity in NTUs at 1-meter depth by zone and month from July 2000 to March 2001.

	July	Aug	Sept	Oct	Nov	Dec	Feb	Mar
RRZ	8.5	18.7	9.8	218.7	78.2	14.9	60.3	32
RRTZ	5.1	6.3	5.5	63.3	42.3	6.3	51.5	18.3
MLZ	3.4	5.2	4	3.4	7.1	2.5	11.4	12.3
WRTZ	4.7	6.6	5.9	6.6	10.5	6.8	36.8	17.4
WRZ	12.5	13.1	12.9	126.9	26.5	26.1	59.4	30.7
BMA	11.1	12.9	10	24.2	31.4	68.5	58.1	52.3

Table 5. Summary of turbidity in NTUs at 1-meter depth from July 2000 to March 2001.

Zone	Min	Max	Median	Mean	SD	N
RRZ	5.3	305.8	32.3	59.2	65.0	663
RRTZ	2.5	177.8	10.1	24.6	27.4	1047
MLZ	1.4	43.7	4.9	6.5	4.5	1716
WRTZ	2.1	67.1	8.1	14.7	14.0	935
WRZ	5.6	318.4	27.9	43.1	44.5	311
BMA	5.9	120.3	30.8	38.1	28.2	223

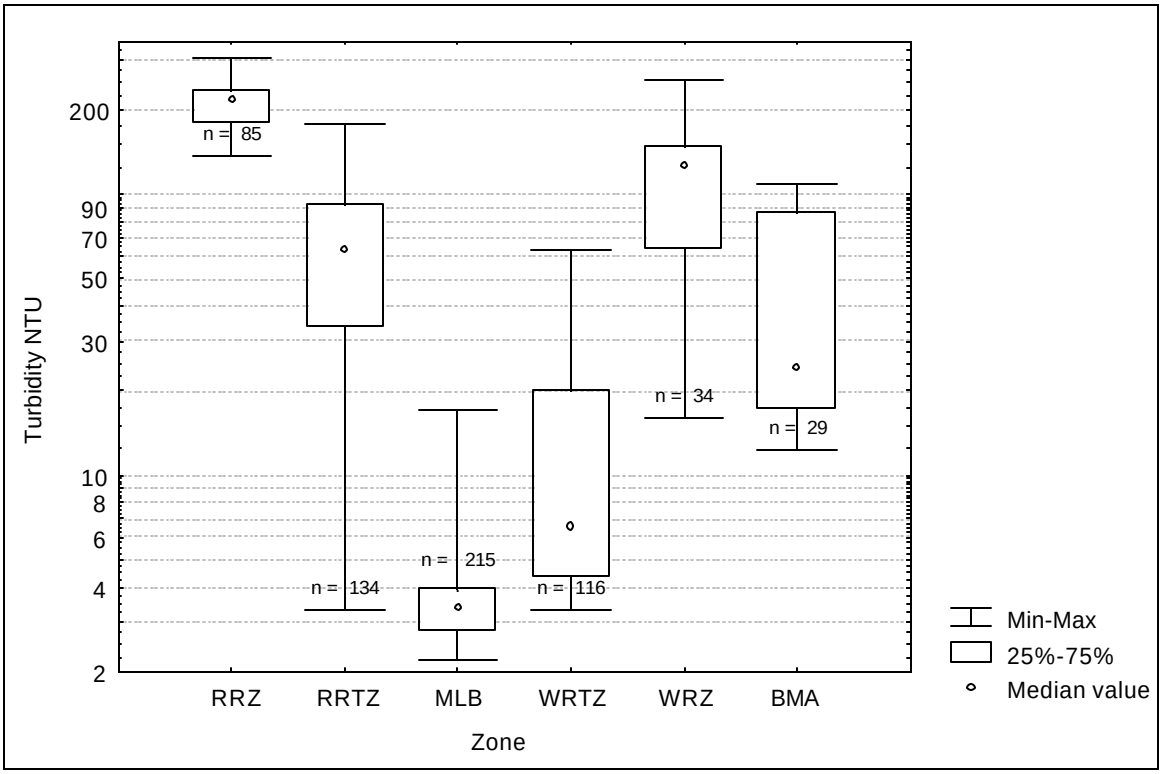

Figure 11. Five number summary of turbidity by zone for October 2000 at 1-meter depth.

The large increase in river discharge in October appeared to change the factors governing turbidity levels in that month and median turbidity in the river arms increased substantially (Figures 10 and 11). With the input of a large volume of sediment-laden water and rising lake levels, water depth was not an important factor in dictating turbidity values in October. November turbidity values were still high due to the increased river discharge, but the highest levels were again associated with shallower water.

The fall flushing event increased median turbidity dramatically in the Red River Transition Zone, but only slightly in the Washita River Transition Zone. Between September and October the Red River Transition Zone saw an increase in median turbidity of 57.8 NTUs, while the Washita River Transition Zone only increased by 0.7

NTUs (Table 4). However, the variation in turbidity increased in both zones. Standard deviations for turbidity in September were 1.2 and 2.3 NTUs for the Red River Transition Zone and the Washita River Transition Zone respectively. In October the same measures were 39.6 and 14.5 NTUs. The increase in variability in the Red River Transition Zone was the result of the strong gradient that was set up in this zone as sediment-laden water moved from the very turbid Red River Zone to the relatively clear Main Lake Body (Map 2:12). The Washita River Transition Zone, which had a smaller increase in variability, displayed a weaker gradient.

The Main Lake Body was the zone of lowest median turbidity throughout the study. Turbidity values across the lake were relatively high in February and March and the Main Lake Body recorded its highest median turbidity value of 12.3 NTUs in March. As mentioned previously, the Main Lake Body resisted large changes in its turbidity values. This ability appeared to stem from the long distance that sediment-laden water, entering at the river zones, had to travel before reaching this zone.

The Big Mineral Arm displayed a delayed reaction to turbidity changes in the lake proper. From July to September turbidity levels in the Big Mineral Arm were stable and generally displayed a decreasing trend as you moved from the shallower end of the arm towards the deeper Red River Transition Zone (Map 1:5). Median Turbidity values were relatively low (Table 4). The fall flushing appeared to push sediment-laded water up the Big Mineral Arm and reverse the decreasing turbidity gradient in October and November (Maps 1:11 and 1:14). However, the highest median turbidity values seen in the Big Mineral Arm occurred in December two months after turbidity spiked in the lake arms

(Table 4). A second lake wide turbidity spike in February reinforced the higher turbidity in the Big Mineral Arm and turbidity values remained high even as the rest of the lake began to clear in March.

Tukey's results for turbidity are given in Table 6. The river arms and the Big Mineral Arm are typically ranked together while the Main Lake Zone is consistently significantly lower than the rest of the lake. The three top ranked zones of the lake share one common feature in that they all have large areas of shallow water.

Table 6. Tukey's multiple comparison ranks for turbidity at 1-meter. Zones followed by the same letter were not significantly different at an alpha level of 0.05. Statistically different classes are labeled in alphabetical order with class A representing the highest concentration and class E the lowest.

July	WRZ(A)	BMA(A)	RRZ(A)	WRTZ(B)	RRTZ(B)	MLZ(C)
August	WRZ(A)	RRZ(A)	BMA(A)	WRTZ(B)	RRTZ(C)	MLZ(D)
September	WRZ(A)	BMA(A)	RRZ(A)	WRTZ(B)	RRTZ(C)	MLZ(D)
October	RRZ(A)	WRZ(B)	RRTZ(C)	BMA(C)	WRTZ(D)	MLZ(E)
November	RRZ(A)	RRTZ(B)	BMA(B)	WRZ(B)	WRTZ(C)	MLZ(D)
December	BMA(A)	WRZ(AB)	RRZ(B)	WRTZ(C)	RRTZ(C)	MLZ(D)
February	RRZ(A)	WRZ(A)	BMA(A)	RRTZ(B)	WRTZ(C)	MLZ(D)
March	BMA(A)	RRZ(AB)	WRZ(B)	RRTZ(C)	WRTZ(D)	MLZ(E)
All Data	RRZ(A)	WRZ(A)	BMA(A)	RRTZ(B)	WRTZ(C)	MLZ(D)

3.4.3 Specific Conductivity

The IAS study established specific conductivity as a reliable surrogate for determining chloride concentration in Lake Texoma (see Section 1.5, Chloride). The general long-term pattern for chloride found by the IAS study was RRZ > RRTZ > MLZ > WRTZ > WRZ (Atkinson et al., 1999). However, Atkinson et al. (1999) also stated that this pattern was not always seen over the short term and that chloride concentrations

in the lake were dependant on total discharge from the Red River. Higher chloride concentrations were associated with periods of lower discharge from the Red River.

Results of the specific conductivity investigation in this study mirror the IAS's chloride findings. The long-term pattern for chloride found by the IAS study was seen in median specific conductivity from July through September (Table 7) and is represented by the August data set (Figure 12).

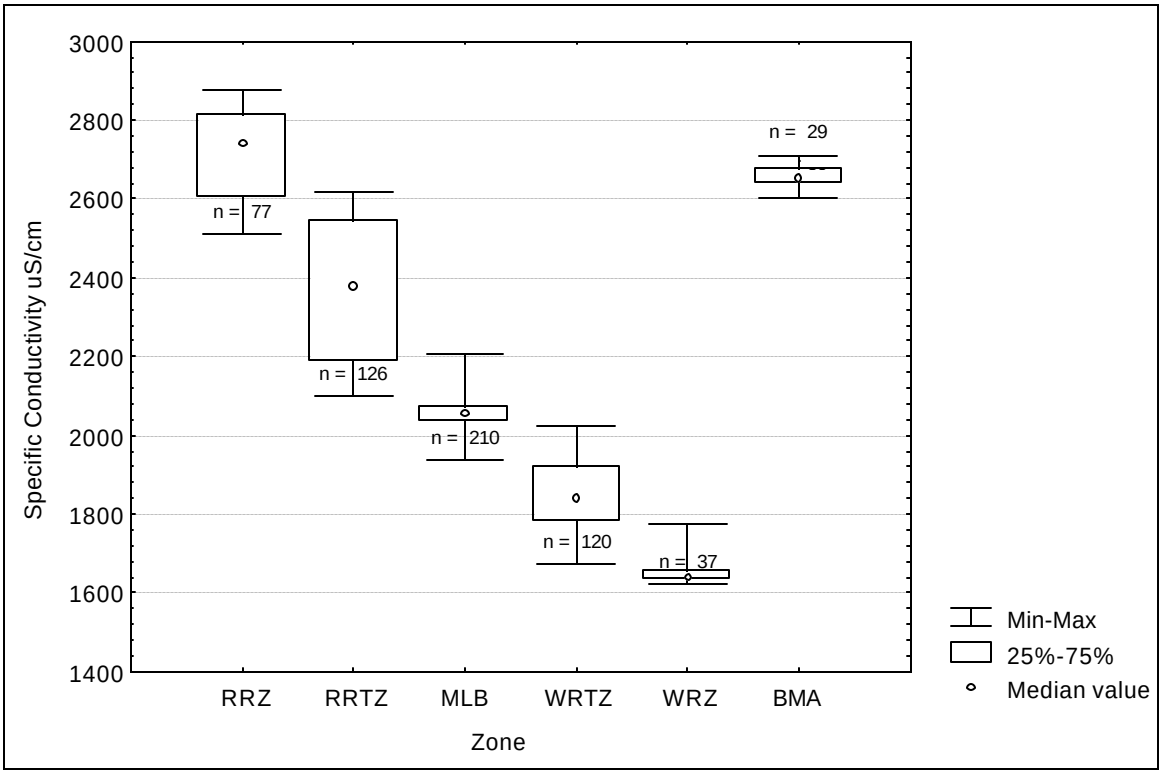

Figure 12. Five number summary of specific conductivity by zone at 1-meter for August 2000.

However, when the complete data set is taken into account the Main Lake Zone actually has the highest average and median specific conductivity (Table 8, Figure 15). This result can be explained by the dynamic nature of the Red River arm and the

relatively stable nature of the Main Lake Zone. The wide swings in specific conductivity seen in the Red River arm during the fall storms translated into much smaller changes in the Main Lake Zone and less variation. This indicates that the Red River Zone's higher base flow chloride concentration, when it is diluted during large inflow events, can drop well below the concentration in the Main Lake Zone.

Table 7. Median specific conductivity in µS/cm at 1-meter by zone and month from July 2000 to March 2001.

Zone	July	Aug	Sept	Oct	Nov	Dec	Feb	Mar
RRZ	2858	2744	2589	622	878	1444	1193	1566
RRTZ	2453	2379	2218	1237	1021	1350	1067	1177
MLB	2131	2059	2185	2157	1678	1454	1295	1096
WRTZ	1783	1838	1996	2003	1170	1099	741	959
WRZ	1439	1639	1908	794	920	963	620	936
BMA	2724	2653	2533	1736	1075	853	644	793

Table 8. Summary of specific conductivity in µS/cm at 1-meter from July 2000 to March 2001.

Zone	Min	Max	Median	Mean	SD	N
RRZ	605	3378	1491	1752	829	663
RRTZ	693	2672	1363	1642	595	1047
MLZ	984	2286	1938	1756	416	1716
WRTZ	549	2182	1458	1442	489	935
WRZ	445	1952	977	1146	439	311
BMA	487	2759	1153	1632	860	223

The increase in discharge from the Red River in October drastically reduced specific conductivity in the Red River and the Red River Transition Zones as predicted by the IAS study (Figure 13). Changes in specific conductivity due to changes in discharge rates from the Washita River were not mentioned in the IAS study, but were apparent in this investigation. When discharge from the Washita River increased in the

fall median specific conductivity in both the Washita River Zone and the Washita River Transition Zone began to decrease (Table 7). This effect was immediate in the Washita River Zone, but did not manifest in the Washita River Transition Zone until November.

Total specific conductivity was heavily influenced by river discharges. Figure 14 represents trends in whole lake specific conductivity over the study period. A comparison of figure 14 to discharge rates from the nearest gauging stations on the Red and Washita Rivers (Figures 16 and 17) shows good agreement with the IAS's predictions.

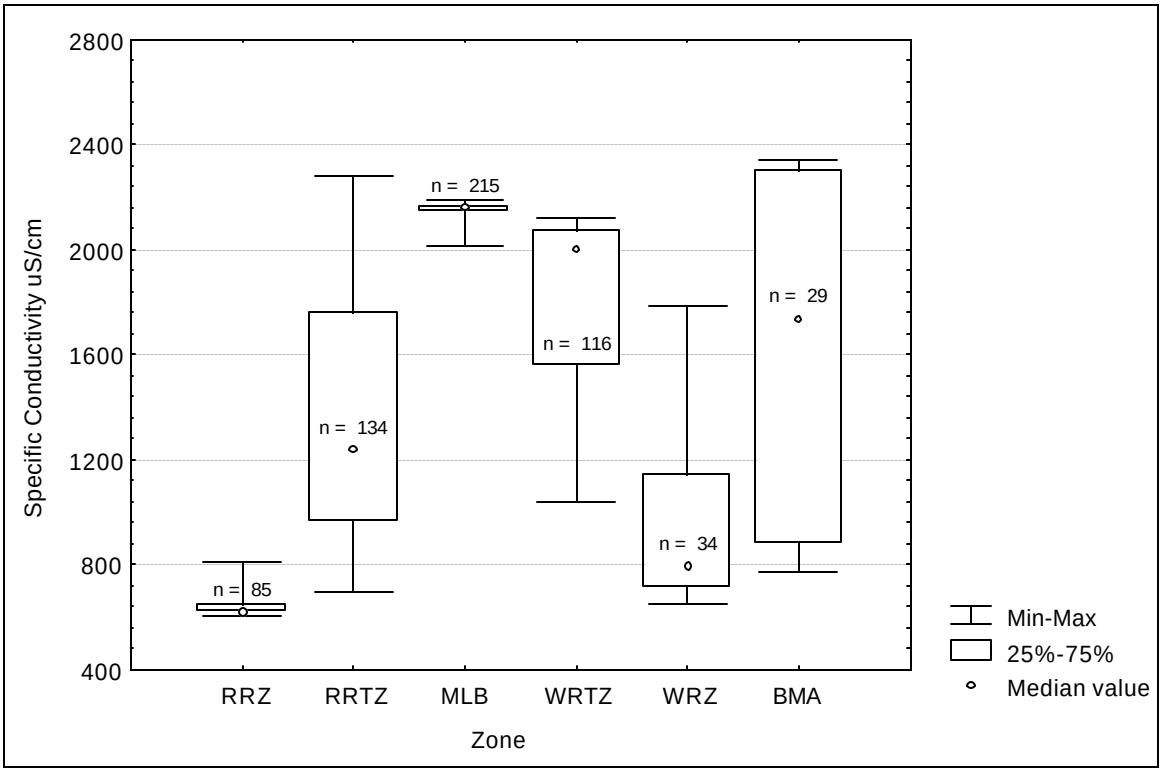

Figure 13. The five number summary of specific conductivity by zone at 1-meter for October 2000.

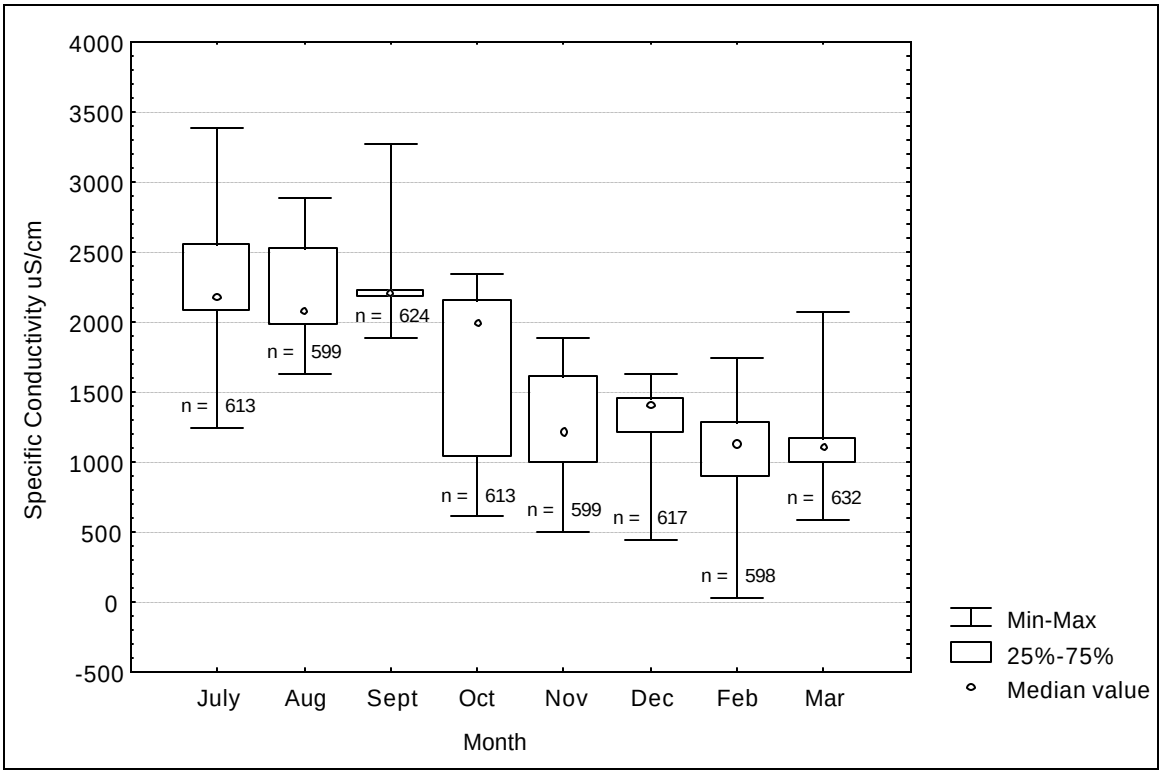

Figure 14. The five number summary of whole lake specific conductivity by month from July 2000 to March 2001 at 1-meter.

Results from Tukey's multiple comparison tests on the specific conductivity data are given in Table 9. All three months of the summer season show the zone ranking order described by Atkinson et al. (1999). The strong influence of the fall flushing event on zone rankings can be seen starting in October. The Red River Zone is reduced from first to last and then slowly returns to first by March. In addition, the delayed reaction of the Big Mineral Arm can be seen in the rankings. During the summer the Big Mineral Arm ranks second in specific conductivity. After the fall storms it slowly descends the ranks until it is eventually ranked last in March just as the other zones are recovering their "normal" summer positions.

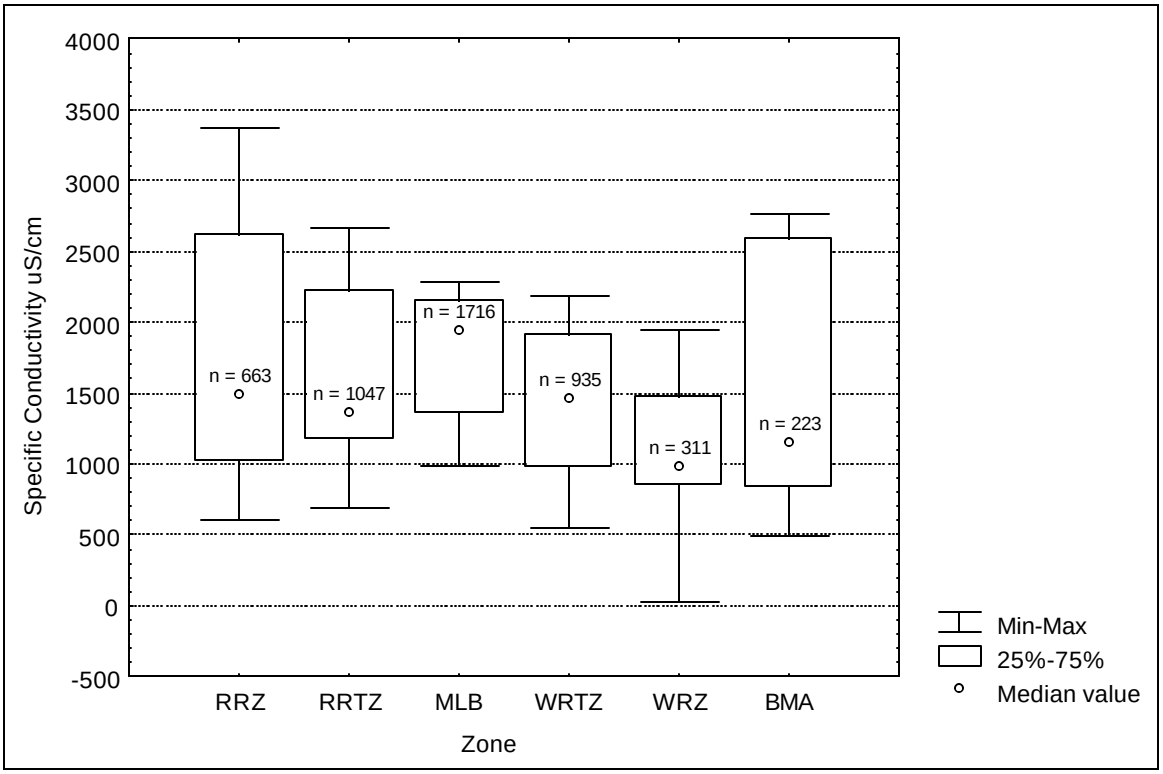

Figure 15. Five number summary of specific conductivity at 1-meter depth from July 2000 to March 2001 for the five zones delineated by the IAS study and the Big Mineral Arm.

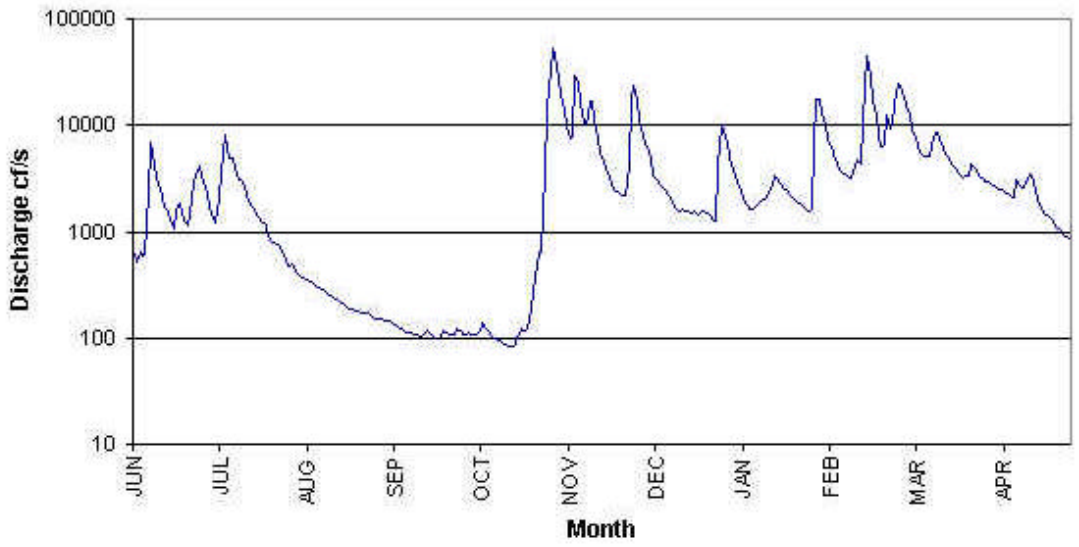

Figure 16. Discharge (cf/s) at the Red River gauging station (07316000) at I-35 near Gainsville, TX during the study period (July 2000 – March 2001).

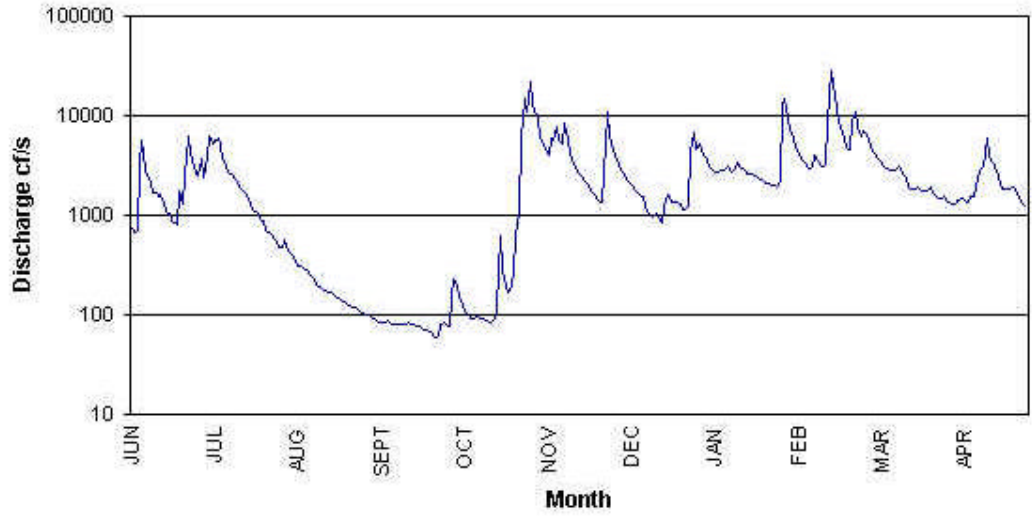

Figure 17. Discharge (cf/s) at the Washita River gauging station (07331000) near Dickson, OK covering the study period (July 2000 – March 2001).

Table 9. Tukey's multiple comparison ranks for specific conductivity at 1-meter. Zones followed by the same letter were not significantly different at an alpha level of 0.05. Statistically different classes are labeled in alphabetical order with class A representing the highest concentration and class E the lowest.

July	RRZ(A)	BMA(A)	RRTZ(B)	MLZ(C)	WRTZ(D)	WRZ(E)
August	RRZ(A)	BMA(A)	RRTZ(B)	MLZ(C)	WRTZ(D)	WRZ(E)
September	RRZ(A)	BMA(A)	RRTZ(B)	MLZ(C)	WRTZ(D)	WRZ(E)
October	MLZ(A)	BMA(B)	WRTZ(B)	RRTZ(C)	WRZ(D)	RRZ(E)
November	MLZ(A)	WRTZ(B)	RRTZ(B)	BMA(B)	RRZ(C)	WRZ(C)
December	MLZ(A)	RRZ(B)	RRTZ(C)	WRTZ(D)	BMA(E)	WRZ(E)
February	MLZ(A)	RRZ(B)	RRTZ(C)	WRTZ(D)	BMA(E)	WRZ(E)
March	RRZ(A)	RRTZ(B)	MLZ(C)	WRTZ(D)	WRZ(D)	BMA(D)
All Data	MLZ(A)	RRZ(B)	RRTZ(B)	BMA(B)	WRTZ(C)	WRZ(D)

3.5 Correlations and Regressions

Correlation analyses were performed to search for possible relationships between chlorophyll-*a*, turbidity, and specific conductivity. Correlation assumes no cause-and-effect relationship between two variables, but identifies situations where the magnitude of one variable changes as the magnitude of another changes (Zar, 1996). The strength of

the relationship is signified by the correlation coefficient (r). The correlation coefficient (r) ranges from -1 to 1 with a negative outcome implying that as one variable increases the other decreases. A positive outcome implies that as one variable increases the other also increases. The strength of the relationship increases as r approaches the extremes with 0 = no correlation, 1 = a perfect positive correlation, and –1 = a perfect negative correlation.

The non-normal nature of the data dictated the use of a non-parametric correlation test. Spearman's rank correlation test was chosen over Kendall's rank correlation because the former is better suited for larger data sets (Zar, 1996). The Spearman method has approximately 90% of the statistical power of the parametric Pearson's method (Beitinger, personal communication).

When statistically significant correlations were found regression analyses were performed. Regression assumes a functional dependence of one variable on the other; a cause-and effect relationship where the magnitude of one variable (termed the *dependent* variable) is a function of the magnitude of another (termed the *independent* variable) (Zar, 1996). The degree of dependence is signified by the coefficient of determination (R^2). The coefficient of determination differs from the correlation coefficient in that R^2 only ranges from 0 to 1. In addition, the value of R^2 expresses, on average, the amount of variation in the dependant variable that is accounted for by variation in the independent variable (Beitinger, personal communication). Chlorophyll-*a* was considered a dependent variable and was regressed against the independent variables turbidity and specific conductivity. Turbidity was also used as a dependant variable and regressed against

specific conductivity. Appendix C contains the results from all statistically significant regression models.

3.5.1 Specific Conductivity and Turbidity

Results from the correlation analyses between specific conductivity and turbidity are given in Figure 18. Differences between sections of Lake Texoma influenced by the Red River and those influenced by the Washita River were clearly evident. From July thru September the Red River arm displayed positive correlations between specific conductivity and turbidity while the Washita River arm showed a negative relationship.

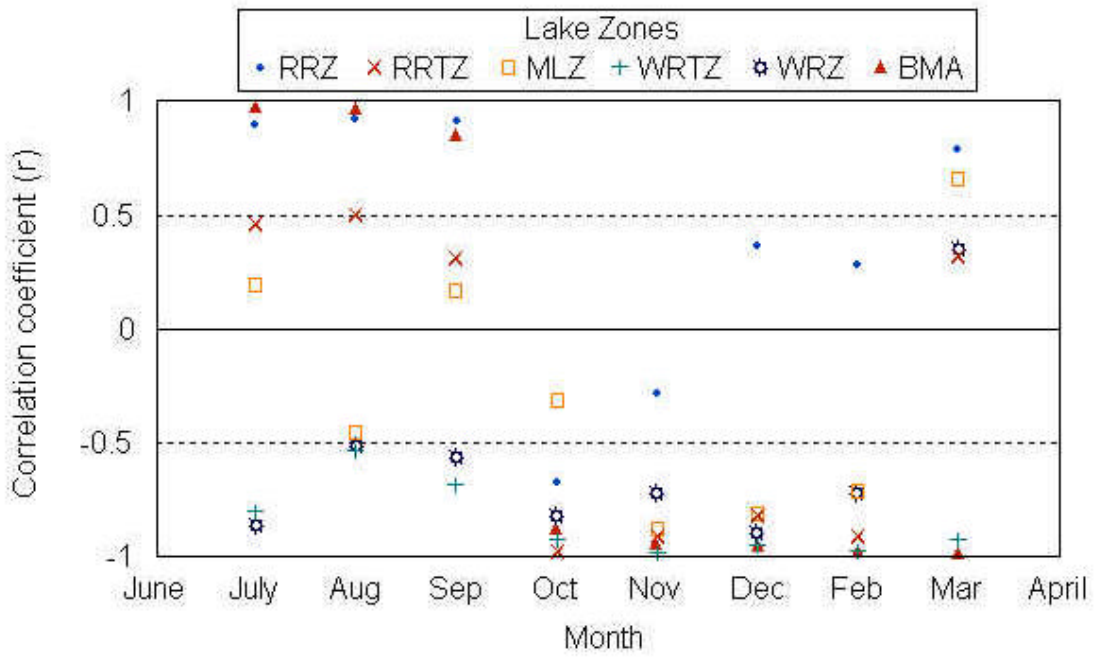

Figure 18. Correlation coefficients between specific conductivity and turbidity by zone from July 2000 to March 2001. Coefficients shown were significant at an Alpha level of 0.05.

The strength of the positive correlation in the Red River arm decreased as you moved down lake from the Red River Zone, but the Washita River arm showed no such change. The Main Lake Zone displayed a slight but statistically significant positive correlation during July and September and a stronger positive correlation later in March. Most of the year, however, specific conductivity and turbidity were negatively correlated in the Main Lake Zone.

The fall flushing event significantly altered the specific conductivity / turbidity pattern and produced strong negative correlations lake-wide in October and November. After November correlations were again positive in the Red River Zone, but the strength of the correlation was reduced. The Red River Transition Zone and the Main Lake Zone continued to display negative correlations between specific conductivity and turbidity until March.

The Washita River arm of the reservoir, with the exception of March, produced negative specific conductivity / turbidity correlations throughout the entire study. This negative association was relatively strong during the summer and became more so after the fall storms. The strength of the correlation was generally higher in the Washita River Transition Zone.

Regression analyses indicated a slight to moderate predictive relationship between specific conductivity and turbidity for all zones of the lake. However, when the analyses were separated by season the predictive ability was greatly reduced or eliminated completely for the summer season (July thru September) (Table 10). The ability of specific conductivity to predict turbidity was much stronger in the winter season (October

thru March) and even increased in the Red River Zone when summer data were removed from the analysis.

Table 10. Regression results for turbidity regressed on specific conductivity by zone and season, alpha level = 0.05. T = turbidity, SC = specific conductivity.

	RRZ	RRTZ	MLZ	WRTZ	WRZ	BMA	All
T/SC All Data	R^2 = 0.45, p<0.0001	R^2 = 0.45, p<0.0001	R^2 = 0.45, p<0.0001	R^2 = 0.54, p<0.0001	R^2 = 0.33, p<0.0001	R^2 = 0.64, p<0.0001	R^2 = 0.26, p<0.0001
T/SC (Summer)	R^2 = 0.05, p=0.0002	R^2 = 0.08, p<0.0001	R^2 = 0.18, p<0.0001	R^2 = 0.17, p<0.0001	Not Significant	Not Significant	R^2 = 0.05, p<0.0001
T/SC (Winter)	R^2 = 0.59, p<0.0001	R^2 = 0.36, p<0.0001	R^2 = 0.39, p<0.0001	R^2 = 0.47, p<0.0001	R^2 = 0.27, p<0.0001	R^2 = 0.49, p<0.0001	R^2 = 0.30, p<0.0001

3.5.2 Chlorophyll-*a* and Specific Conductivity

Correlation analyses between specific conductivity and chlorophyll-*a* produced some complex results (Figure 19). The zones in the Red River branch of the reservoir, including the Big Mineral Arm, generally displayed positive correlations between specific conductivity and chlorophyll-*a*, but only the Red River Zone produced positive correlations throughout the entire study. The Washita River branch tended to show negative correlations between specific conductivity and chlorophyll-*a*, but again, these were not consistent. The Washita River Transition Zone either displayed a negative association or no statistically significant correlation. The association between specific conductivity and chlorophyll-*a* was highly variable in the Washita River Zone and, over the course of the study, was positively correlated, negatively correlated, or not correlated.

Regressions of chlorophyll-*a* against specific conductivity produced results similar to the regressions of turbidity against specific conductivity. Strong predictive relationships were apparent in some zones, but disappeared when data were analyzed by

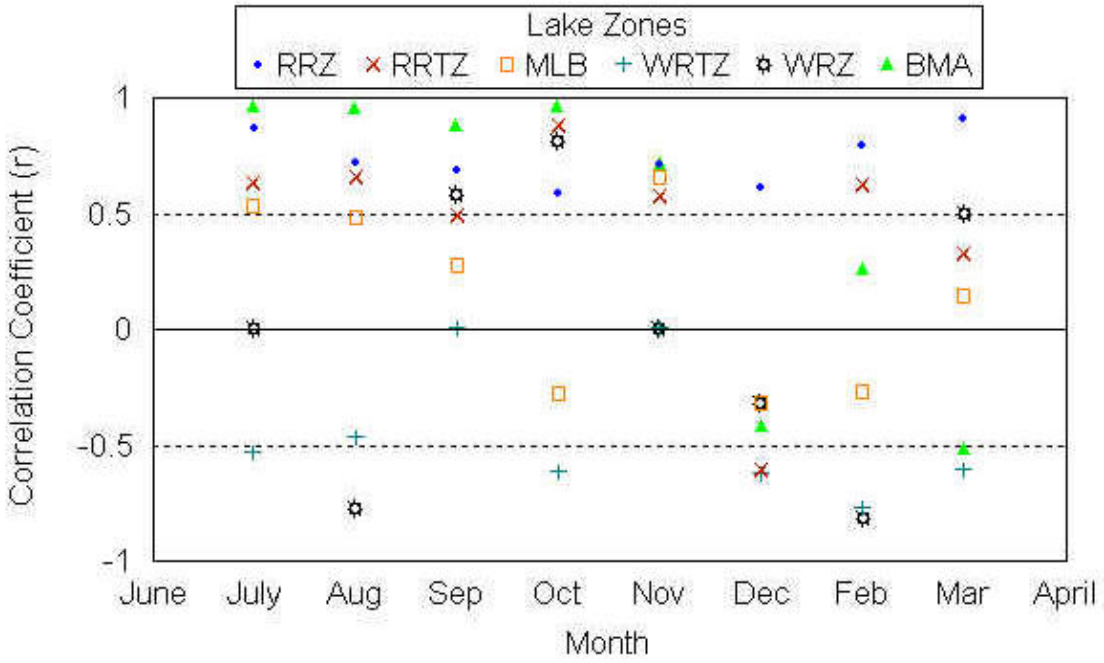

Figure 19. Correlation coefficients between specific conductivity and chlorophyll-*a* by zone from July 2000 to March 2001. Coefficients shown were significant at an Alpha level of 0.05.

Table 11. Regression results for chlorophyll-*a* regressed on specific conductivity by zone and season, alpha level = 0.05. Ch = chlorophyll-*a*, SC = specific conductivity.

	RRZ	RRTZ	MLZ	WRTZ	WRZ	BMA	All
Ch/SC All Data	R^2 = 0.90, p<0.0001	R^2 = 0.84, p<0.0001	R^2 = 0.43, p<0.0001	R^2 = 0.47, p<0.0001	R^2 = 0.70, p<0.0001	R^2 = 0.81, p<0.0001	R^2 = 0.57, p<0.0001
Ch/SC (Summer)	R^2 = 0.41, p<0.0001	R^2 = 0.18, p<0.0001	R^2 = 0.05, p<0.0001	Not Significant	R^2 = 0.06, p = 0.008	Not Significant	R^2 = 0.29, p<0.0001
Ch/SC (Winter)	R^2 = 0.69, p<0.0001	R^2 = 0.39, p<0.0001	R^2 = 0.14, p<0.0001	R^2 = 0.09, p<0.0001	R^2 = 0.08, p<0.0001	R^2 = 0.81, p<0.0001	R^2 = 0.09, p<0.0001

season (Table 11). The seasonal discrepancy in regressions between chlorophyll-*a* and specific conductivity were least in the Red River Zone where these parameters were positively correlated throughout the study. High R^2 values found when seasonal influences were not considered may be the result of seasonal changes and river discharge effects and do not necessarily indicate a significant biological relationship.

3.5.3 Chlorophyll-*a* and Turbidity

Turbidity and chlorophyll-*a* were positively correlated to varying degrees throughout much of the study (Figure 20). The Red River branch produced the clearest pattern; turbidity and chlorophyll-*a* were positively correlated there during the summer

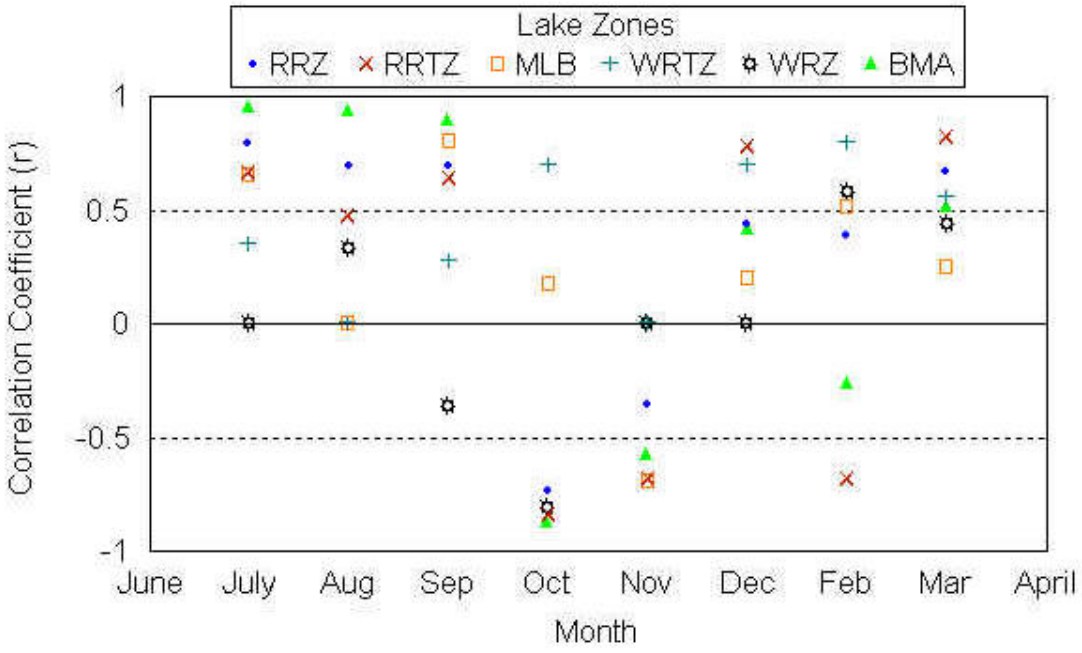

Figure 20. Correlation coefficients between turbidity and chlorophyll-*a* by zone from July 2000 to March 2001. Coefficients shown were significant at an Alpha level of 0.05.

when turbidity levels were relatively low and became negatively correlated in October when turbidity levels were very high. As turbidity decreased in November the strength of the negative correlation diminished and eventually became positive again in December. A subsequent increase in turbidity in February produced another negative correlation period in the Red River Transition Zone, but not in the Red River Zone.

The only zone that never saw a negative correlation between turbidity and chlorophyll-*a* was the Washita River Transition Zone. This zone showed either a positive correlation or no correlation. The no correlation results occurred both in the summer when turbidity was relatively low and in the fall when turbidity was higher.

Regression analyses of chlorophyll-*a* against turbidity showed only a very slight predictive relationship (Table 12). The one exception was the Big Mineral Arm, which displayed a moderate relationship. Contrary to the other regression results, the R^2 for the chlorophyll-*a*/turbidity regressions tended to be higher in the summer. This was especially true in the less dynamic zones of the Main Lake and the Big Mineral Arm. This pattern may indicate that the nutrients associated with turbidity help maintain the relatively high summer production rates in these less active areas. Large increases in turbidity that reduce light penetration in the river zones, because they translate to smaller increases down lake, may have little impact on Main Lake Zone production.

Table 12. Regression results for chlorophyll-*a* regressed on turbidity by zone and season, alpha level = 0.05. Ch = chlorophyll-*a*, T = turbidity.

	RRZ	RRTZ	MLZ	WRTZ	WRZ	BMA	All
Ch/T All Data	R^2 = 0.26, p<0.0001	R^2 = 0.21, p<0.0001	R^2 = 0.09, p<0.0001	R^2 = 0.16, p<0.0001	R^2 = 0.16, p<0.0001	R^2 = 0.40, p<0.0001	R^2 = 0.04, p<0.0001
Ch/T (Summer)	R^2 = 0.03, p=0.0092	R^2 = 0.37, p<0.0001	R^2 = 0.21, p<0.0001	R^2 = 0.02, p=0.0043	Not significant	R^2 = 0.65, p<0.0001	R^2 = 0.23, p<0.0001
Ch/T (Winter)	R^2 = 0.15, p<0.0001	Not Significant	Not significant	Not significant	Not significant	R^2 = 0.22, p<0.0001	Not significant

Multiple regression analyses of chlorophyll-*a* against turbidity and specific conductivity produced the best regression results (Table 13). However, the effects of seasonal influences were again apparent. The zones of the Red River arm produced the

strongest predictive models for chlorophyll-*a* with moderate R^2 values for the summer season.

Table 13. Regression results for chlorophyll-*a* regressed on specific conductivity and turbidity by zone and season, alpha level = 0.05. Ch = chlorophyll-*a*, SC = specific conductivity, T = turbidity.

	RRZ	RRTZ	MLZ	WRTZ	WRZ	BMA	All
Ch/SC&T All Data	R^2 = 0.94, p<0.0001	R^2 = 0.88, p<0.0001	R^2 = 0.46, p<0.0001	R^2 = 0.49, p<0.0001	R^2 = 0.71, p<0.0001	R^2 = 0.84, p<0.0001	R^2 = 0.61, p<0.0001
Ch/SC&T (Summer)	R^2 = 0.41, p<0.0001	R^2 = 0.44, p<0.0001	R^2 = 0.21, p<0.0001	R^2 = 0.05, p<0.0001	R^2 = 0.06, p=0.0295	R^2 = 0.66, p<0.0001	R^2 = 0.43, p<0.0001
Ch/SC&T (Winter)	R^2 = 0.83, p<0.0001	R^2 = 0.68, p<0.0001	R^2 = 0.19, p<0.0001	R^2 = 0.19, p<0.0001	R^2 = 0.14, p<0.0001	R^2 = 0.86, p<0.0001	R^2 = 0.14, p<0.0001

CHAPTER 4

DISCUSSION

4.1 Mapping system

The system proved to be an effective method for mapping the near surface distribution of chlorophyll-*a* and other physical and chemical parameters. Statistical results from the data collected with the mapping system mirrored the results from the Institute of Applied Sciences (IAS) study. Additionally, many fine details of variation and distribution that cannot be derived from stationary sampling schemes were apparent within the maps. This was especially true of stream arms and shallow littoral zones that were often dissimilar in character from the deeper water of the major lake zones.

Mapping also revealed clear patterns within the lake and the effects of a strong flushing event on parameter gradients (for example the turbidity maps for September and October). September shows a marked division down the middle of the Red River Transition Zone (Maps 1:8 and 2:11). This division marks an area of the lake that is split by a series of small islands. The main channel of the old Red River is located on the south side of these islands and is relatively deep and clear whereas the north side is relatively shallow and turbid. When comparing the September turbidity maps with the turbidity maps from October (Maps 1:11 and 2:12), one can see how the slug of turbid water introduced by the fall storm events overpowers this spatial division.

One important caveat concerning our mapping procedure must be considered: when analyzing chlorophyll *in situ* fluorescence from sources other than chlorophyll can be a problem. The chlorophyll probe is not selective – it will record the fluorescence of everything in the water that emits light in the 650 to 700 nm range when excited. Soluble fluorescence, fluorescence inherent in the water after algal bodies have been removed, can be a serious source of error with this technique. Carlson and Shapiro (1981) reviewed the problem of soluble fluorescence and investigated its effects on *in vivo* chlorophyll measurements in Minnesota lakes. They found a positive relationship between water color, thought to be derived from humic substances and soluble fluorescence. Soluble fluorescence contributed from 14 – 100% of the total fluorescence in the lakes they tested. In addition, they speculated that humic substances, while generally uniformly distributed in a lake, could display a heterogenic distribution when there is a rich influx of material.

A correction factor was applied to raw chlorophyll data to compensate for the fluorescence effects of suspended sediments before regression equations were developed. This correction was often vital to developing equations when samples came from highly turbid water. However, the adjustment factor suggested by Yellow Springs Instruments (YSI), (0.03 µg/L)turbidity, worked only until overall turbidity increased following the fall storms. After October the adjustment factor needed to be higher and was not consistent across the entire lake. These results were not unexpected since rainfall increases the influx of humic substances from land sources. Our adjustment factor may have been essentially a correction for soluble fluorescence. In the future it may be more

effective to develop an adjustment factor for each month based on soluable fluorescence as opposed to turbidity.

4.2 Spatial and Temporal Variability

The zonal differences described by Atkinson et al. (1999) and others were clearly present in our data when they were treated as zonal during statistical analysis. However, our method was clearly better suited at portraying gradients across the lake. The maps we developed showed gradients in turbidity, specific conductivity and summer chlorophyll-*a* at the 1-meter depth. Low flow gradients of turbidity and chlorophyll-*a* revealed decreasing concentrations from the river zones to the Main Lake Zone. The low flow specific conductivity gradient decreased from the Red River Zone to the Washita River Zone. The changing character of the gradients during storm events was also clearly evident in the maps. Specific conductivity and chlorophyll-*a* gradients at 1-meter were reversed in the Red River arm during large inflow events while the turbidity gradient was strengthened. In the Washita River arm both turbidity and specific conductivity gradients were strengthened, but the chlorophyll-*a* gradient was reversed. Gradient changes in turbidity and specific conductivity appear to be due to the large inputs of fresh sediment laden water. Whether the gradient reversals for chlorophyll-*a* represent biological changes or flushing of algae down lake is unknown.

We also demonstrated that the character of the Big Mineral Arm is distinct from the Red River Transition Zone. For lake management purposes the Big Mineral Arm should be regarded as a separate zone.

4.3 Specific Conductivity and Turbidity

When attempting to understand the interactions between specific conductivity, turbidity and chlorophyll-*a* in Lake Texoma, it is important to consider the characteristics of the individual lake zones. Steep unprotected banks and areas of shallow water are common in the river arms. Wave action, both natural and boat induced, works to re-suspend sediments in these zones. Additionally, the river arms are greatly affected by events in the catchment and are subject to large erosional inputs from the surrounding land and their respective rivers. As water moves from shallow, dynamic river zones to deeper water (e.g. Main Lake Zone) suspended sediments fall out and pronounced turbidity gradients are formed.

While turbidity and the physical mechanisms that cause it are similar between the Red and Washita River Arms, specific conductivity is quite different. The Red River is the primary source of chlorides and other dissolved solids contributing to Lake Texoma's salinity (Atkinson et al., 1999). Thus, at the base flow level the Red River Zone has both higher dissolved solids concentrations and higher specific conductivity than the Washita River Zone. Dilution decreases specific conductivity as water moves down lake from the Red River Zone to the Main Lake Zone. In the Washita River arm the situation is the opposite and specific conductivity actually increases as the dilute water of the Washita River Zone moves down lake and mixes with water influenced by the Red River.

The similarity between turbidity gradients in the river arms, coupled with the dissimilar characters of their respective specific conductivity gradients helps to explain the specific conductivity / turbidity correlation results. During summer months river

discharges were low (Figures 16 and 17) and turbidity and specific conductivity both showed declining gradients from the Red River Zone to the Main Lake Body. A series of transects progressing up lake from the Main Lake Zone to the Red River Zone would be expected to demonstrate positive correlations between specific conductivity and turbidity. In the Washita River arm turbidity showed a declining gradient from the Washita River Zone to the Main Lake Zone, but specific conductivity showed an increasing gradient. Thus transects in the Washita arm yielded negative correlations between specific conductivity and turbidity.

During the summer, transition zones displayed a specific conductivity / turbidity correlation status similar to their respective river zones, but only the Red River Transition Zone showed a clear decrease in correlation strength (Figure 18). Clearly, as one moves further away from the Red River Zone and towards the Main Lake Zone the positive association weakens. Eventually in the Main Lake Zone itself the association became very weakly positive or even negative, as was the case in August. No reduction in correlation strength was seen in the negative association in the Washita River arm suggesting that some mechanism in addition to dilution may be acting to reduce the positive specific conductivity / turbidity correlation in the Red River arm.

The storms in October and November brought copious amounts of fresh water to the Red River Basin and dramatically increased discharge from both rivers (Figures 16 and 17). Increased flow from the Red River produced a large increase in turbidity and a large decrease in specific conductivity in the Red River arm resulting in negative correlations as higher turbidity levels became linked to less saline water. The specific

conductivity / turbidity association in the Washita arm was reinforced and negative correlations became stronger during these storm events.

The effect of ionic strength on turbidity levels in the river zones is overshadowed by the dynamic nature of those environments and the many factors contributing to turbidity. Furthermore, effects in the Red River Transition Zone would also be difficult to discern due to large expanses of shallow water that may contribute to local turbidity. Deeper waters of the Main Lake Zone and the Washita River Transition Zone were relatively resistant to rapid catchment and / or re-suspension induced changes in their turbidity levels and should show the clearest evidence of the effects of ionic strength on turbidity.

During the summer specific conductivity / turbidity correlations in the Main Lake Zone were weakly positive in July and September and moderately negative in August (Figure 18). The swing from slightly positive to moderately negative took place in association with small increases in both chlorophyll-*a* and turbidity (Table 14). Although these increases were not great they may have been enough to change the association between specific conductivity and turbidity. When median turbidities began to increase after the fall storms the specific conductivity / turbidity association in the Main Lake Zone became strongly negative (Figure 18). This indicates that ionic strength may influence water clarity when turbidity is high and dominated by mineral turbidity.

Specific conductivity and turbidity were strongly negatively correlated in the Washita River Transition Zone throughout the entire study indicating that ionic strength may be an important factor influencing turbidity levels in this zone.

Table 14. Summary of chlorophyll-*a*, turbidity, and specific conductivity at 1-meter depth in the Main Lake Zone from July 2000 to September 2000.						
July	Min	Max	Median	Mean	SD	N
Chl-*a* µg/L	9.9	20.9	14.6	14.5	2.4	218
Turb NTU	2.4	6.7	3.4	3.6	0.9	218
SpCond µS/cm	1954	2286	2131	2144	60.0	218
August	Min	Max	Median	Mean	SD	N
Chl-*a* µg/L	8.7	27.3	16.8	17.0	3.5	210
Turb NTU	4.0	15.4	5.2	5.4	1.3	210
SpCond µS/cm	1937	2208	2059	2059	40.6	210
September	Min	Max	Median	Mean	SD	N
Chl-*a* µg/L	5.7	30.0	9.5	11.4	5.1	216
Turb NTU	2.3	10.3	4.0	4.0	1.1	216
SpCond µS/cm	2160	2222	2185	2190	11.7	216

Variations in specific conductivity explained little of the variation in turbidity during the summer (Table 10), but regression coefficients improved after the fall flush increased turbidity levels throughout the lake. These results support the hypothesis that ionic strength is more likely to be a factor in water clarity at high mineral turbidity levels.

4.4 Chlorophyll-*a* and Turbidity

The measurement of turbidity in water typically involves shining a light beam into a sample and measuring the amount of light scattered by suspended particles (YSI, 1999). Phytoplankton in the water column will scatter light as any other suspended particles and will constitute a component of turbidity measurements. Therefore, some degree of autocorrelation should be expected. The duel effect turbidity has on phytoplankton productivity further complicates the picture. On the one hand, suspended sediments provide nutrients for phytoplankton production (Persson, 1990). On the other hand, high turbidity can reduce light penetration and inhibit phytoplankton productivity (Torro et al.,

1996). Understanding how these effects interact to influence turbidity readings in a specific local is vital to understanding the correlation and regression associations found in this study.

Previous studies have characterized turbidity, total suspended solids (TSS), and light attenuation in Lake Texoma. Atkinson et al. (1999) found that turbidity explained 76% of the variation in light attenuation and 88% of the variation in Secchi depth. Chlorophyll-*a* concentration, however, was not correlated with either light attenuation or Secchi depth. They concluded that the lake exhibited substantial nonalgal turbidity, especially in the river arms. Rolbiecki (1998) reported strong correlations between TSS and turbidity in 4 out of 5 sampling stations. Station 17 near the dam, where water clarity is generally highest, had correlation coefficients of 0.66 between TSS and turbidity and 0.12 between chlorophyll-a and turbidity. This evidence suggests that algal bodies do not add substantially to turbidity readings in Lake Texoma and that positive correlations between turbidity and chlorophyll-*a* found in this study are only weakly influenced by autocorrelation.

The association between scouring rainfall events, high turbidity readings, and relatively low chlorophyll-*a* values suggests further evidence for this assumption. In the same vain, higher chlorophyll-*a* values were seen in the summer and were associated with lower turbidity. Also, parallel increases in chlorophyll-*a* and turbidity were seen in August (Table 14) resulting in a decreased correlation (Figure 20). Nevertheless, autocorrelation studies were not undertaken for these data and it should be considered a

factor in the high positive correlations found in some zones and in the summer regression R^2 values.

Factors influencing chlorophyll-*a* concentrations in Lake Texoma were examined by Gibbs (1998) and negative correlations between chlorophyll-*a* and turbidity in the Red River Transition Zone and the Washita River Zone were found. Additionally, turbidity and TSS were important variables in chlorophyll-*a* models developed for the Main Lake Zone ($R^2 = 0.37$) and the Red River Transition Zone ($R^2 = 0.77$). Her analyses were for the full 13-month study period and did not consider seasonal factors. In her conclusions she suggested that light attenuation might control phytoplankton production in the river arms, while nutrient limitations were suggested to dominate the Main Lake Zone. Atkinson et al. (1999) also suggested a negative association between chlorophyll-*a* and turbidity.

The findings of this study differ in that negative correlations were not observed between chlorophyll-*a* and turbidity until turbidity levels were elevated during increased river discharge events. This suggests that, with the possible exception of the Washita River Zone, light limitation may not be a dominant factor at the 1-meter depth during base flow conditions. The generally poor ability to predict chlorophyll-*a* from turbidity (Table 12) implies that other factors are controlling productivity at 1-meter. The one exception may be the Big Mineral Arm where turbidity explained 65% of the variation in summer chlorophyll-*a*. The Big Mineral Arm is dominated by relatively shallow water, is not fed by a large river system, and displays fairly stable turbidity during base flow with

an increasing trend moving up the arm (Maps 2:9, 2:10, and 2:11). Further research should examine this relationship to determine the extent of autocorrelation.

4.5 Chlorophyll-*a* and Specific Conductivity

A hypothesized association between ionic strength and chlorophyll-*a* rests on two assumptions: (1) productivity is a function of light transmission in at least some zones of the lake and (2) ionic strength increases particle coagulation and thus settling which in turn increases light penetration. If these assumptions are correct we would expect to see a positive association in the Red River branch where both turbidity and ionic strength are high.

This study did find positive correlations between chlorophyll-*a* and specific conductivity in the Red River branch. The strength of the correlations also tended to decrease as specific conductivity decreased. A notable exception was the Big Mineral Arm; in the summer months this zone had a median specific conductivity slightly lower than the Red River Zone, but the chlorophyll-*a* / specific conductivity association was much stronger.

It is important to note that the Red River Zone, the zone highest in both turbidity and specific conductivity, displayed positive correlations throughout the entire study. During the fall flushing event, associations between other parameters changed from positive to negative in the Red River Zone, but the chlorophyll-*a* / specific conductivity correlation remained positive. In addition, the Red River Transition Zone, which normally displayed a weaker correlation then the Red River Zone, showed a stronger

correlation during the fall flush. This may be considered evidence for the hypothesized association between ionic strength and light limitation. However, another interpretation is possible. The flushing event reverses the “normal” decreasing specific conductivity gradient and also moves algae laden water down lake. The character of the Red River arm then becomes one of increasing salinity and increasing chlorophyll-*a* as one moves down lake from the mouth of the Red River. This situation would also result in strong positive correlations between chlorophyll-*a* and specific conductivity in the Red River branch.

Interestingly, support for the association between ionic strength and turbidity may have come from the zone where it was least expected to apply. The Washita River Transition Zone consistently showed positive correlations between chlorophyll-*a* / turbidity and negative correlations between specific conductivity / turbidity and chlorophyll-*a* / specific conductivity. This may imply a nutrient limited situation where higher conductivity may help bind nutrients in the water column.

Regressions of chlorophyll-*a* on specific conductivity indicate that ionic strength may play an important role in the Red River arm of the reservoir (Table 11). The best models for predicting chlorophyll-*a* were created when both specific conductivity and turbidity were included in the model. In addition, the regression coefficients associated with these models improved in the winter season when turbidity was high. This is further evidence that ionic strength may be an important factor at high turbidity levels.

4.6 Conclusions

The primary objective of this study was to develop a system capable of rapid and continuous collection of water quality data on Lake Texoma. The system developed was capable of:

- Collecting data on several important water quality parameters including chlorophyll-*a*, turbidity, specific conductivity, temperature, pH, and dissolved oxygen concentration and percent saturation,
- Collecting simultaneous position data to facilitate mapping.
- Surveying the entire lake within a 4-day window.
- Collecting data with a density of one point every 330 to 400 meters at top speed. The systems data collection speed is limited by the Data Collection Platform's communications protocol. Reduced speeds will increase data density, but increase survey time.
- Portability.

A secondary objective for this project was to use the system to collect monthly water quality data on Lake Texoma for 1 year (12 months). This objective was not completely met since only 8 sampling trips were completed. Some trips experienced delays due to weather and the trip for January was canceled due to illness. Trips for the spring and summer of 2001, however, were canceled due to equipment problems. The communications protocol for YSI's 6200 Data Collection Platform was the primary

technical problem with the system. This problem was corrected, but not in time to complete the scheduled sampling trips.

The system was designed to facilitate mapping water quality parameters on lakes and thus one important objective of this study was to use the data collected during sampling trips to develop distribution maps for chlorophyll-*a*, turbidity, and specific conductivity. Two sets of maps were created for the 8 months sampled and are presented in Appendix A and Appendix B.

Assessing the performance of the system, its ability to detect patterns in the lake, and the accuracy of the maps created, was an integral part of this project. Data reported by the University of North Texas' Institute of Applied Sciences served as the basis for evaluating our data. No serious deviations from the IAS data were seen and specific similarities include:

- Overall lake zone chlorophyll-*a* rankings were similar to the IAS study and showed the same decreasing gradients from the river arms to the Main Lake Zone. System: RRZ > WRZ > RRTZ > WRTZ > MLZ
  IAS: RRZ > WRZ = WRTZ >RRTZ > MLZ
- Both studies found the RRZ generally had the highest chlorophyll-*a* concentration and the Main Lake Zone generally had the lowest.
- Overall lake zone turbidity rankings were similar to the IAS study and showed the same decreasing gradients from the river arms to the Main Lake Zone. System: RRZ > WRZ > RRTZ > WRTZ > MLZ.
  IAS: WRZ > RRZ > RRTZ > WRTZ > MLZ

- Summer lake zone specific conductivity rankings were the same as the IAS chloride rankings and showed the same decreasing gradient going from the Red River Zone to the Washita River Zone: RRZ > RRTZ > MLZ > WRTZ > WRZ
- Both studies noted that specific conductivity was heavily influenced by river discharges and during high discharge periods the Main Lake Zone became the zone of highest specific conductivity.

Some differences were noted between this study and the IAS report, specifically:

- We reported chlorophyll-*a* maximums that were lower then those reported in the IAS study. Percent differences between this study and the IAS report: RRZ -6%, RRTZ -25%, MLZ -40%, WRTZ -17%, WRZ -55%.
- We reported chlorophyll-*a* minimums much lower then those reported in the IAS study. Percent differences between this study and the IAS report: RRZ -85%, RRTZ -78%, MLZ -95%, WRTZ, -86%, WRZ -78%.
- We reported turbidity maximums much higher than those reported in the IAS study. Percent differences between this study and the IAS report: RRZ +81%, RRTZ +84%, MLZ +81%, WRTZ +80%, WRZ +75%.

Differences in turbidity maximums can be explained by our increased spatial sampling regime and our ability to sample in shallow areas where turbidity is often very high. The reduced chlorophyll-*a* statistics are not easily explained. The differences seen in the chlorophyll-*a* minimums may lie partially in the fact that much of our sampling

was conducted during low productivity periods in the fall and winter. However, the fact that data recorded during high productivity was markedly lower then what the IAS study found could indicate that our method underestimates actual chlorophyll-*a* concentrations, or that concentrations were in fact lower. Lower chlorophyll-*a* concentrations found in this study, if accurate, may indicate a reduction in productivity from the time of the IAS study performed in 1996 - 1997. Further refinement of the chlorophyll-*a* estimating techniques, including more rapid extraction and testing of grab samples, should increase the accuracy of chlorophyll-*a* estimates and resolve these questions.

The proposed chloride control projects and their possible effects on turbidity and productivity in Lake Texoma is the driving force behind this research thus an analysis of the spatial and temporal relationships between specific conductivity, turbidity, and chlorophyll-*a* was an important goal of this research. Patterns noted in this study include:

- Specific conductivity and turbidity show a positive association in the Red River branch of the reservoir during low discharge periods with a decreasing strength of correlation as you move down lake from the Red River Zone toward the Main Lake Zone (Figure 18).
- Specific conductivity and turbidity show a negative association in the Washita River branch of the reservoir during low discharge periods with no decreasing pattern (Figure 18).
- The association between specific conductivity and turbidity becomes negative across the entire lake during high discharge periods after large storm events (Figure 18).

- Specific conductivity and chlorophyll-*a* in the Red River branch generally show a positive association with decreasing strength of correlation as you move down lake from the Red River Zone toward the Main Lake Zone (Figure 19).
- The Washita River Transition Zone generally shows a negative association between specific conductivity and chlorophyll-*a* (Figure 19).
- Most zones of the lake show positive associations between chlorophyll-*a* and turbidity during low discharge periods and negative associations during high discharge (Figure 20).
- The Big Mineral Arm acts as a distinct zone and is usually very different in character from the Red River Transition Zone.
- Specific conductivity and turbidity may be important predictors of chlorophyll-*a* in the Red River Zones and the Big Mineral Arm especially at high turbidity levels (Table 13).

4.7 Future Research

Although our chlorophyll-*a* maps correlated well with the general IAS study results, a degree of uncertainty exists in the chlorophyll-*a* estimates. Future work should focus on refining the chlorophyll-*a* estimates. More specifically, the factors effecting the conversion of YSI estimates to more accurate chlorophyll-*a* levels need to be investigated thoroughly. The percentage of YSI chlorophyll-*a* estimates that can be attributed to soluble fluorescence and or other fluorescing compounds needs to be quantified under

various conditions. Likewise, the degree of uncertainty within the extrapolation process used to create the final maps should be explored. We suggest that future studies with the system include random grab samples off transect in areas that will be interpolated during the mapping process. Chlorophyll-*a* extracts from these samples can be compared to the final extrapolation values to develop a measure of uncertainty for the mapping process.

APPENDIX A
MAP SET 1

Distribution Maps for Chlorophyll-*a*, Turbidity, and Specific Conductivity on Lake Texoma from July 2000 to March 2001

This map set was designed to show maximum detail for the individual month using 10 categories per month.

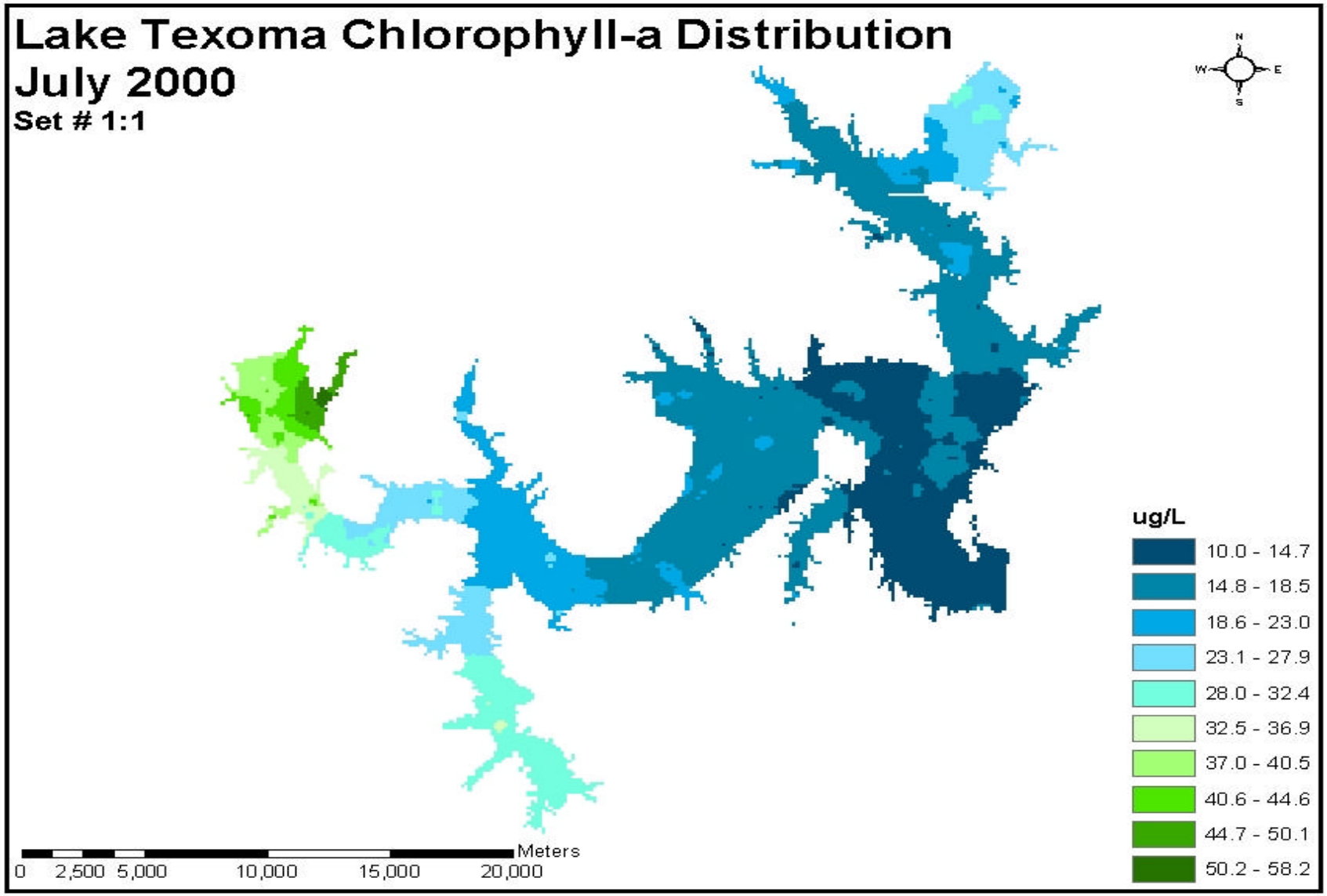
Lake Texoma Chlorophyll-a Distribution
July 2000
Set # 1:1
N
W
E
S
ug/L
10.0 - 14.7
14.8 - 18.5
18.6 - 23.0
23.1 - 27.9
28.0 - 32.4
32.5 - 36.9
37.0 - 40.5
40.6 - 44.6
44.7 - 50.1
50.2 - 58.2
Meters
0
2,500
5,000
10,000
15,000
20,000

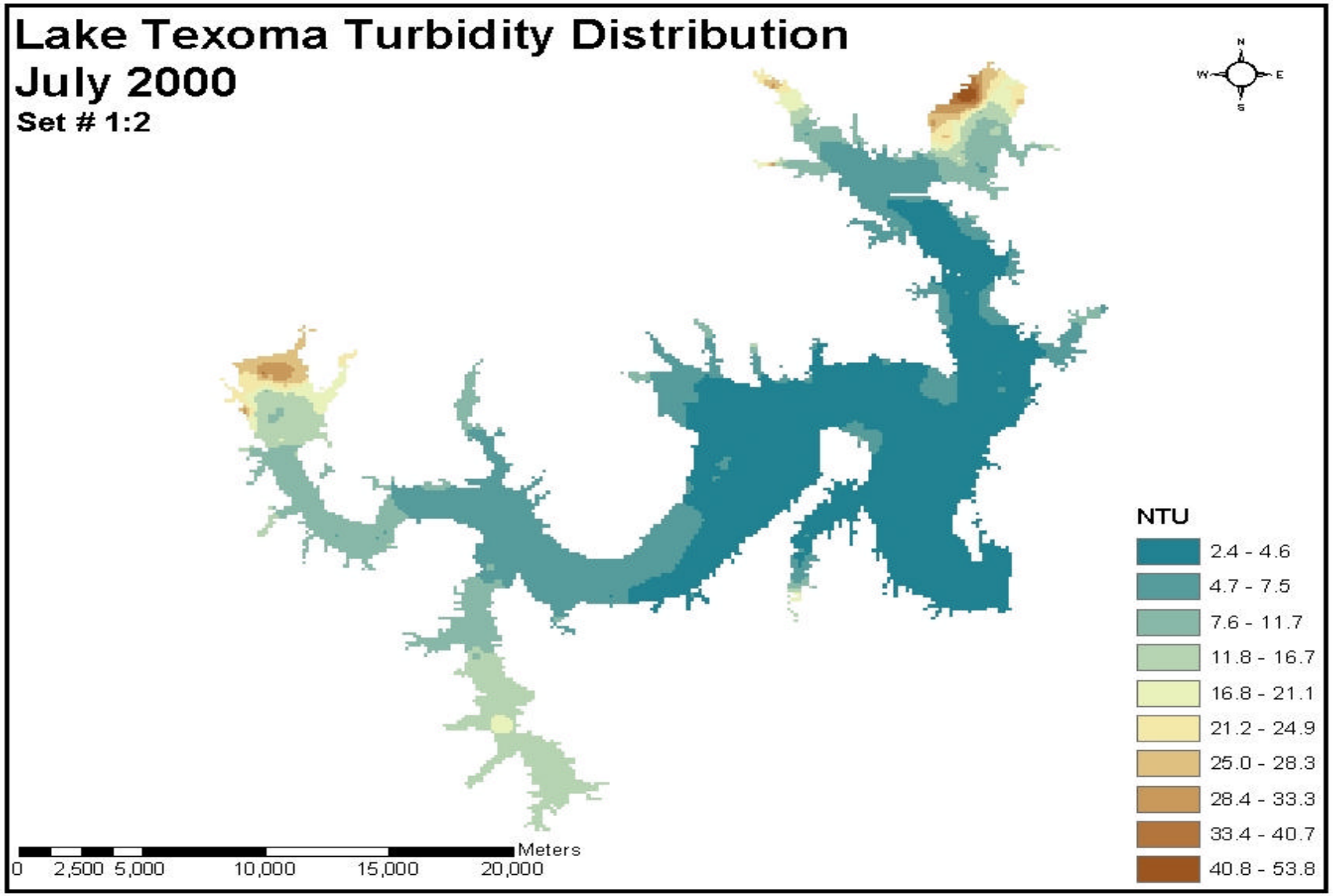
Lake Texoma Turbidity Distribution
July 2000
Set # 1:2
N
W
E
S
NTU
2.4 - 4.6
4.7 - 7.5
7.6 - 11.7
11.8 - 16.7
16.8 - 21.1
21.2 - 24.9
25.0 - 28.3
28.4 - 33.3
33.4 - 40.7
40.8 - 53.8
Meters
0
2,500
5,000
10,000
15,000
20,000

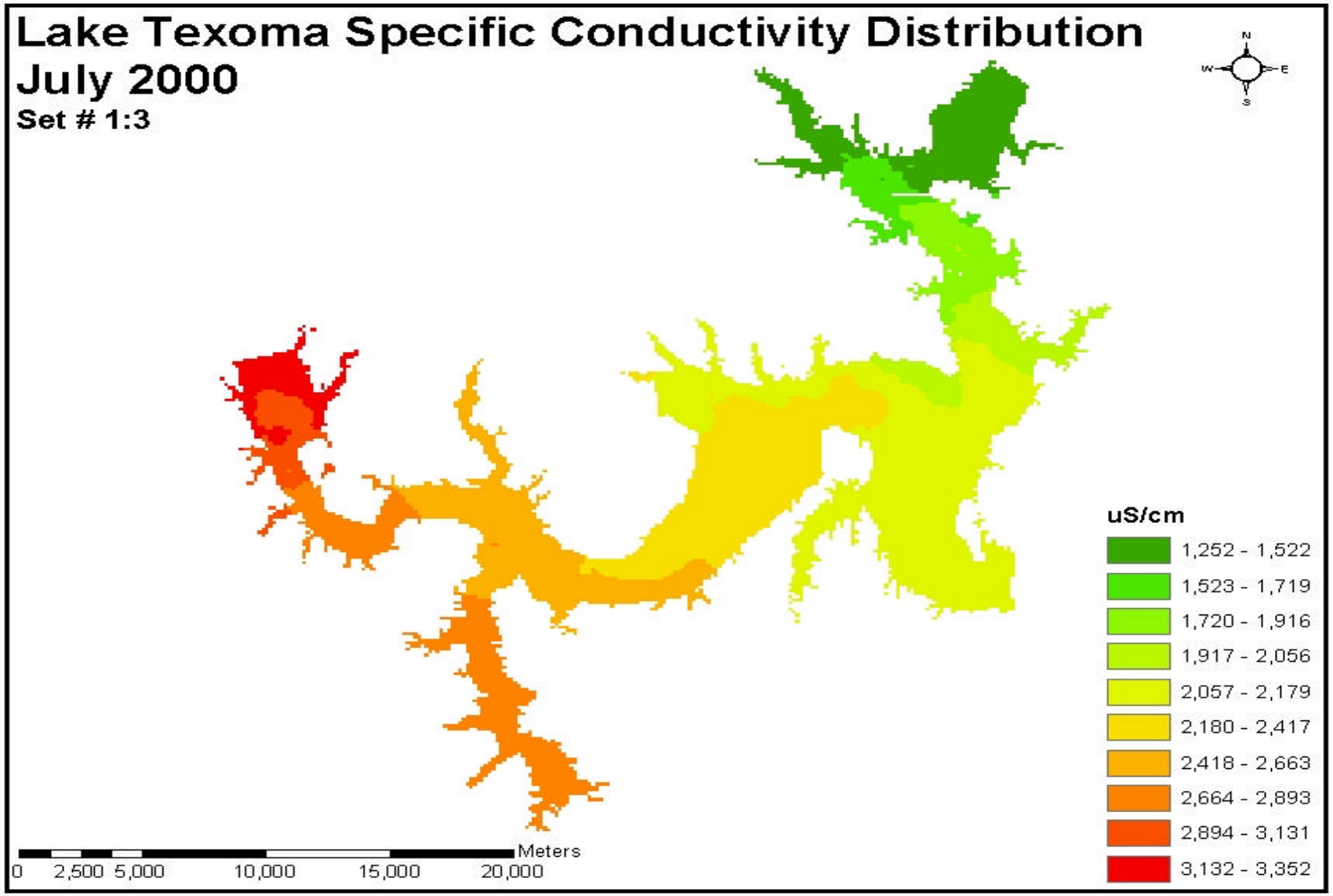
Lake Texoma Specific Conductivity Distribution
July 2000
Set # 1:3
N
W
E
S
uS/cm
1,252 - 1,522
1,523 - 1,719
1,720 - 1,916
1,917 - 2,056
2,057 - 2,179
2,180 - 2,417
2,418 - 2,663
2,664 - 2,893
2,894 - 3,131
3,132 - 3,352
Meters
0 2,500 5,000 10,000 15,000 20,000

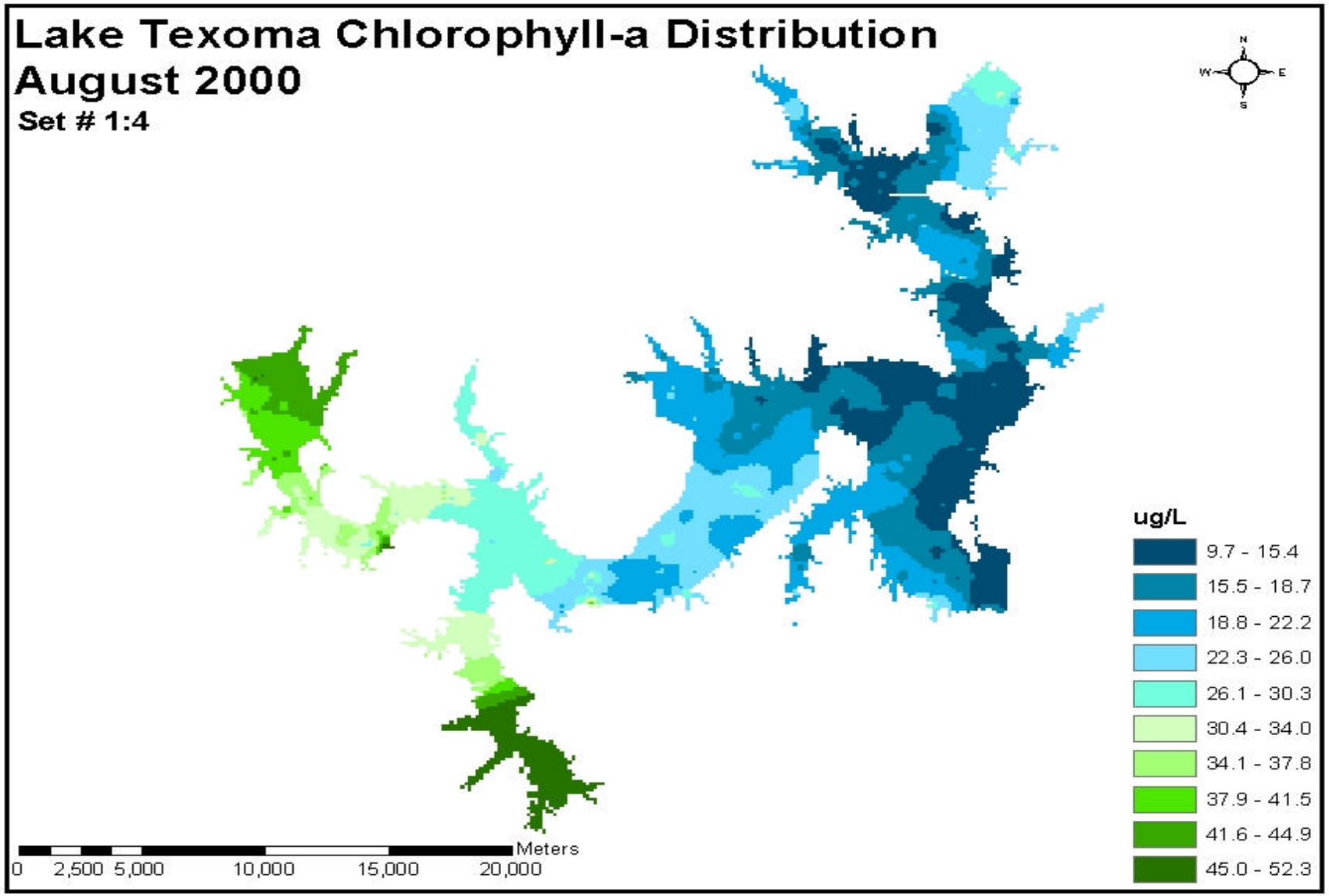
Lake Texoma Chlorophyll-a Distribution
August 2000
Set # 1:4
N
W
E
S
ug/L
9.7 - 15.4
15.5 - 18.7
18.8 - 22.2
22.3 - 26.0
26.1 - 30.3
30.4 - 34.0
34.1 - 37.8
37.9 - 41.5
41.6 - 44.9
45.0 - 52.3
Meters
0
2,500
5,000
10,000
15,000
20,000

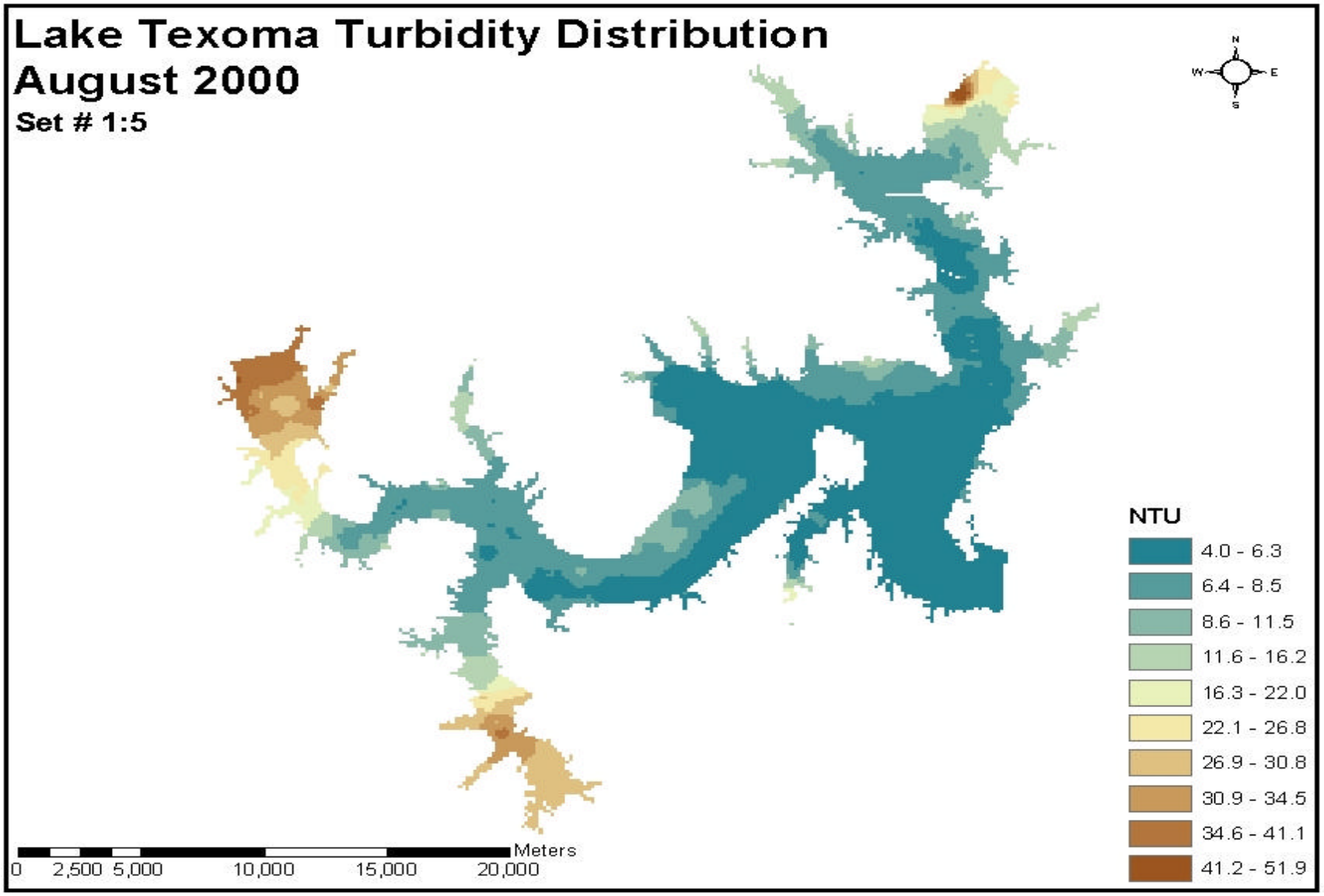
Lake Texoma Turbidity Distribution
August 2000
Set # 1:5
N
W
E
S
NTU
4.0 - 6.3
6.4 - 8.5
8.6 - 11.5
11.6 - 16.2
16.3 - 22.0
22.1 - 26.8
26.9 - 30.8
30.9 - 34.5
34.6 - 41.1
41.2 - 51.9
Meters
0 2,500 5,000 10,000 15,000 20,000

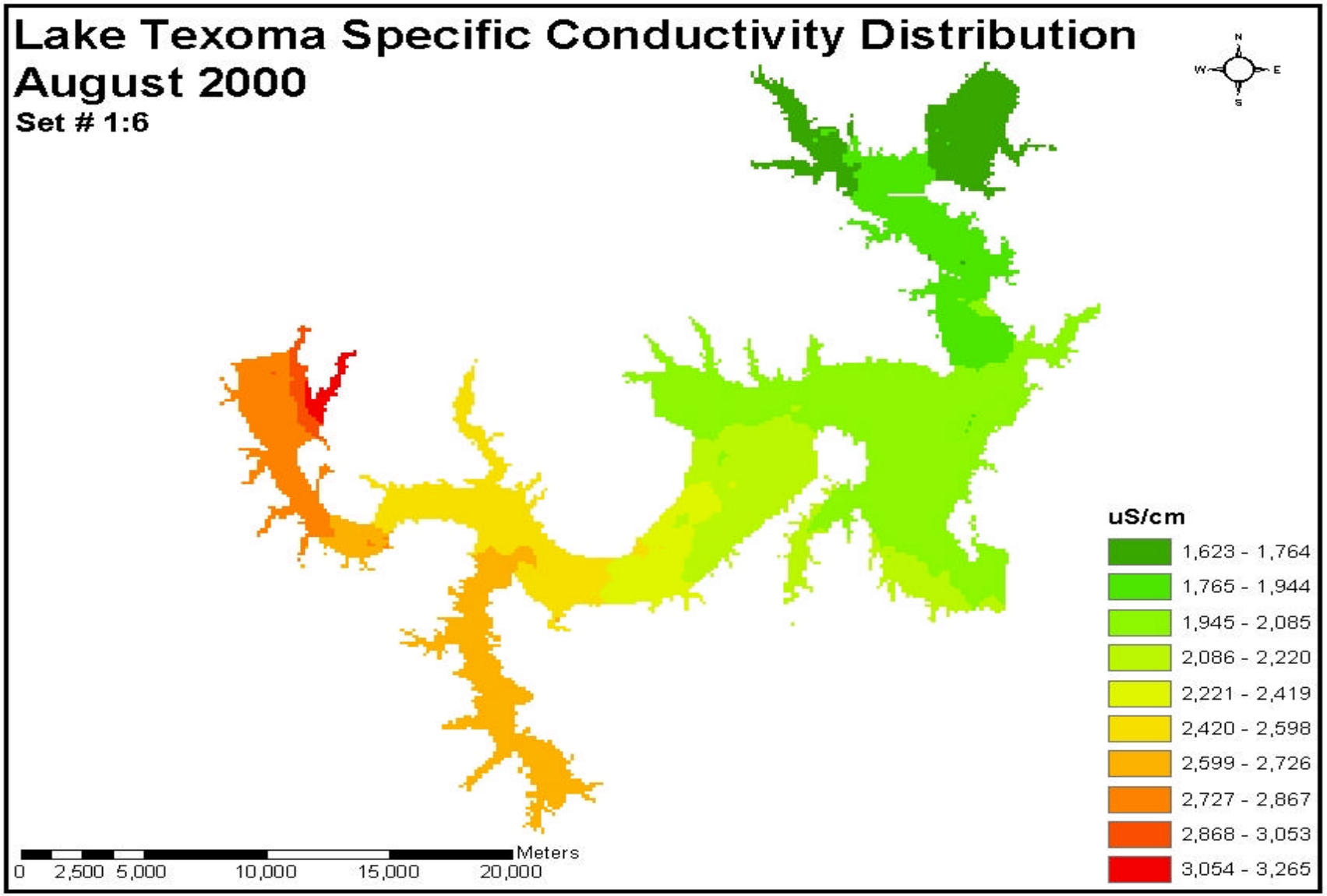
Lake Texoma Specific Conductivity Distribution
August 2000
Set # 1:6
N
W
E
S
uS/cm
1,623 - 1,764
1,765 - 1,944
1,945 - 2,085
2,086 - 2,220
2,221 - 2,419
2,420 - 2,598
2,599 - 2,726
2,727 - 2,867
2,868 - 3,053
3,054 - 3,265
Meters
0 2,500 5,000 10,000 15,000 20,000

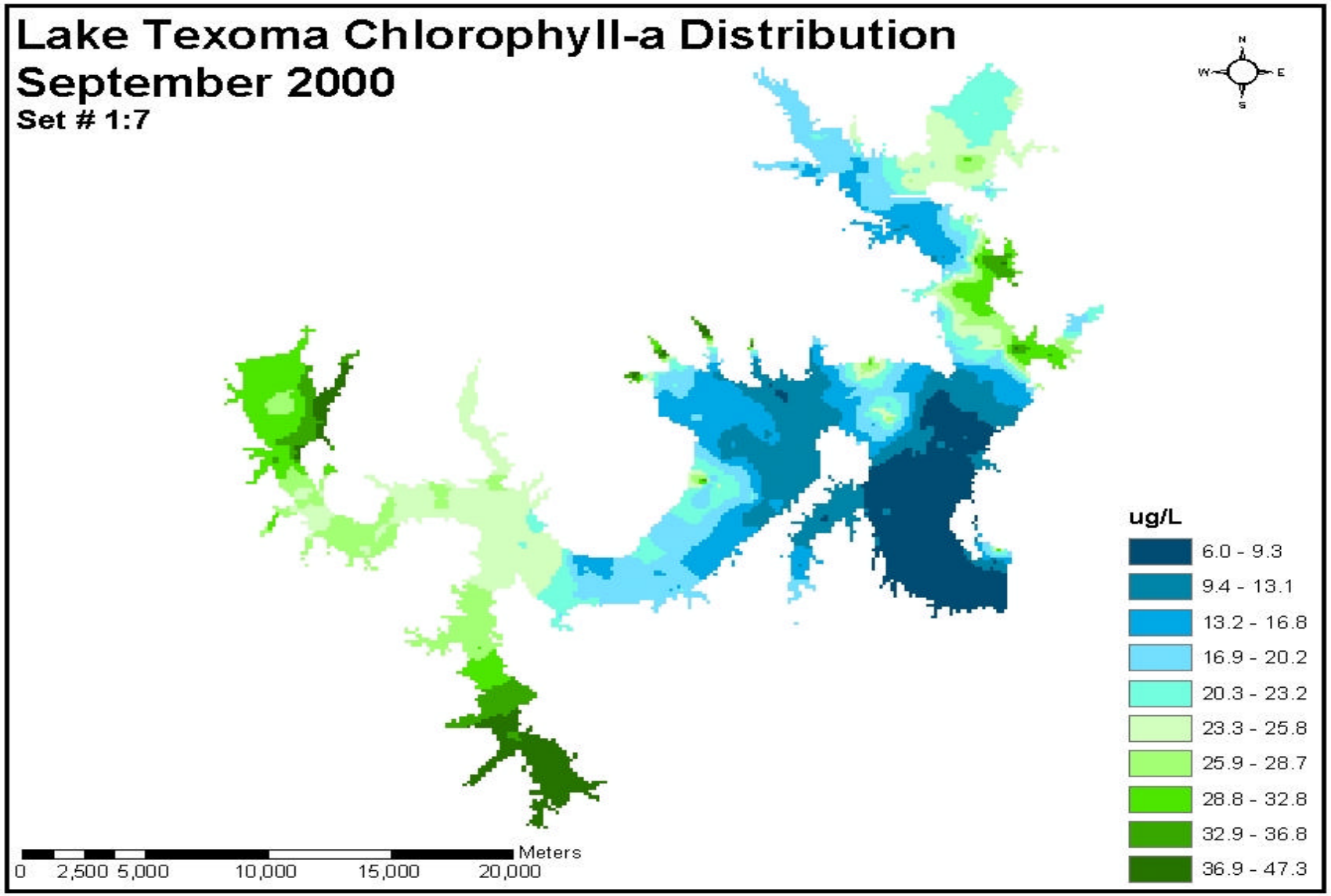
Lake Texoma Chlorophyll-a Distribution
September 2000
Set # 1:7
N
W
E
S
ug/L
6.0 - 9.3
9.4 - 13.1
13.2 - 16.8
16.9 - 20.2
20.3 - 23.2
23.3 - 25.8
25.9 - 28.7
28.8 - 32.8
32.9 - 36.8
36.9 - 47.3
Meters
0 2,500 5,000 10,000 15,000 20,000

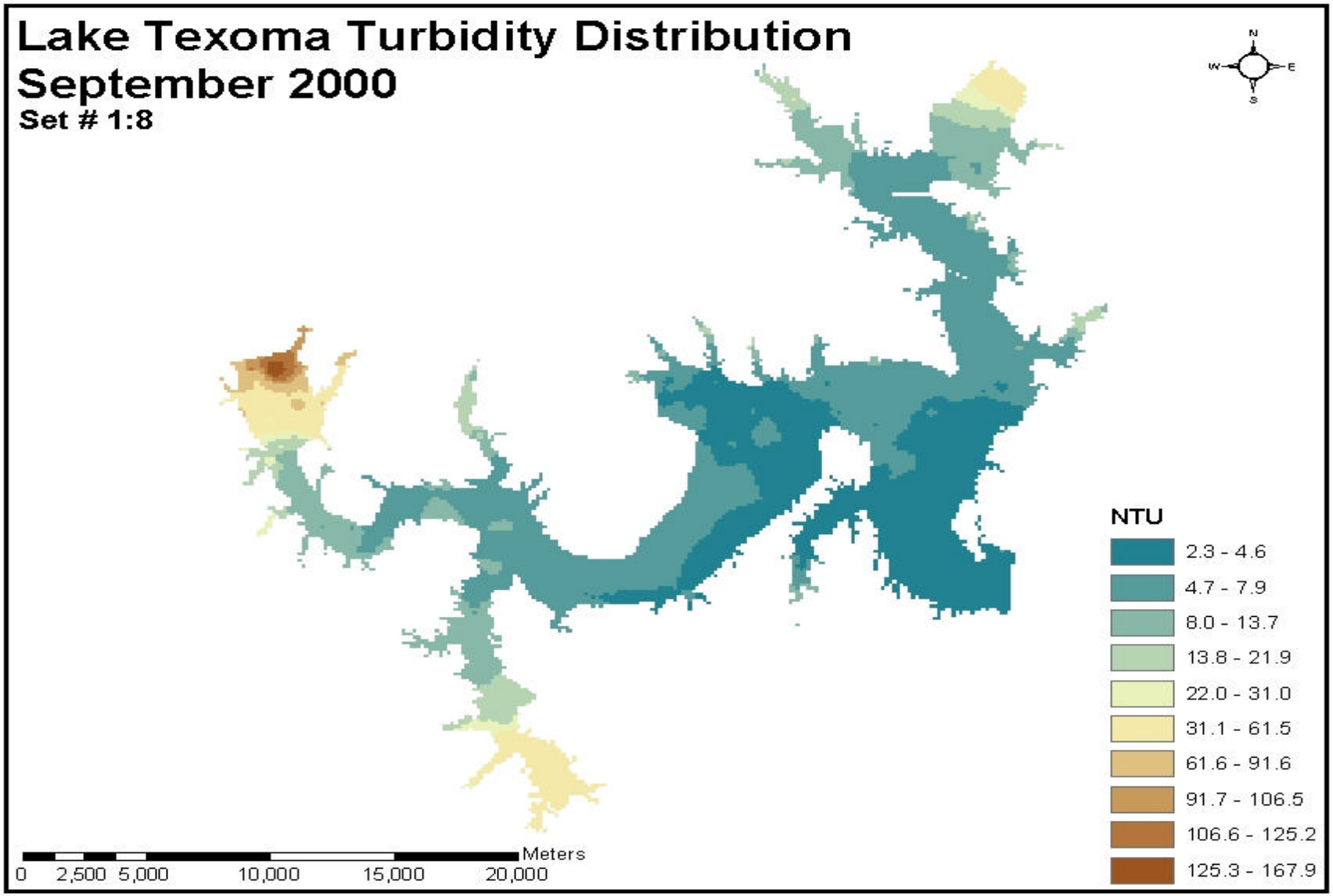
Lake Texoma Turbidity Distribution
September 2000
Set # 1:8
N
W
E
S
NTU
2.3 - 4.6
4.7 - 7.9
8.0 - 13.7
13.8 - 21.9
22.0 - 31.0
31.1 - 61.5
61.6 - 91.6
91.7 - 106.5
106.6 - 125.2
125.3 - 167.9
Meters
0 2,500 5,000 10,000 15,000 20,000

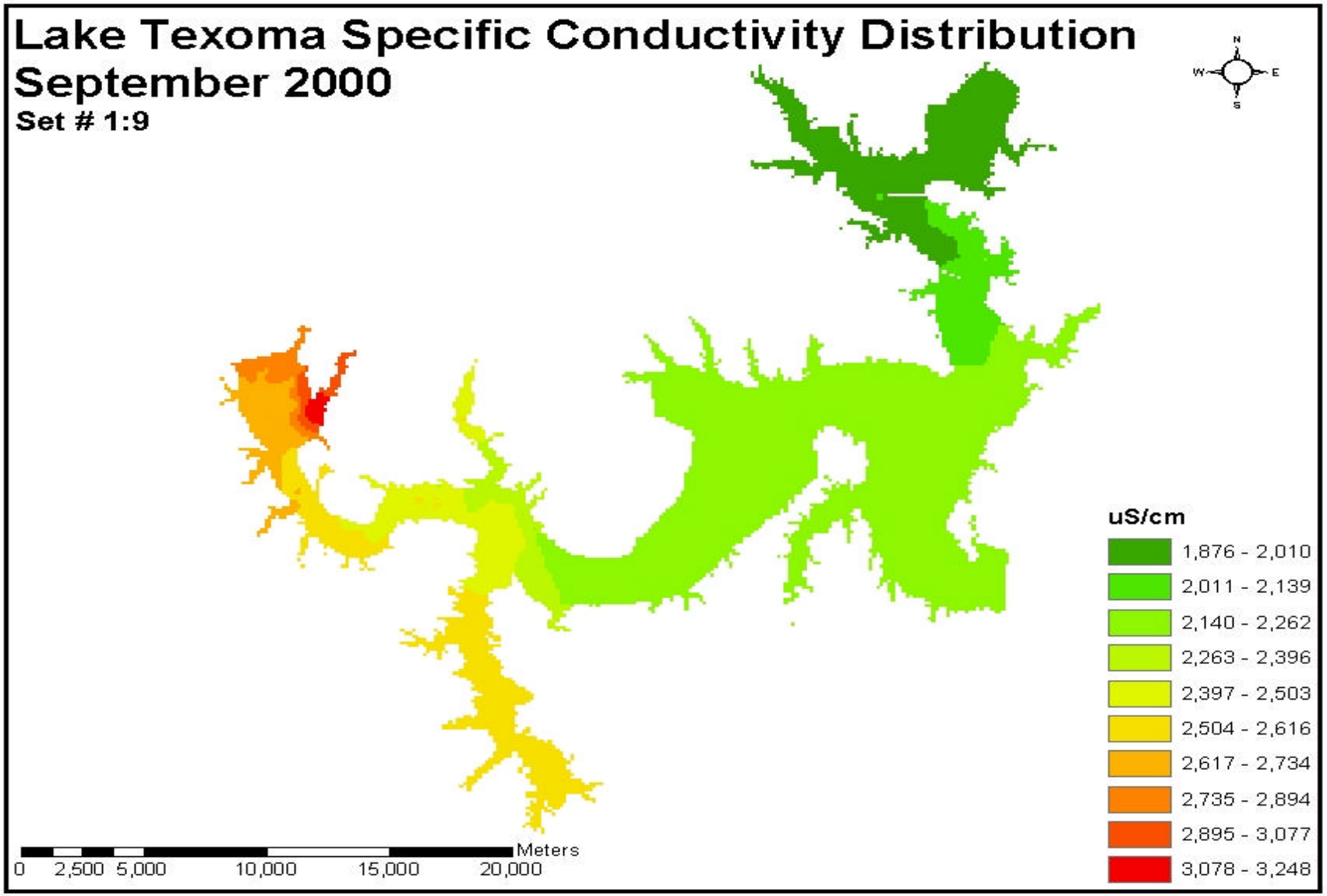
Lake Texoma Specific Conductivity Distribution
September 2000
Set # 1:9
N
W
E
S
uS/cm
1,876 - 2,010
2,011 - 2,139
2,140 - 2,262
2,263 - 2,396
2,397 - 2,503
2,504 - 2,616
2,617 - 2,734
2,735 - 2,894
2,895 - 3,077
3,078 - 3,248
0 2,500 5,000 10,000 15,000 20,000
Meters

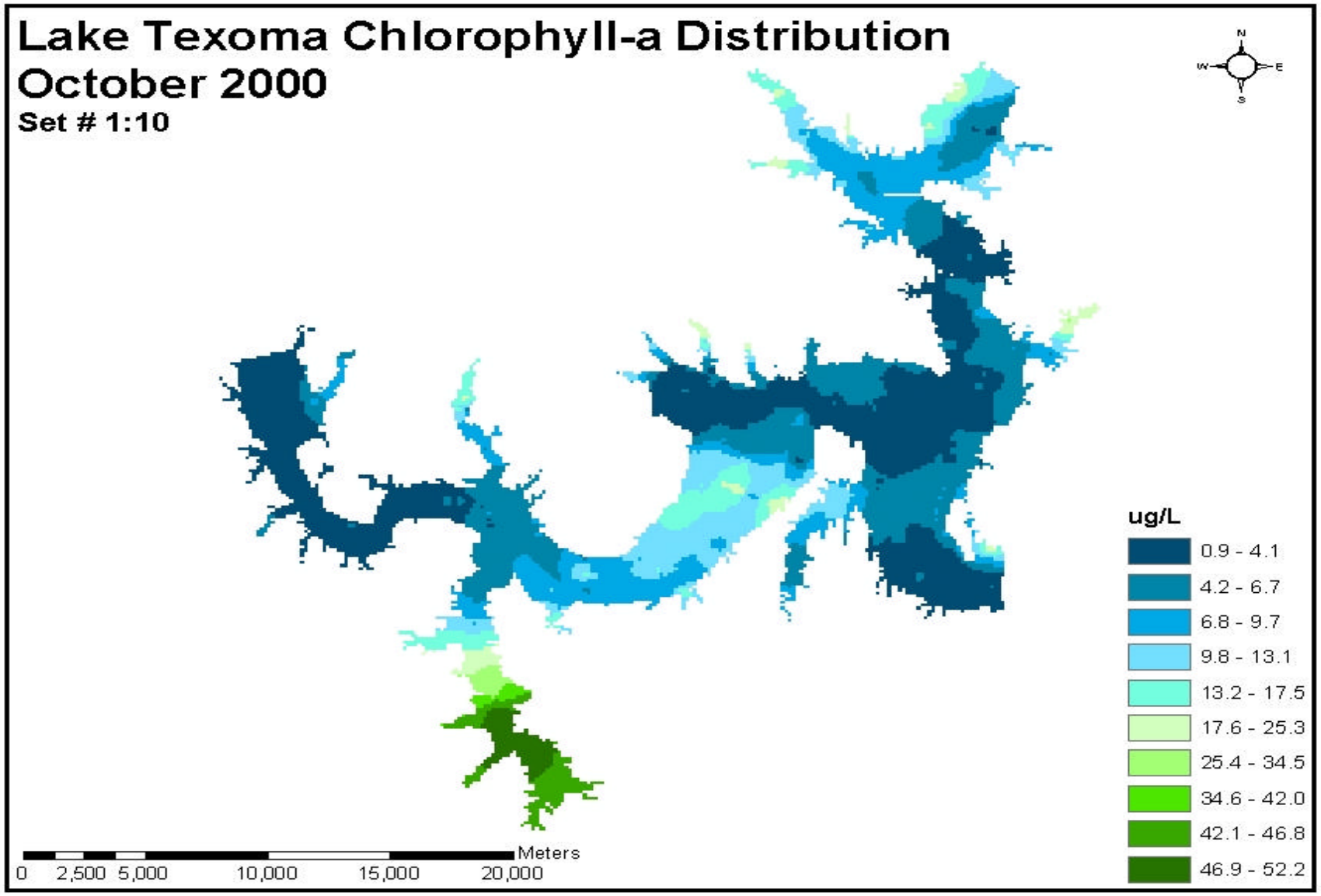
Lake Texoma Chlorophyll-a Distribution
October 2000
Set # 1:10
N
W
E
S
ug/L
0.9 - 4.1
4.2 - 6.7
6.8 - 9.7
9.8 - 13.1
13.2 - 17.5
17.6 - 25.3
25.4 - 34.5
34.6 - 42.0
42.1 - 46.8
46.9 - 52.2
Meters
0 2,500 5,000 10,000 15,000 20,000

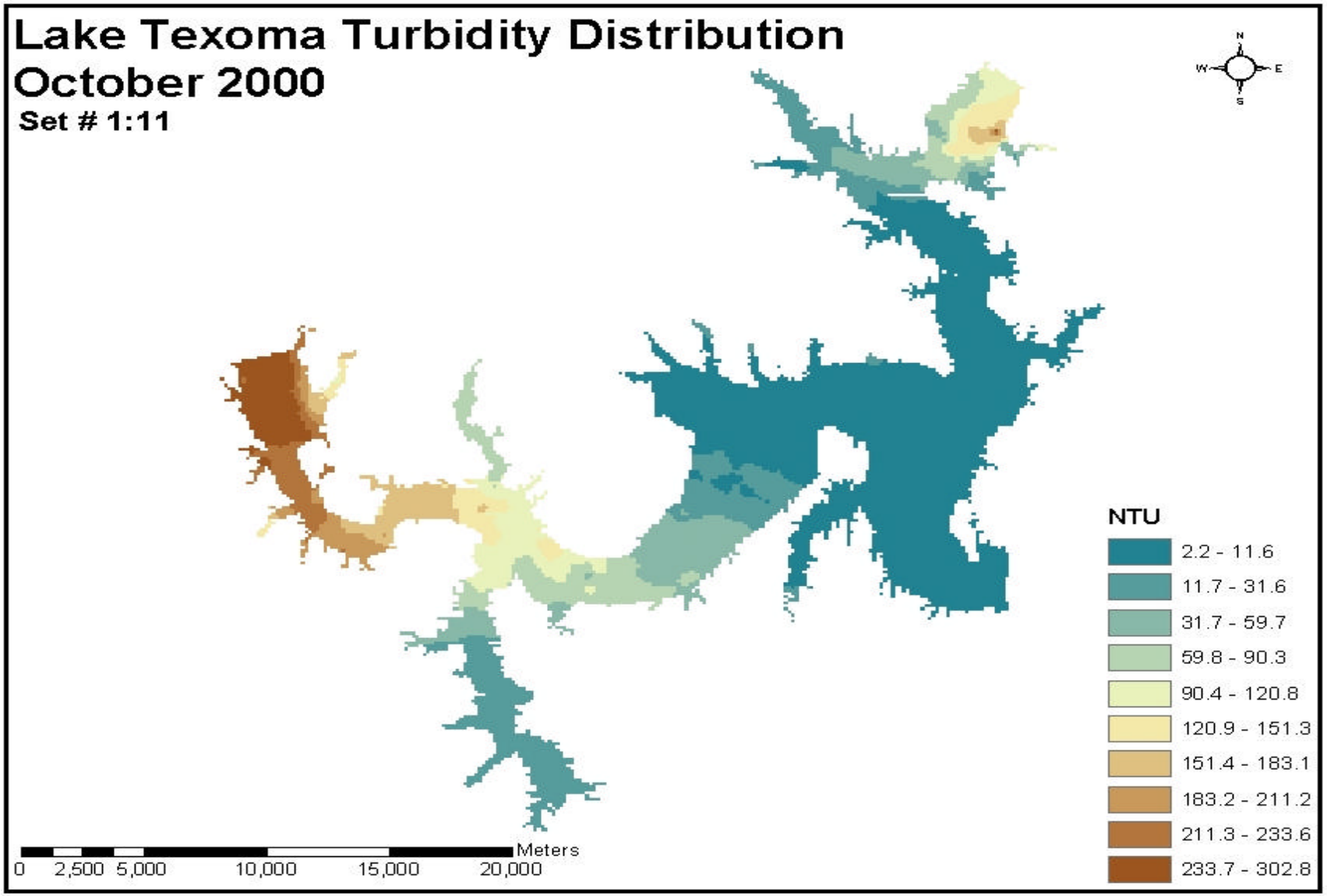
Lake Texoma Turbidity Distribution
October 2000
Set # 1:11
N
W
E
S
NTU
2.2 - 11.6
11.7 - 31.6
31.7 - 59.7
59.8 - 90.3
90.4 - 120.8
120.9 - 151.3
151.4 - 183.1
183.2 - 211.2
211.3 - 233.6
233.7 - 302.8
Meters
0 2,500 5,000 10,000 15,000 20,000

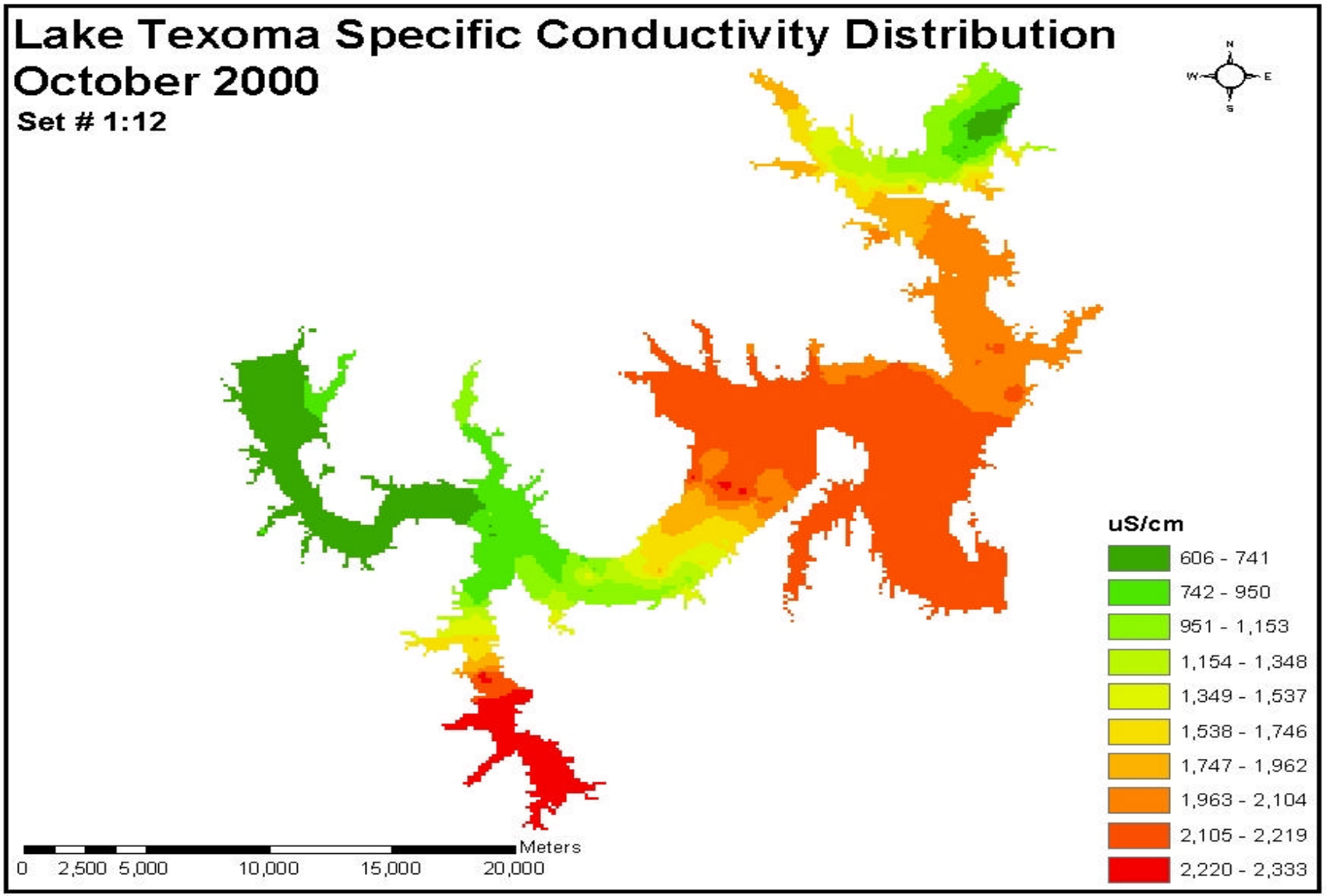
Lake Texoma Specific Conductivity Distribution
October 2000
Set # 1:12
N
W
E
S
uS/cm
606 - 741
742 - 950
951 - 1,153
1,154 - 1,348
1,349 - 1,537
1,538 - 1,746
1,747 - 1,962
1,963 - 2,104
2,105 - 2,219
2,220 - 2,333
Meters
0
2,500
5,000
10,000
15,000
20,000

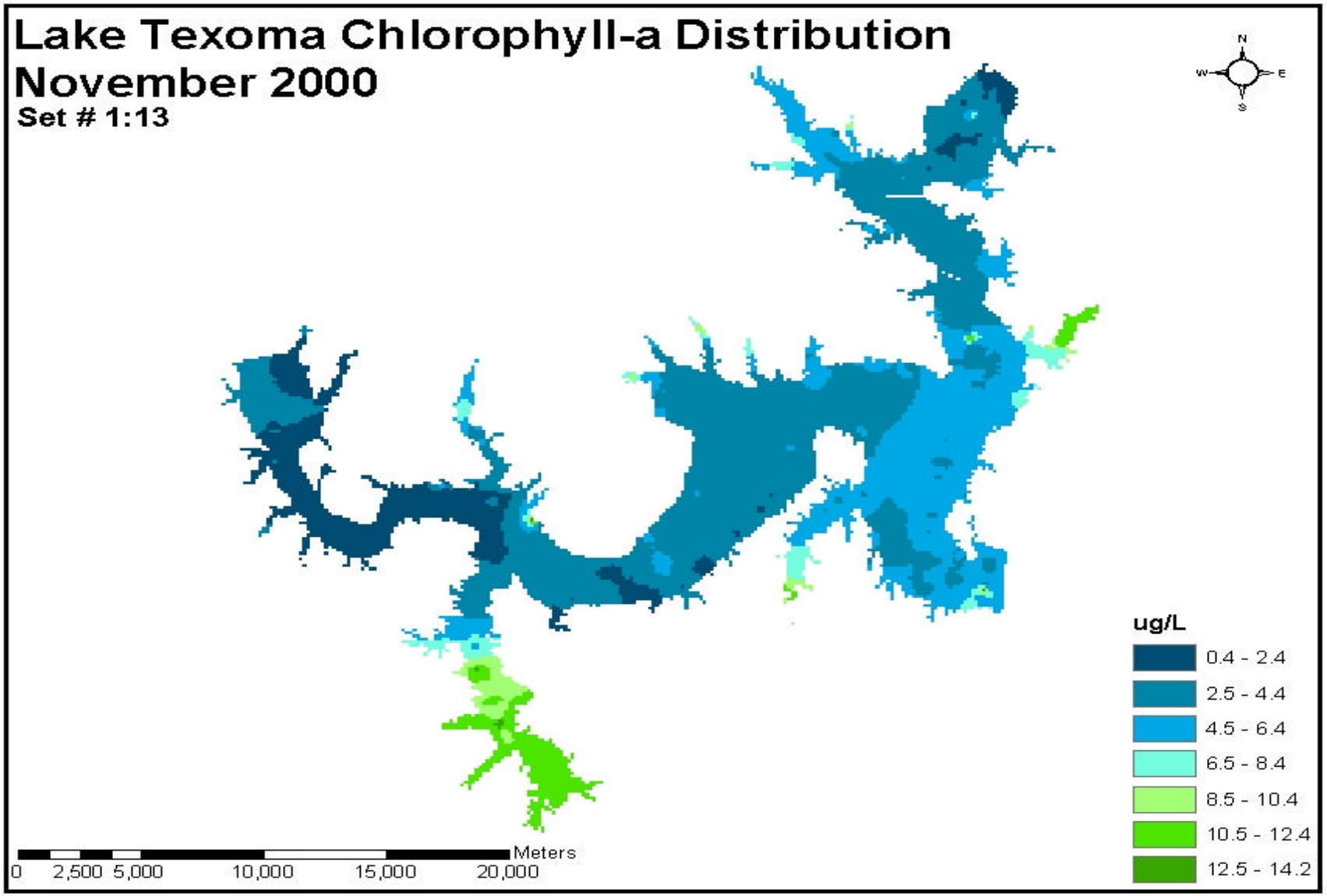
Lake Texoma Chlorophyll-a Distribution
November 2000
Set # 1:13
N
W
E
S
ug/L
0.4 - 2.4
2.5 - 4.4
4.5 - 6.4
6.5 - 8.4
8.5 - 10.4
10.5 - 12.4
12.5 - 14.2
Meters
0 2,500 5,000 10,000 15,000 20,000

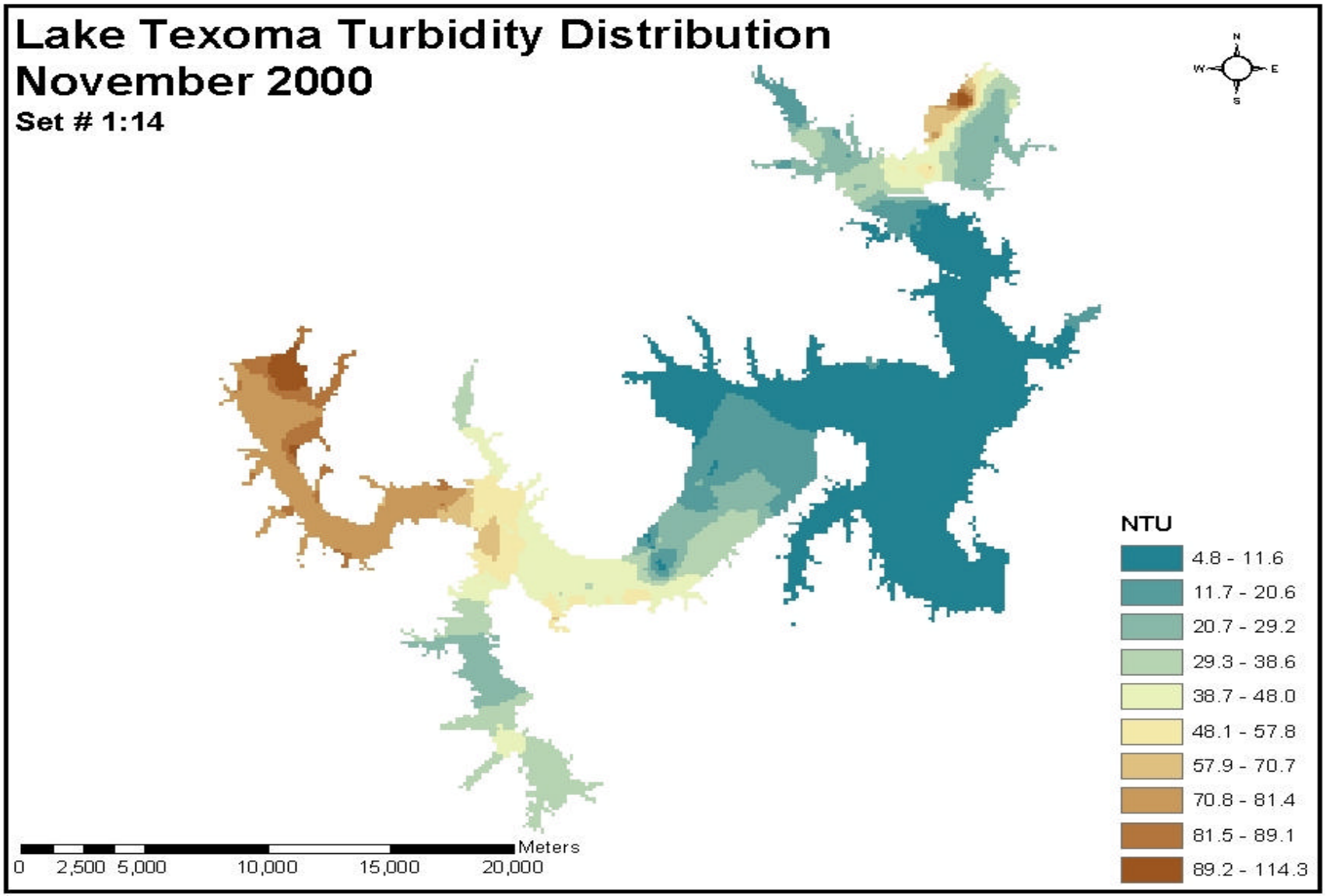
Lake Texoma Turbidity Distribution
November 2000
Set # 1:14
N
W
E
S
NTU
4.8 - 11.6
11.7 - 20.6
20.7 - 29.2
29.3 - 38.6
38.7 - 48.0
48.1 - 57.8
57.9 - 70.7
70.8 - 81.4
81.5 - 89.1
89.2 - 114.3
Meters
0
2,500
5,000
10,000
15,000
20,000

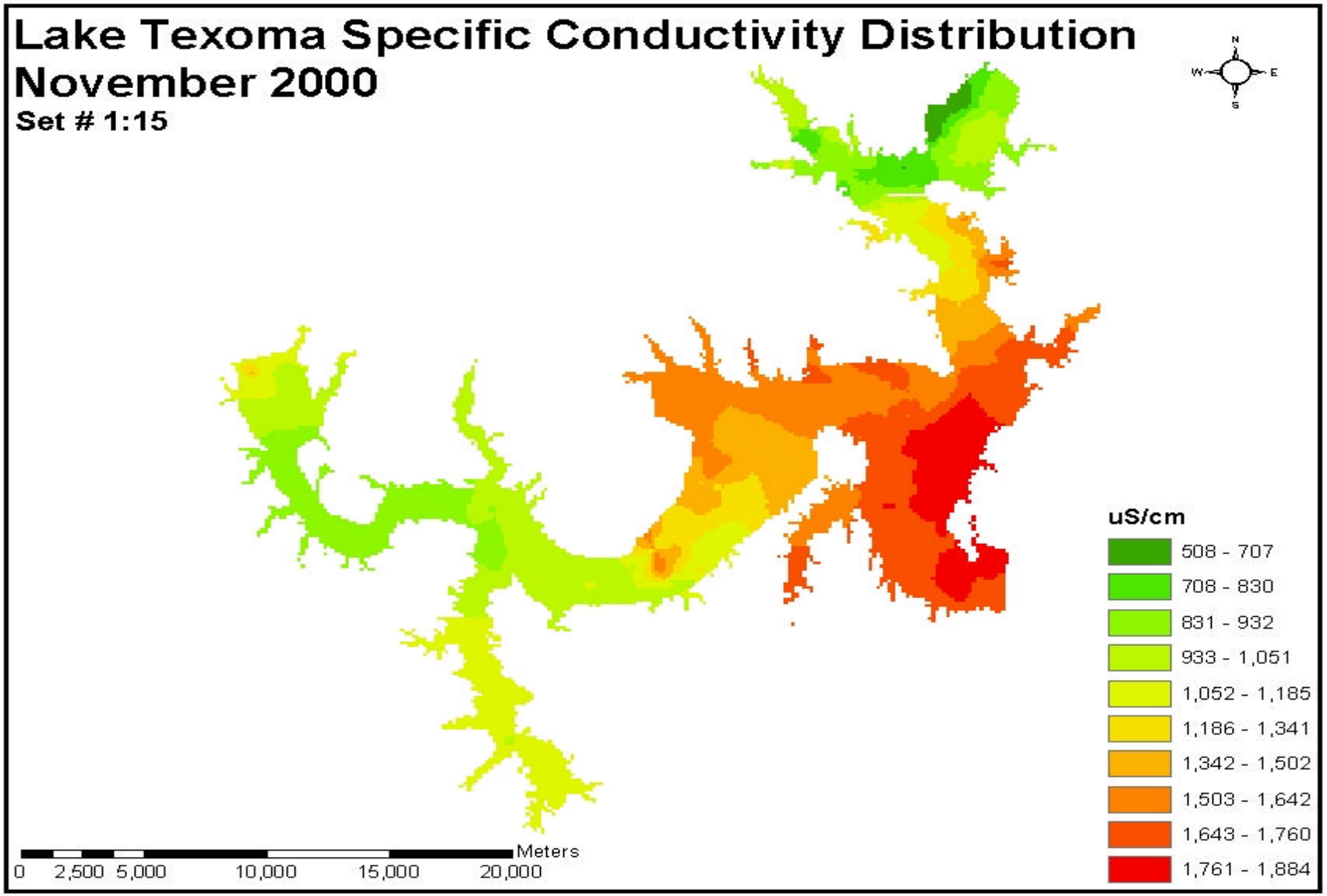
Lake Texoma Specific Conductivity Distribution
November 2000
Set # 1:15
N
W
E
S
uS/cm
508 - 707
708 - 830
831 - 932
933 - 1,051
1,052 - 1,185
1,186 - 1,341
1,342 - 1,502
1,503 - 1,642
1,643 - 1,760
1,761 - 1,884
Meters
0 2,500 5,000 10,000 15,000 20,000

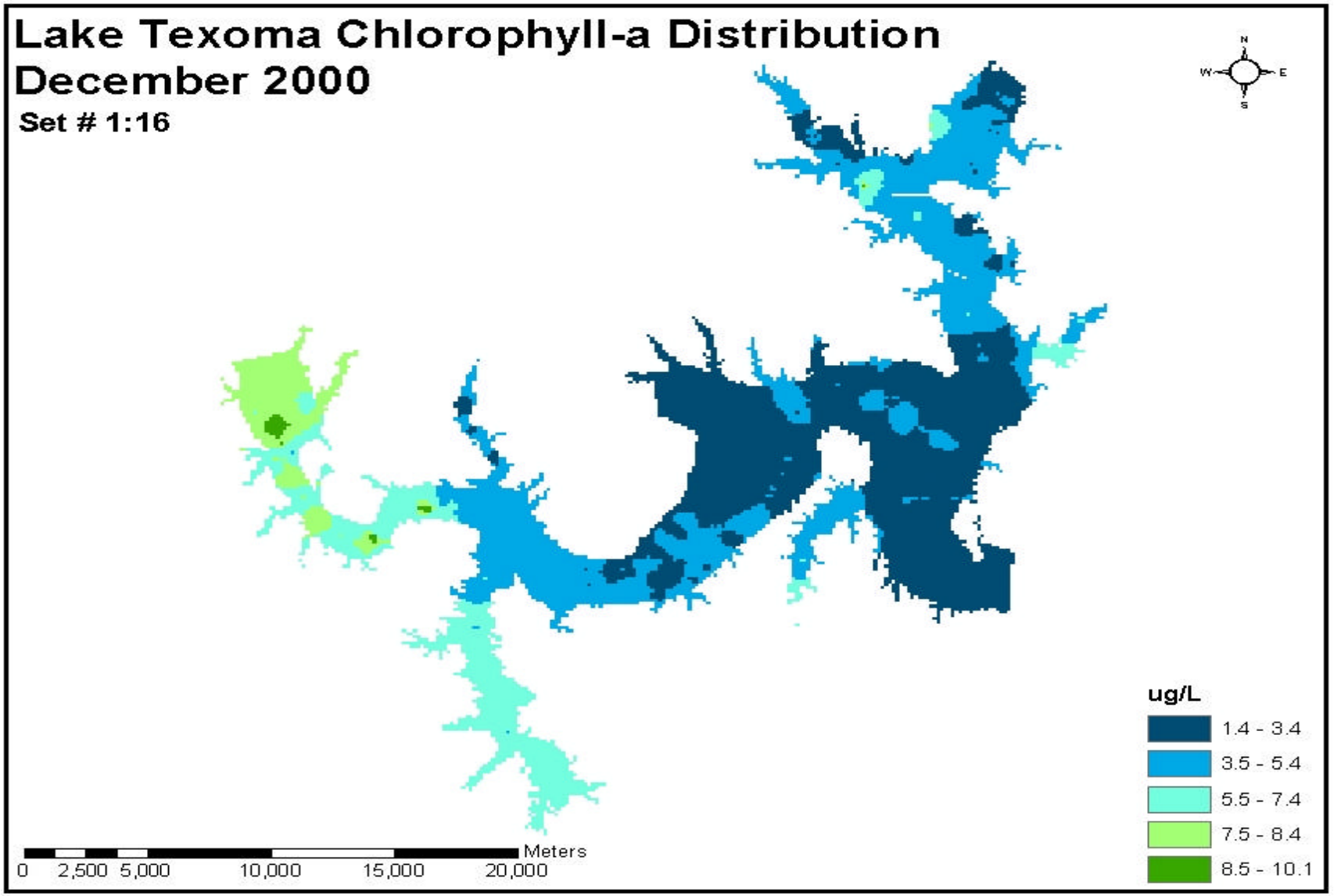
Lake Texoma Chlorophyll-a Distribution
December 2000
Set # 1:16
N
W
E
S
ug/L
1.4 - 3.4
3.5 - 5.4
5.5 - 7.4
7.5 - 8.4
8.5 - 10.1
0
2,500
5,000
10,000
15,000
20,000
Meters

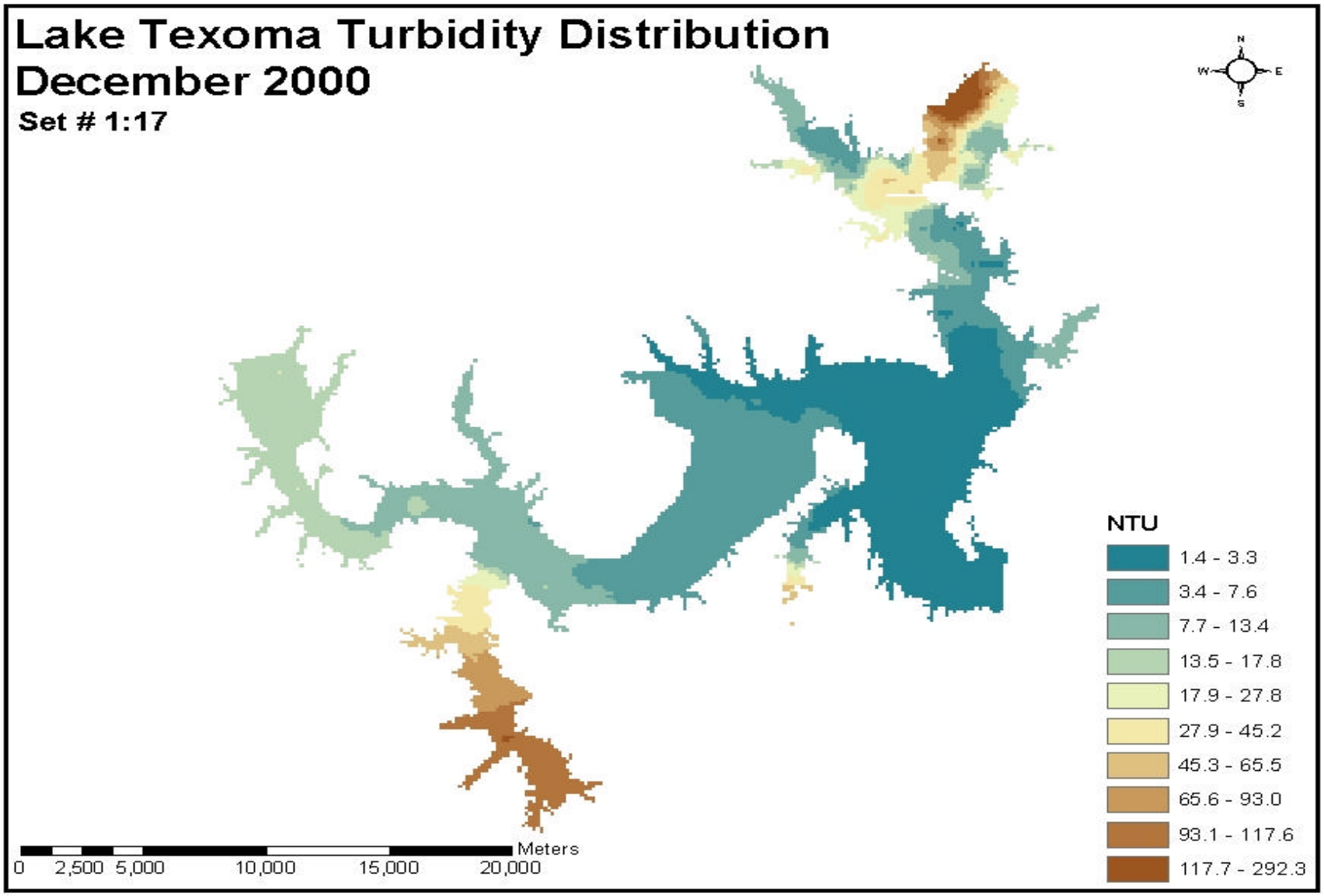
Lake Texoma Turbidity Distribution
December 2000
Set # 1:17
N
W
E
S
NTU
1.4 - 3.3
3.4 - 7.6
7.7 - 13.4
13.5 - 17.8
17.9 - 27.8
27.9 - 45.2
45.3 - 65.5
65.6 - 93.0
93.1 - 117.6
117.7 - 292.3
Meters
0
2,500
5,000
10,000
15,000
20,000

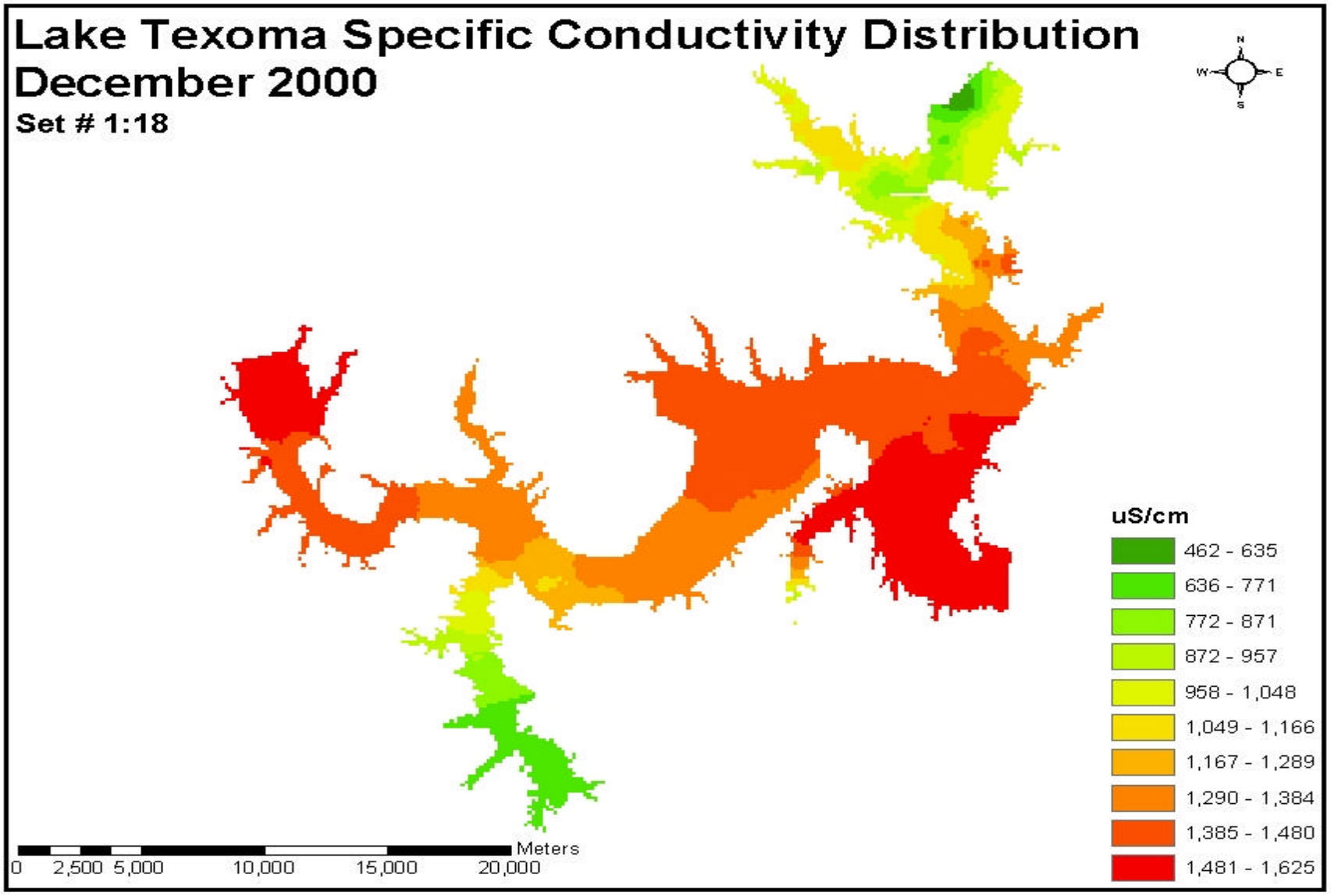
Lake Texoma Specific Conductivity Distribution
December 2000
Set # 1:18
N
W
E
S
uS/cm
462 - 635
636 - 771
772 - 871
872 - 957
958 - 1,048
1,049 - 1,166
1,167 - 1,289
1,290 - 1,384
1,385 - 1,480
1,481 - 1,625
Meters
0
2,500
5,000
10,000
15,000
20,000

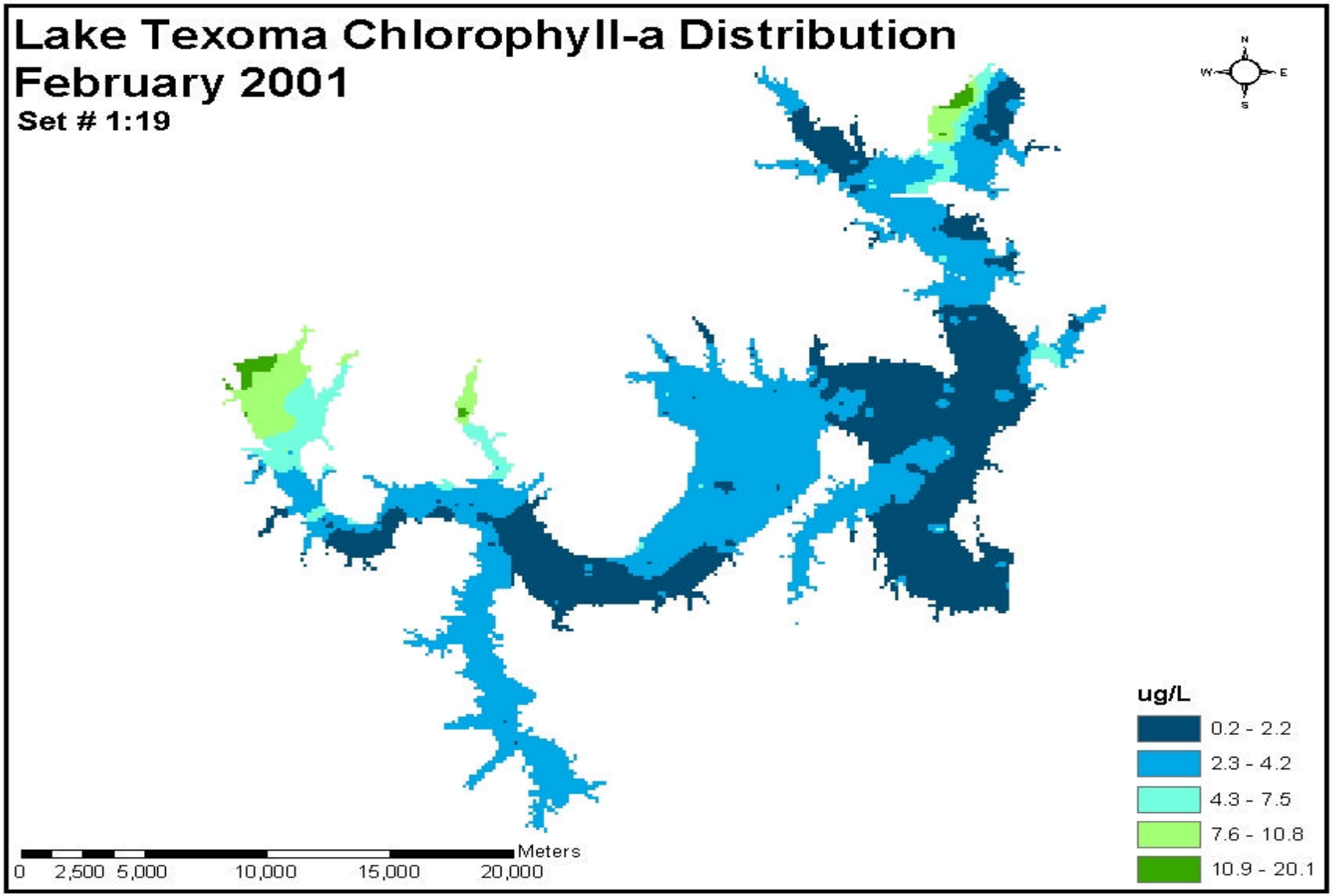
Lake Texoma Chlorophyll-a Distribution
February 2001
Set # 1:19
N
W
E
S
ug/L
0.2 - 2.2
2.3 - 4.2
4.3 - 7.5
7.6 - 10.8
10.9 - 20.1
Meters
0
2,500
5,000
10,000
15,000
20,000

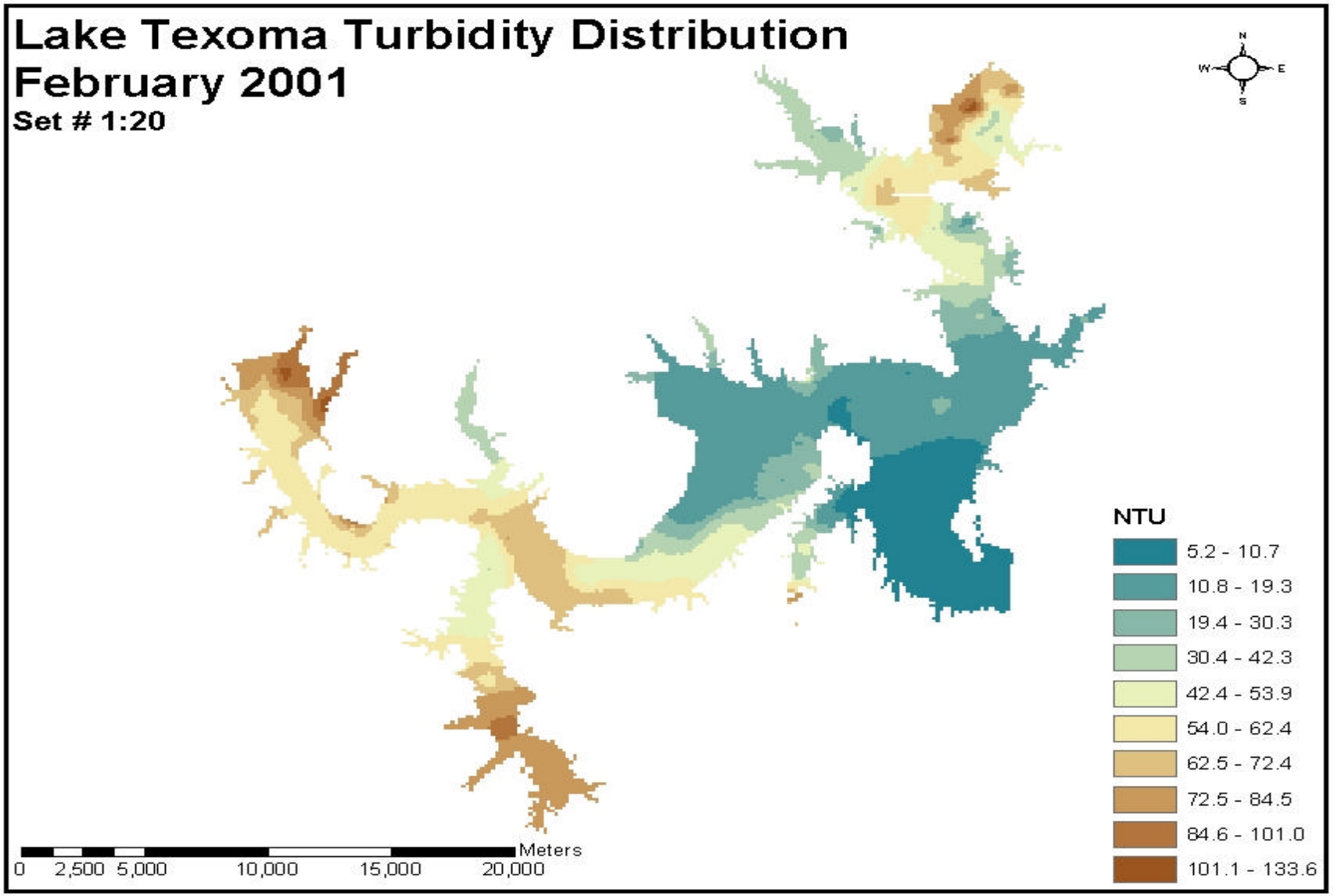
Lake Texoma Turbidity Distribution
February 2001
Set # 1:20
N
W
E
S
NTU
5.2 - 10.7
10.8 - 19.3
19.4 - 30.3
30.4 - 42.3
42.4 - 53.9
54.0 - 62.4
62.5 - 72.4
72.5 - 84.5
84.6 - 101.0
101.1 - 133.6
Meters
0 2,500 5,000 10,000 15,000 20,000

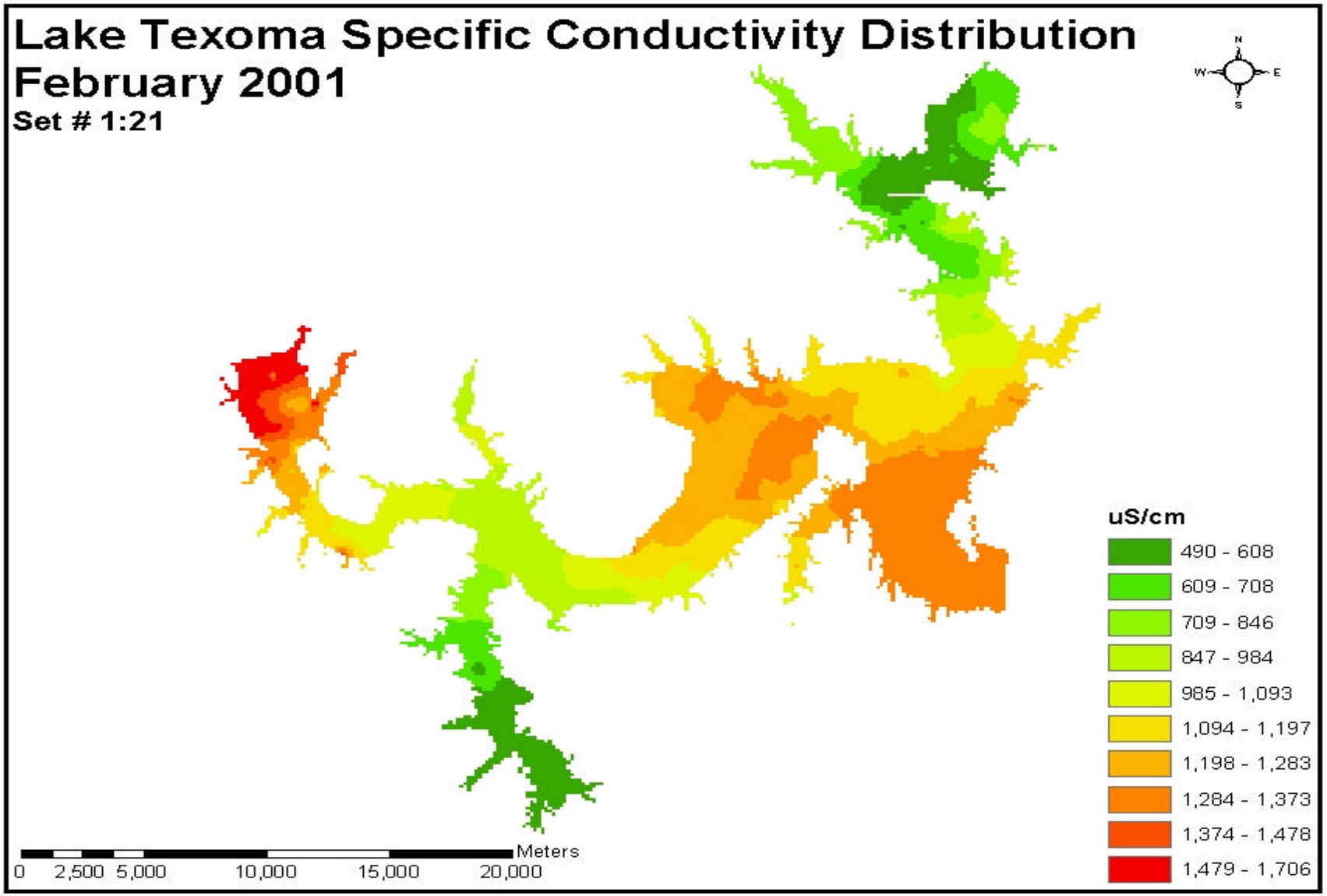
Lake Texoma Specific Conductivity Distribution
February 2001
Set # 1:21
N
W
E
S
uS/cm
490 - 608
609 - 708
709 - 846
847 - 984
985 - 1,093
1,094 - 1,197
1,198 - 1,283
1,284 - 1,373
1,374 - 1,478
1,479 - 1,706
Meters
0 2,500 5,000 10,000 15,000 20,000

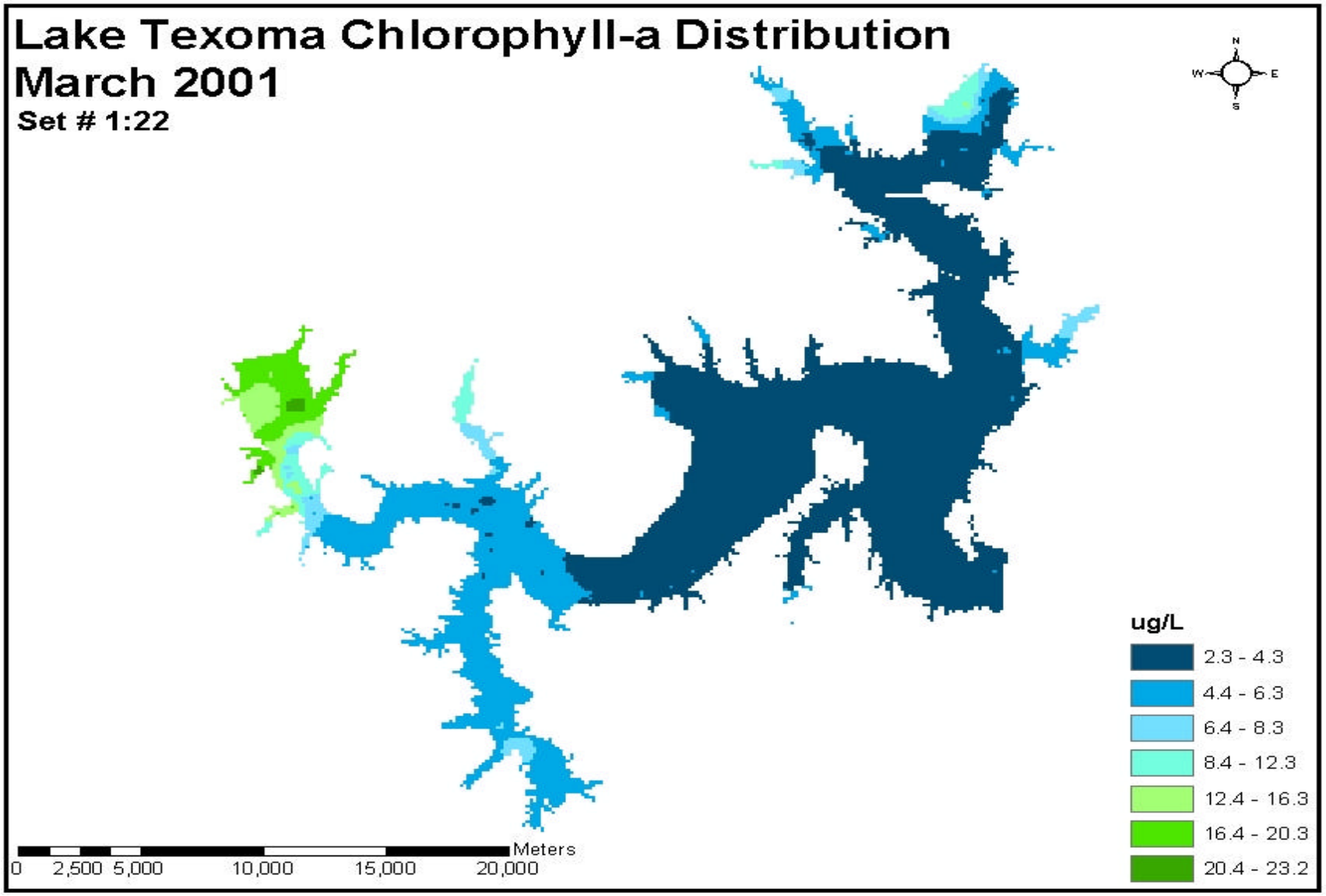
Lake Texoma Chlorophyll-a Distribution
March 2001
Set # 1:22
N
W
E
S
ug/L
2.3 - 4.3
4.4 - 6.3
6.4 - 8.3
8.4 - 12.3
12.4 - 16.3
16.4 - 20.3
20.4 - 23.2
Meters
0
2,500
5,000
10,000
15,000
20,000

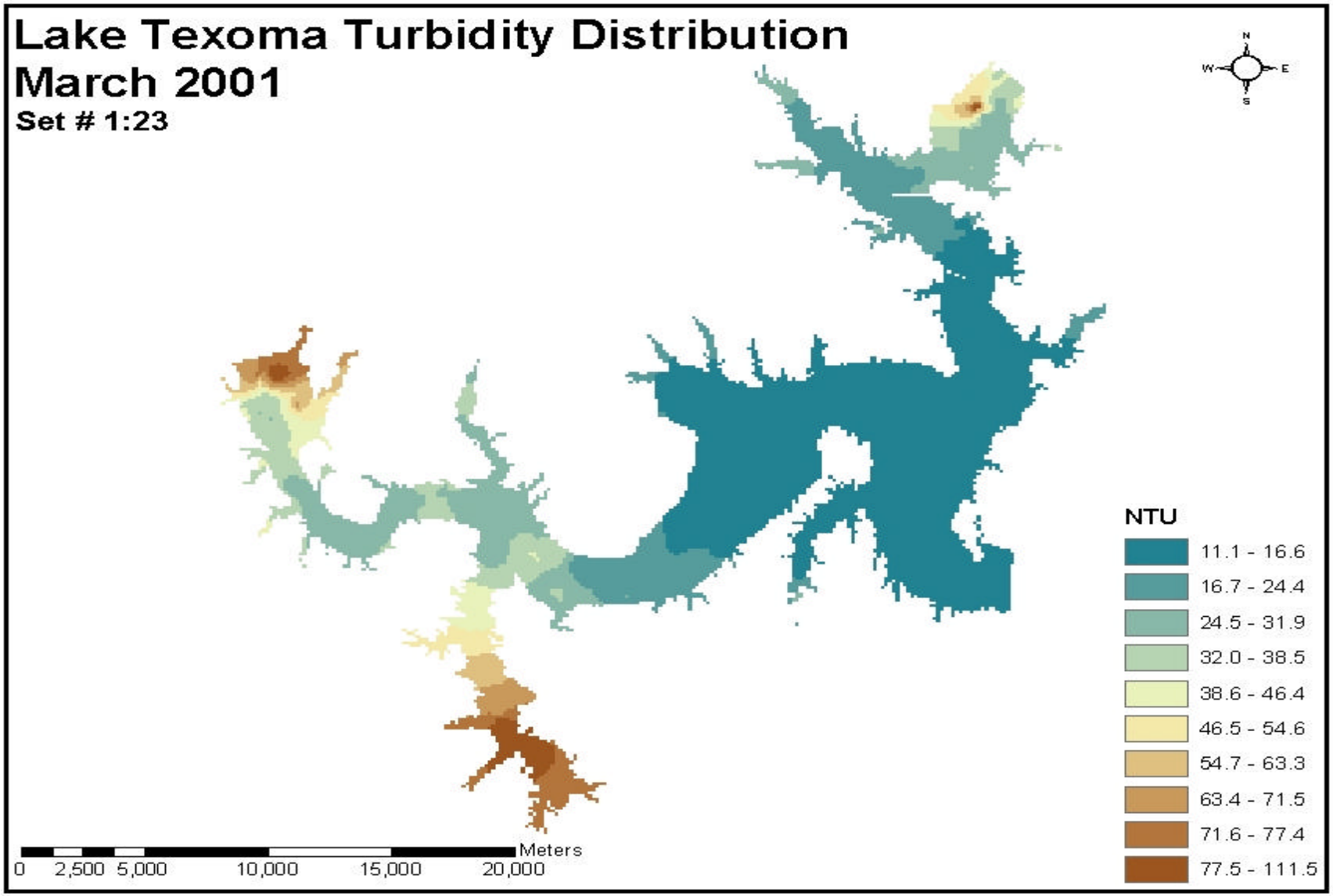
Lake Texoma Turbidity Distribution
March 2001
Set # 1:23
N
W
E
S
NTU
11.1 - 16.6
16.7 - 24.4
24.5 - 31.9
32.0 - 38.5
38.6 - 46.4
46.5 - 54.6
54.7 - 63.3
63.4 - 71.5
71.6 - 77.4
77.5 - 111.5
Meters
0 2,500 5,000 10,000 15,000 20,000

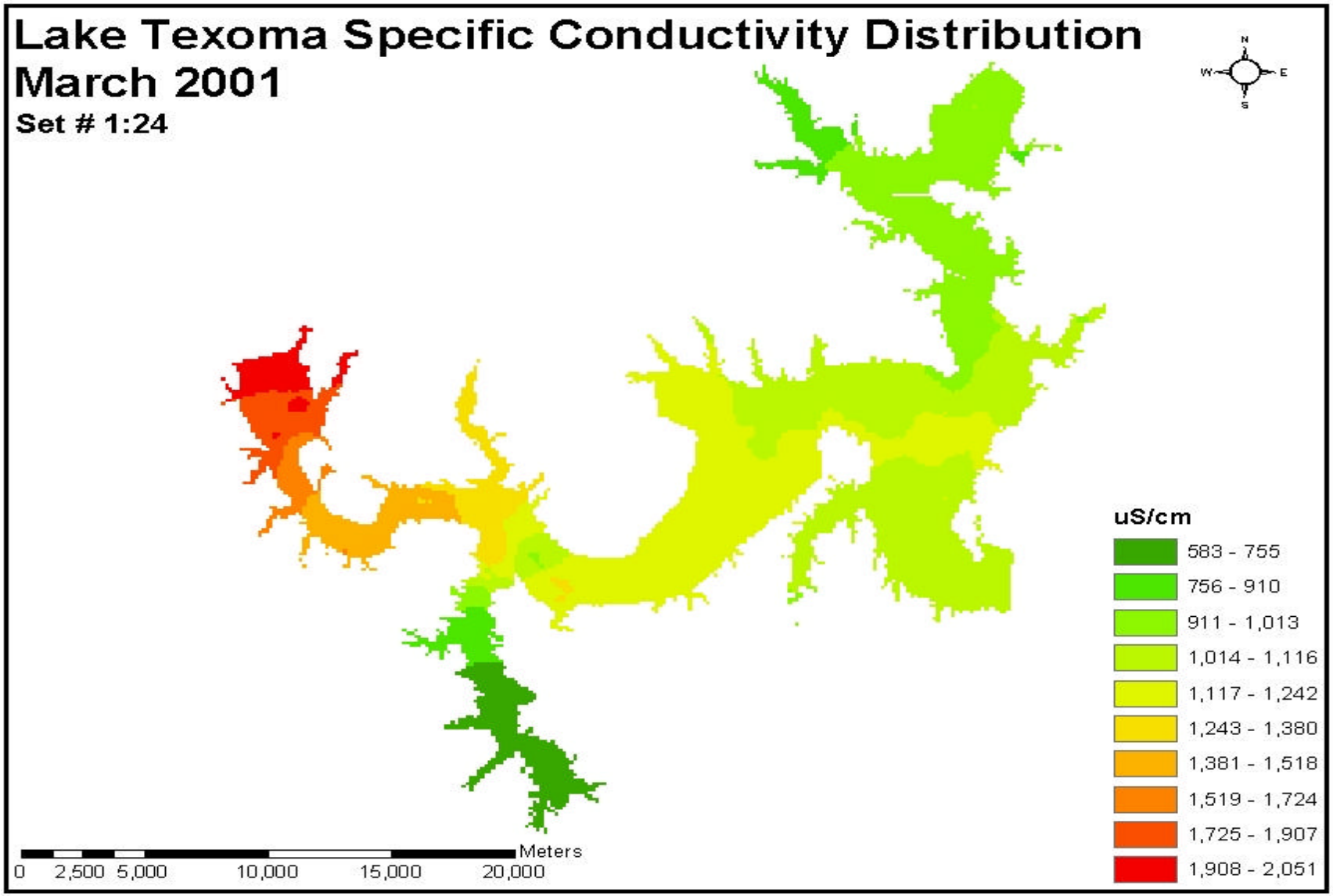
Lake Texoma Specific Conductivity Distribution
March 2001
Set # 1:24
N
W
E
S
uS/cm
583 - 755
756 - 910
911 - 1,013
1,014 - 1,116
1,117 - 1,242
1,243 - 1,380
1,381 - 1,518
1,519 - 1,724
1,725 - 1,907
1,908 - 2,051
Meters
0
2,500
5,000
10,000
15,000
20,000

APPENDIX B
MAP SET 2

Distribution Maps for Chlorophyll-*a*, Turbidity, and Specific Conductivity on Lake Texoma from July 2000 through March 2001

This map set was designed to compare values across months using 10 fixed categories that cover the combined data range of all months.

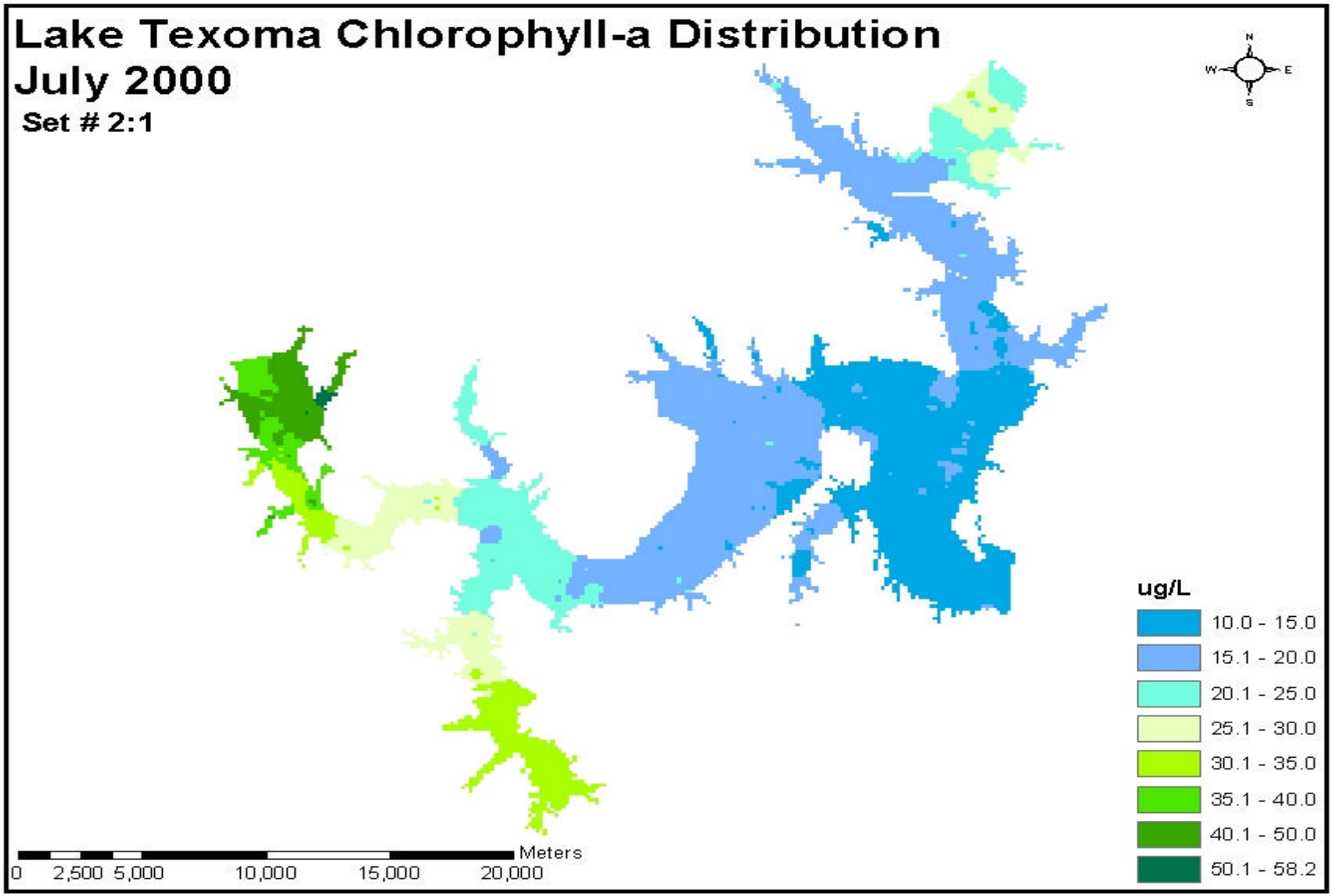
Lake Texoma Chlorophyll-a Distribution
July 2000
Set # 2:1
N
W
E
S
ug/L
10.0 - 15.0
15.1 - 20.0
20.1 - 25.0
25.1 - 30.0
30.1 - 35.0
35.1 - 40.0
40.1 - 50.0
50.1 - 58.2
Meters
0
2,500
5,000
10,000
15,000
20,000

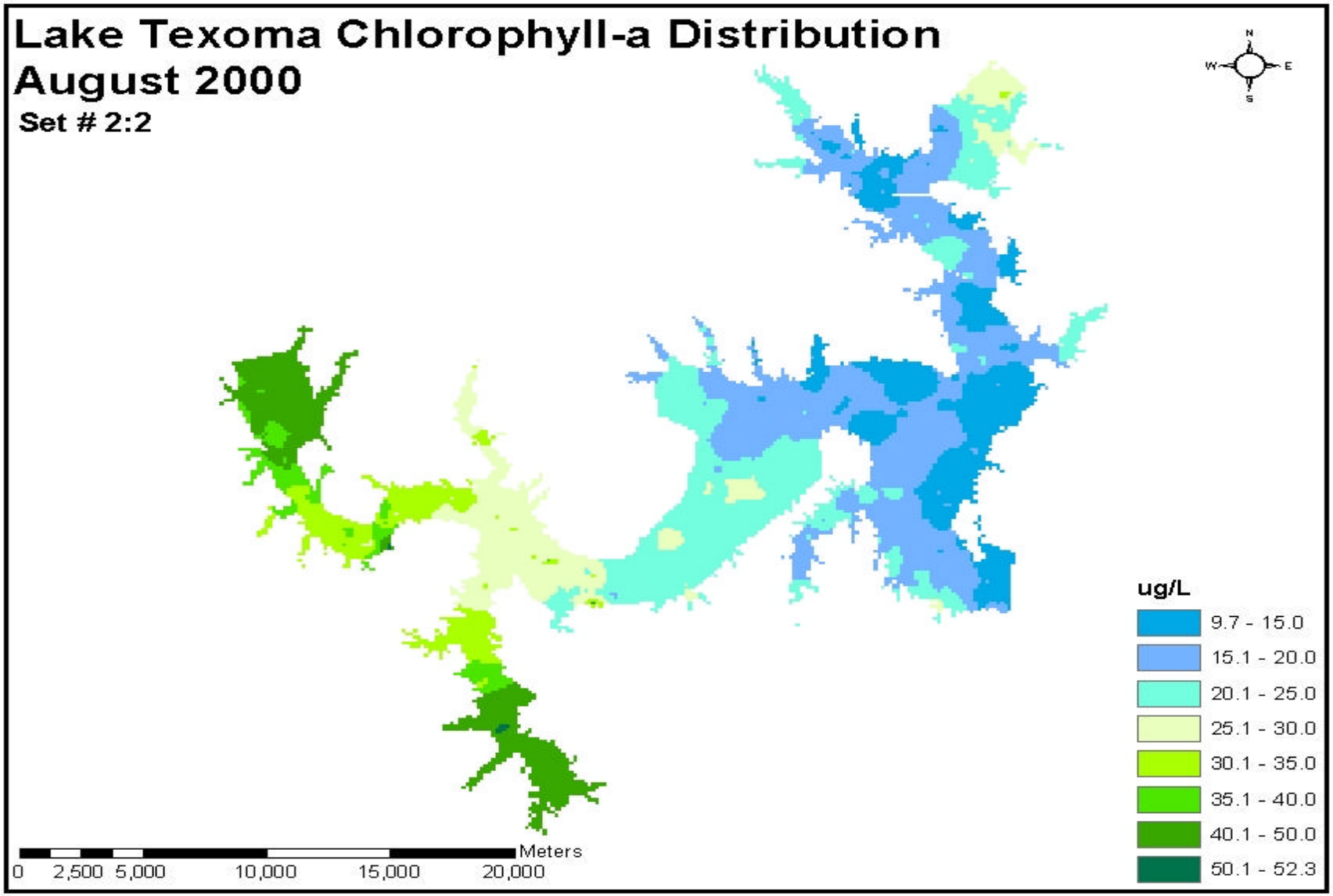
Lake Texoma Chlorophyll-a Distribution
August 2000
Set # 2:2
N
W
E
S
ug/L
9.7 - 15.0
15.1 - 20.0
20.1 - 25.0
25.1 - 30.0
30.1 - 35.0
35.1 - 40.0
40.1 - 50.0
50.1 - 52.3
Meters
0
2,500
5,000
10,000
15,000
20,000

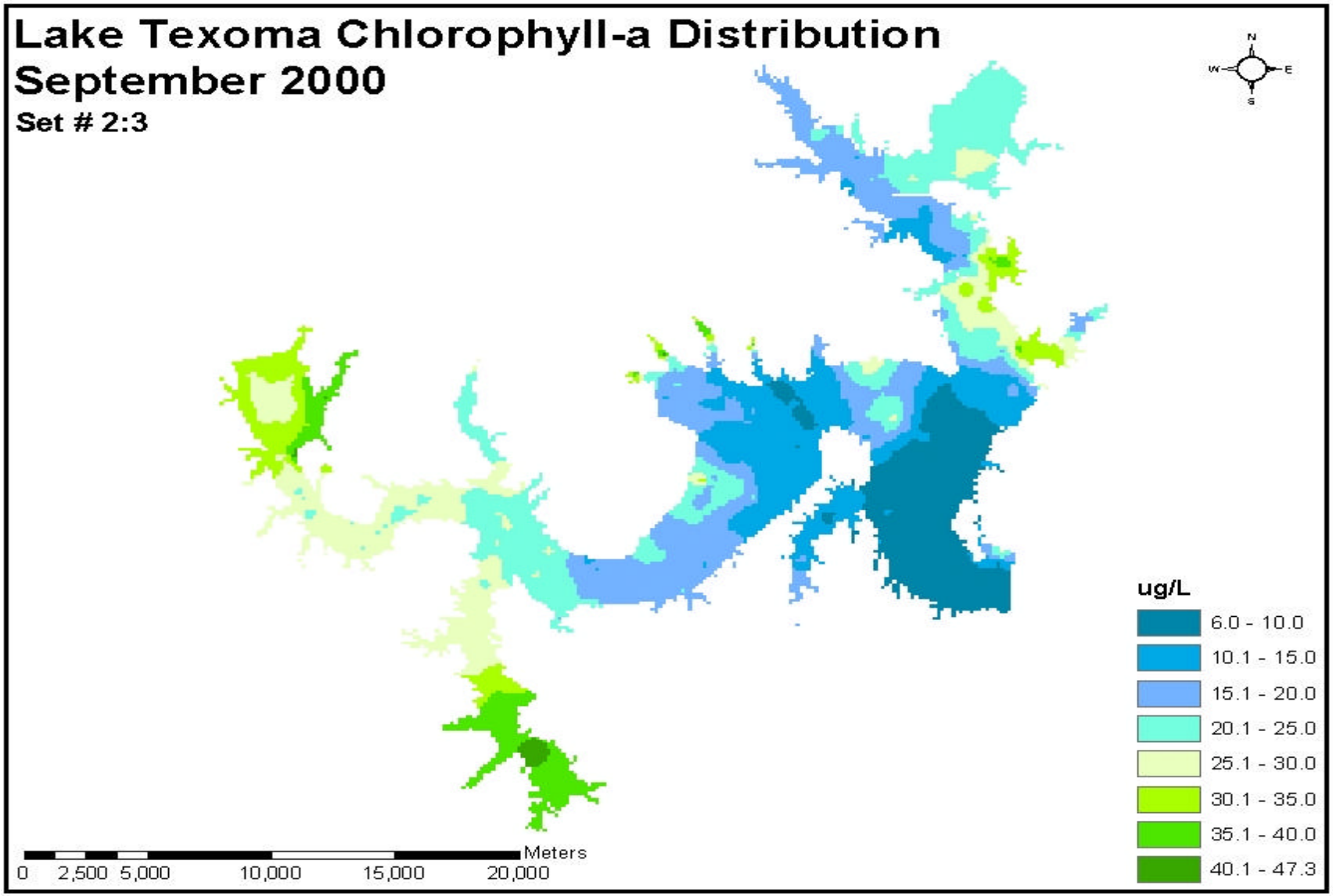
Lake Texoma Chlorophyll-a Distribution
September 2000
Set # 2:3
N
W
E
S
ug/L
6.0 - 10.0
10.1 - 15.0
15.1 - 20.0
20.1 - 25.0
25.1 - 30.0
30.1 - 35.0
35.1 - 40.0
40.1 - 47.3
Meters
0 2,500 5,000 10,000 15,000 20,000

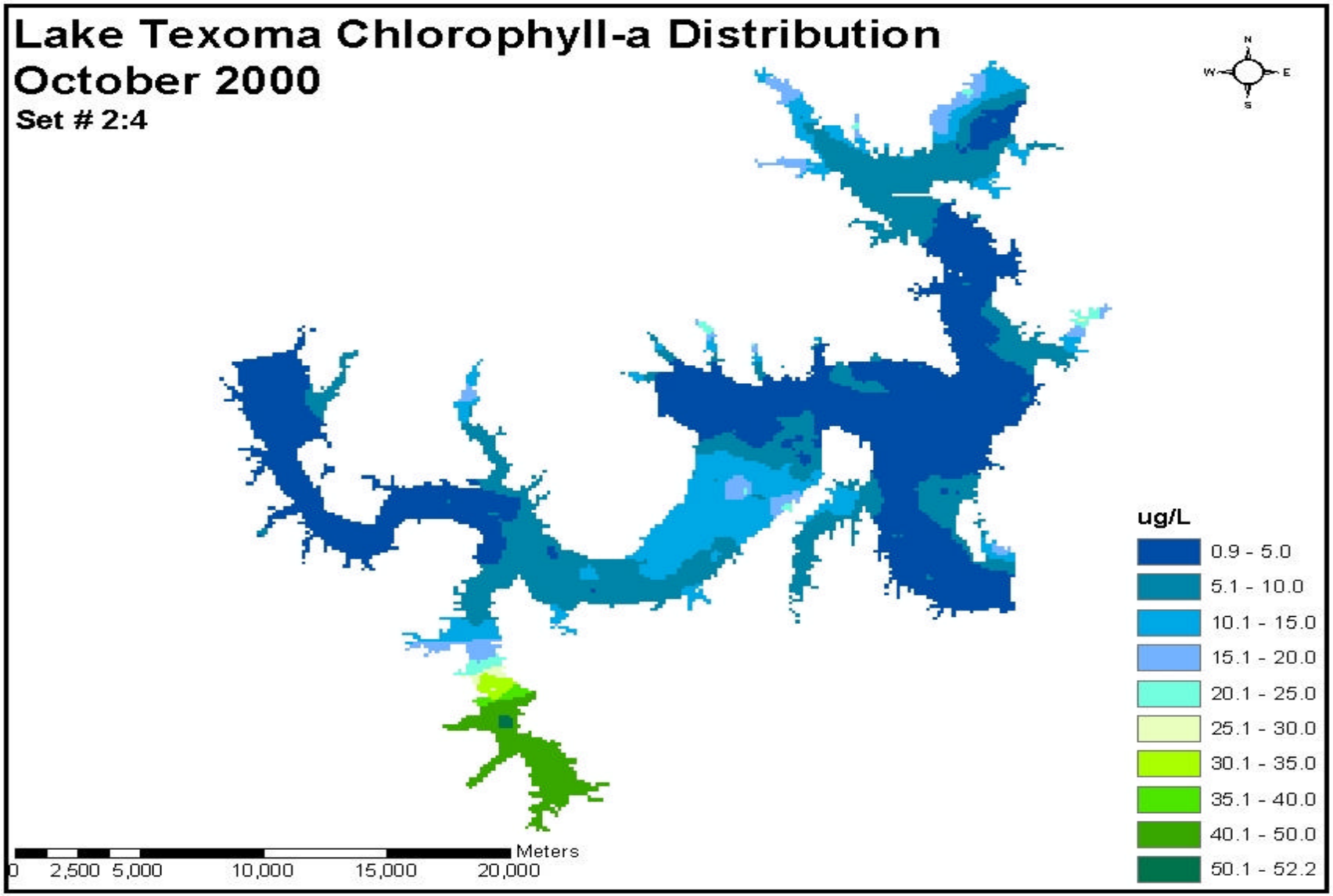
Lake Texoma Chlorophyll-a Distribution
October 2000
Set # 2:4
N
W
E
S
ug/L
0.9 - 5.0
5.1 - 10.0
10.1 - 15.0
15.1 - 20.0
20.1 - 25.0
25.1 - 30.0
30.1 - 35.0
35.1 - 40.0
40.1 - 50.0
50.1 - 52.2
Meters
0
2,500
5,000
10,000
15,000
20,000

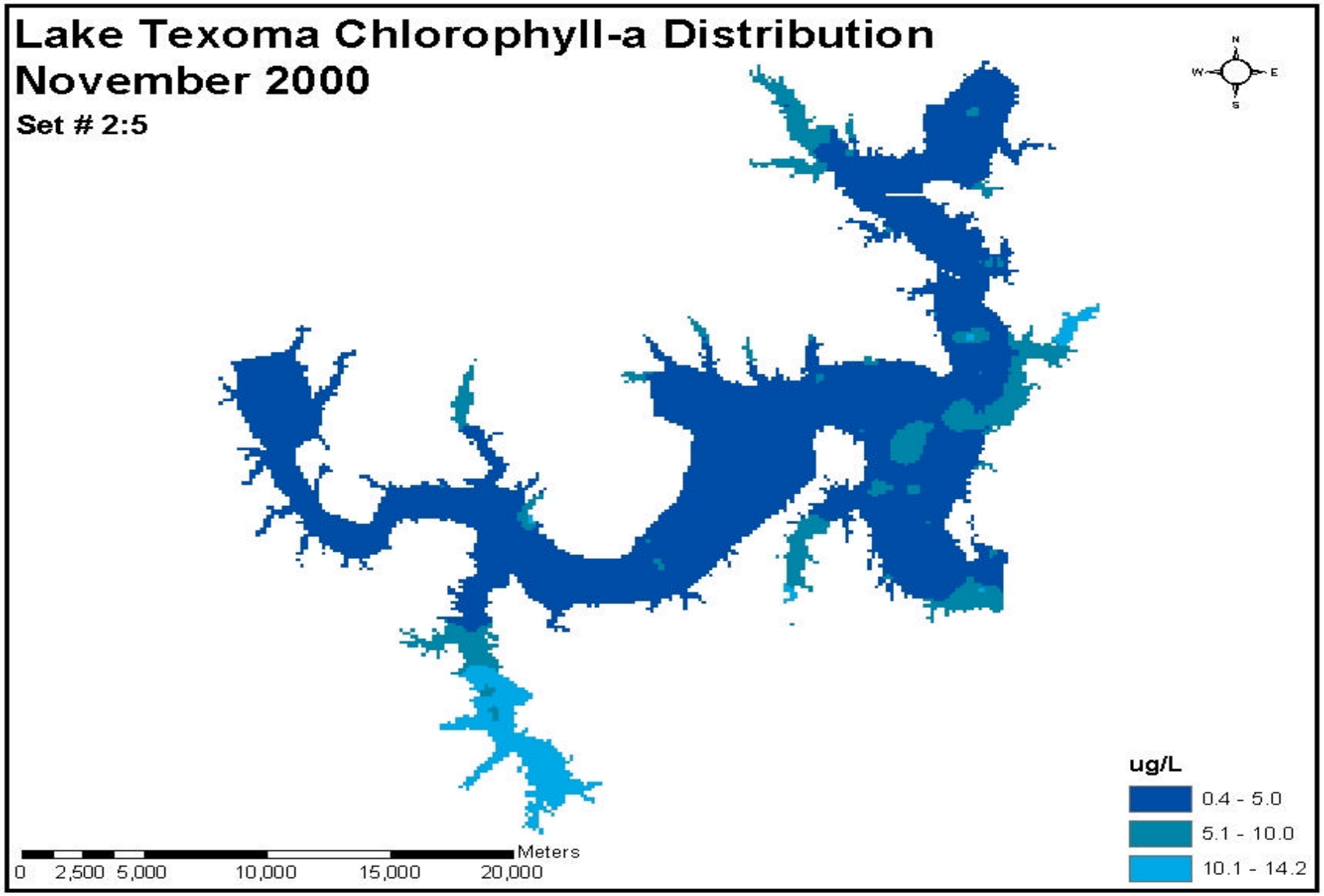
Lake Texoma Chlorophyll-a Distribution
November 2000
Set # 2:5
N
W
E
S
ug/L
0.4 - 5.0
5.1 - 10.0
10.1 - 14.2
Meters
0
2,500
5,000
10,000
15,000
20,000

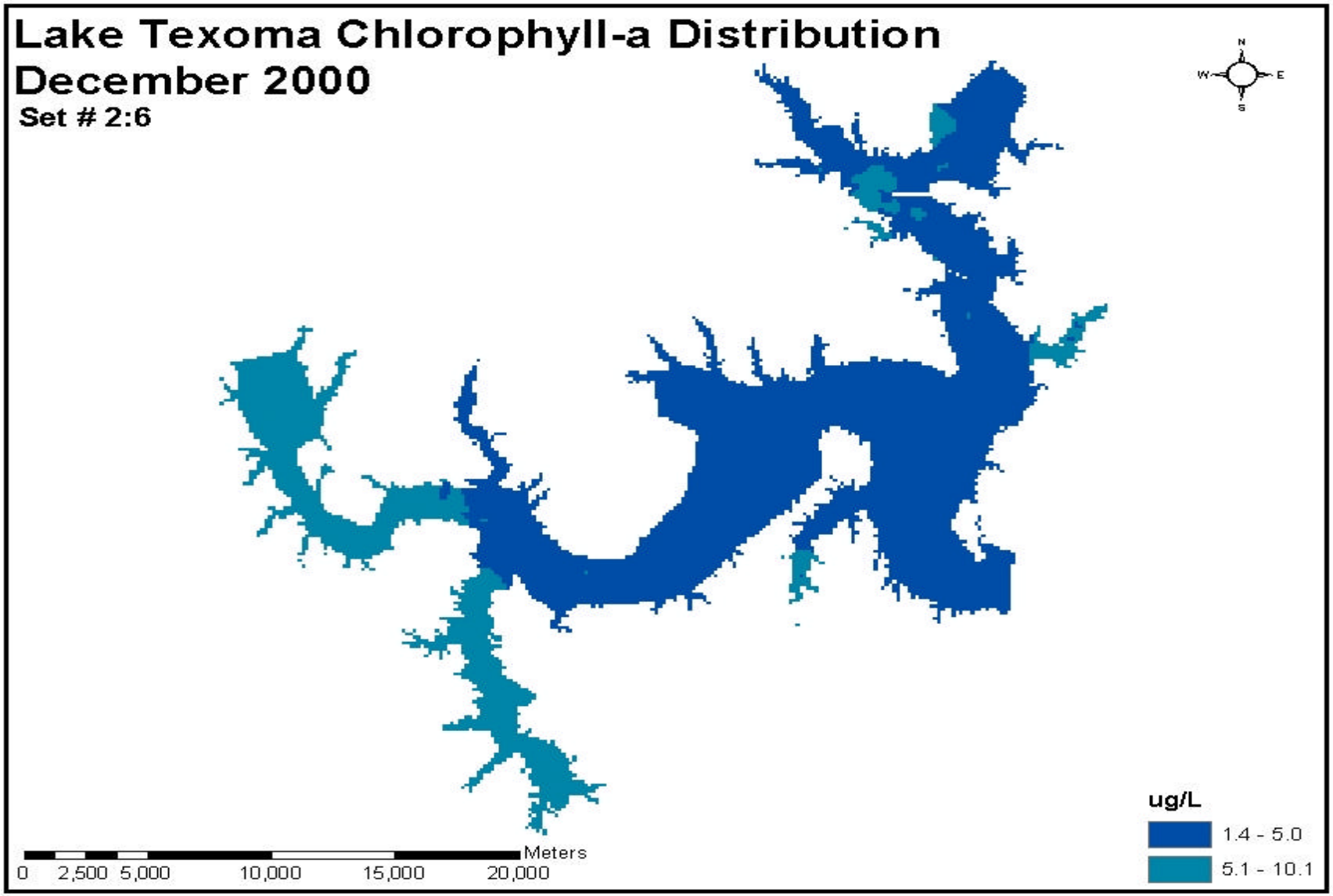
Lake Texoma Chlorophyll-a Distribution
December 2000
Set # 2:6
N
W
E
S
Meters
0
2,500
5,000
10,000
15,000
20,000
ug/L
1.4 - 5.0
5.1 - 10.1

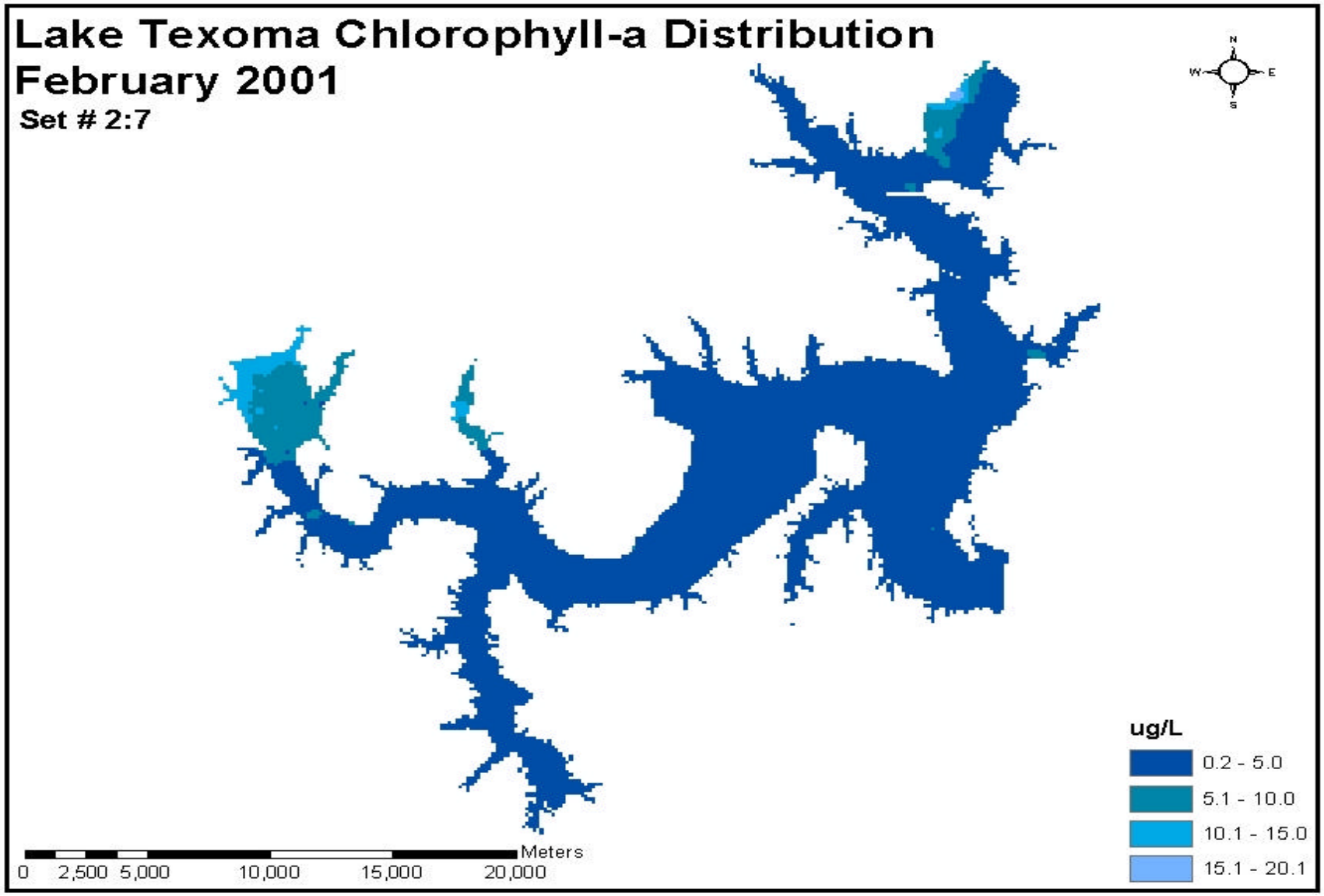
Lake Texoma Chlorophyll-a Distribution
February 2001
Set # 2:7
N
W
E
S
ug/L
0.2 - 5.0
5.1 - 10.0
10.1 - 15.0
15.1 - 20.1
Meters
0 2,500 5,000 10,000 15,000 20,000

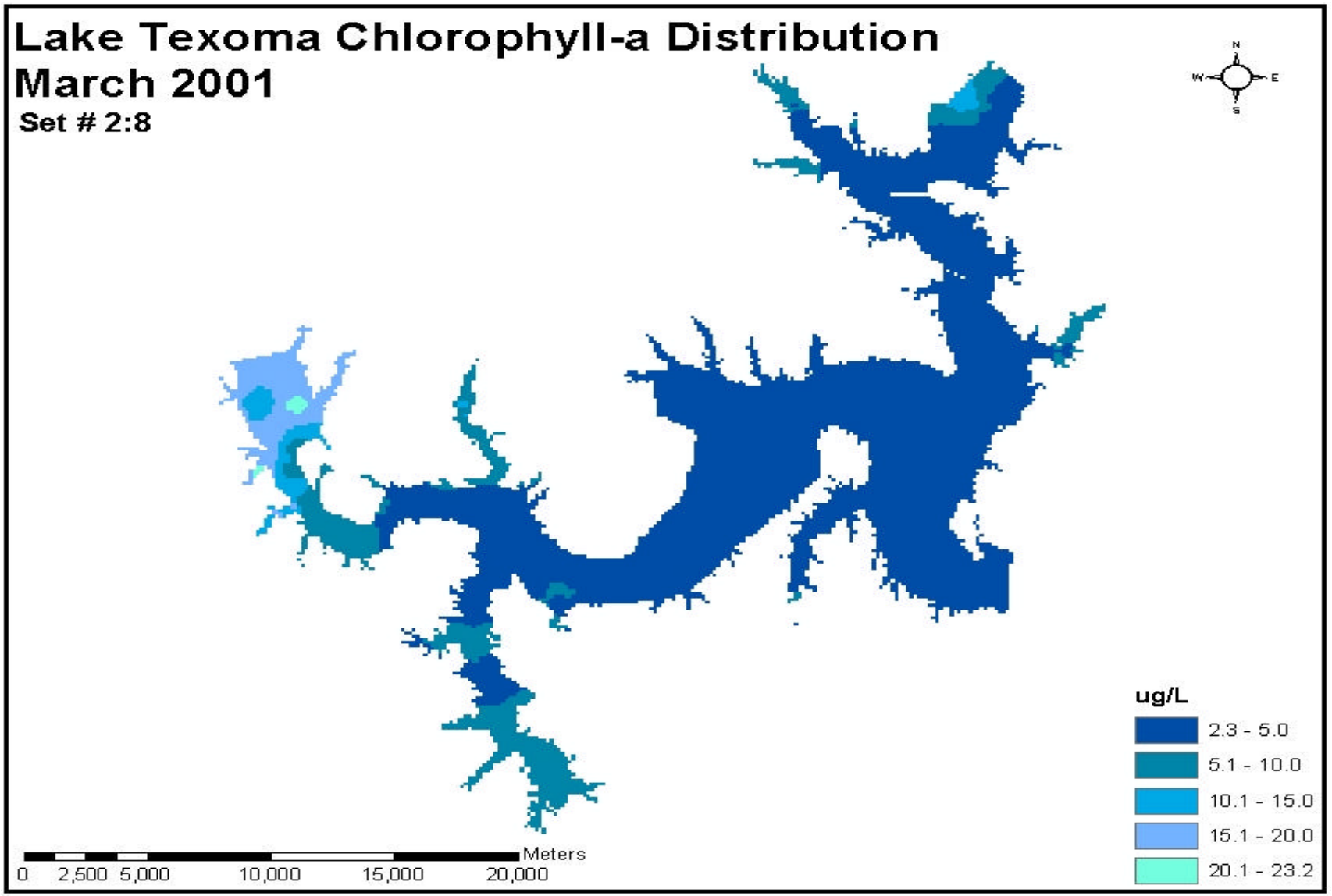
Lake Texoma Chlorophyll-a Distribution
March 2001
Set # 2:8
N
W
E
S
ug/L
2.3 - 5.0
5.1 - 10.0
10.1 - 15.0
15.1 - 20.0
20.1 - 23.2
Meters
0 2,500 5,000 10,000 15,000 20,000

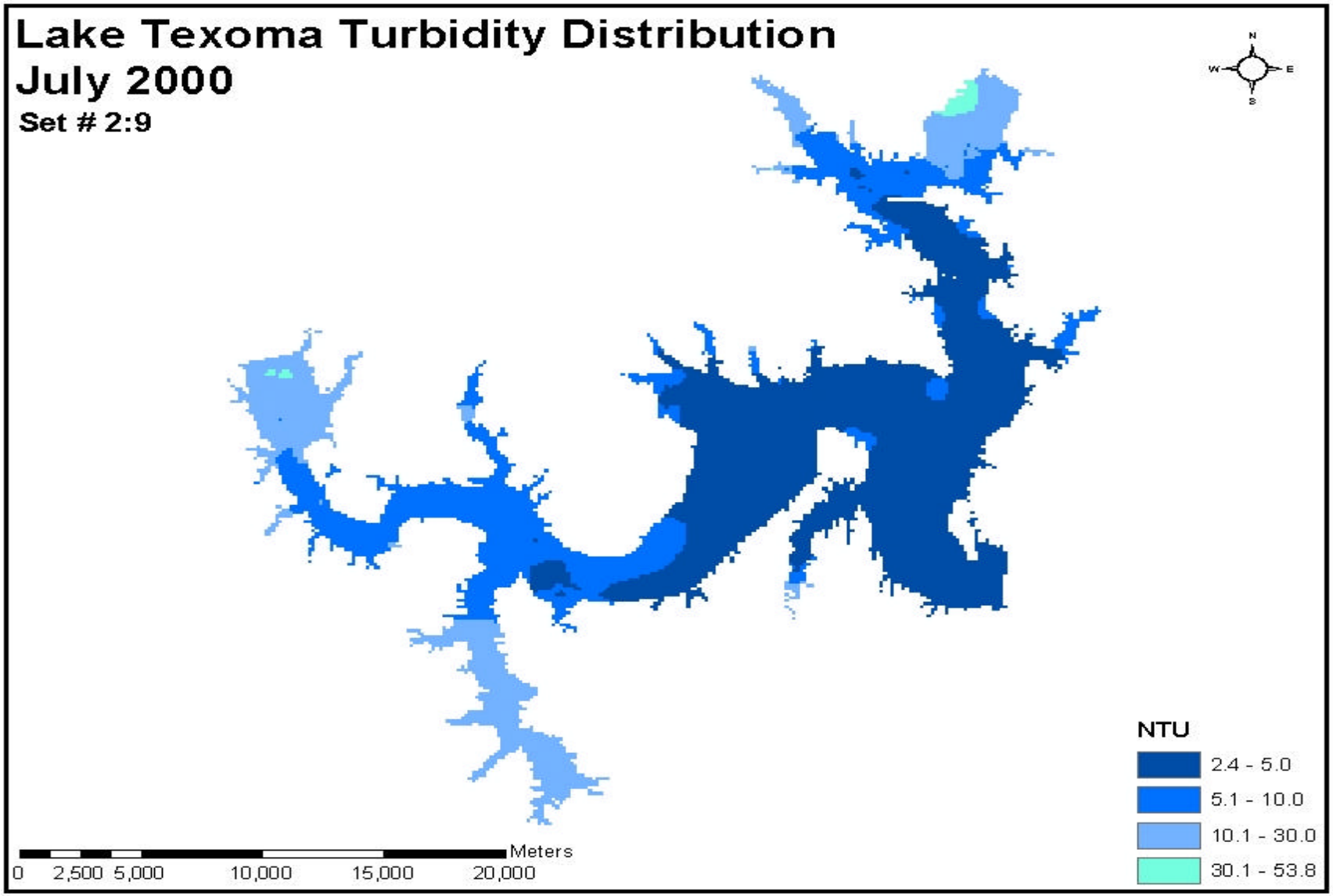
Lake Texoma Turbidity Distribution
July 2000
Set # 2:9
N
W
E
S
NTU
2.4 - 5.0
5.1 - 10.0
10.1 - 30.0
30.1 - 53.8
Meters
0
2,500
5,000
10,000
15,000
20,000

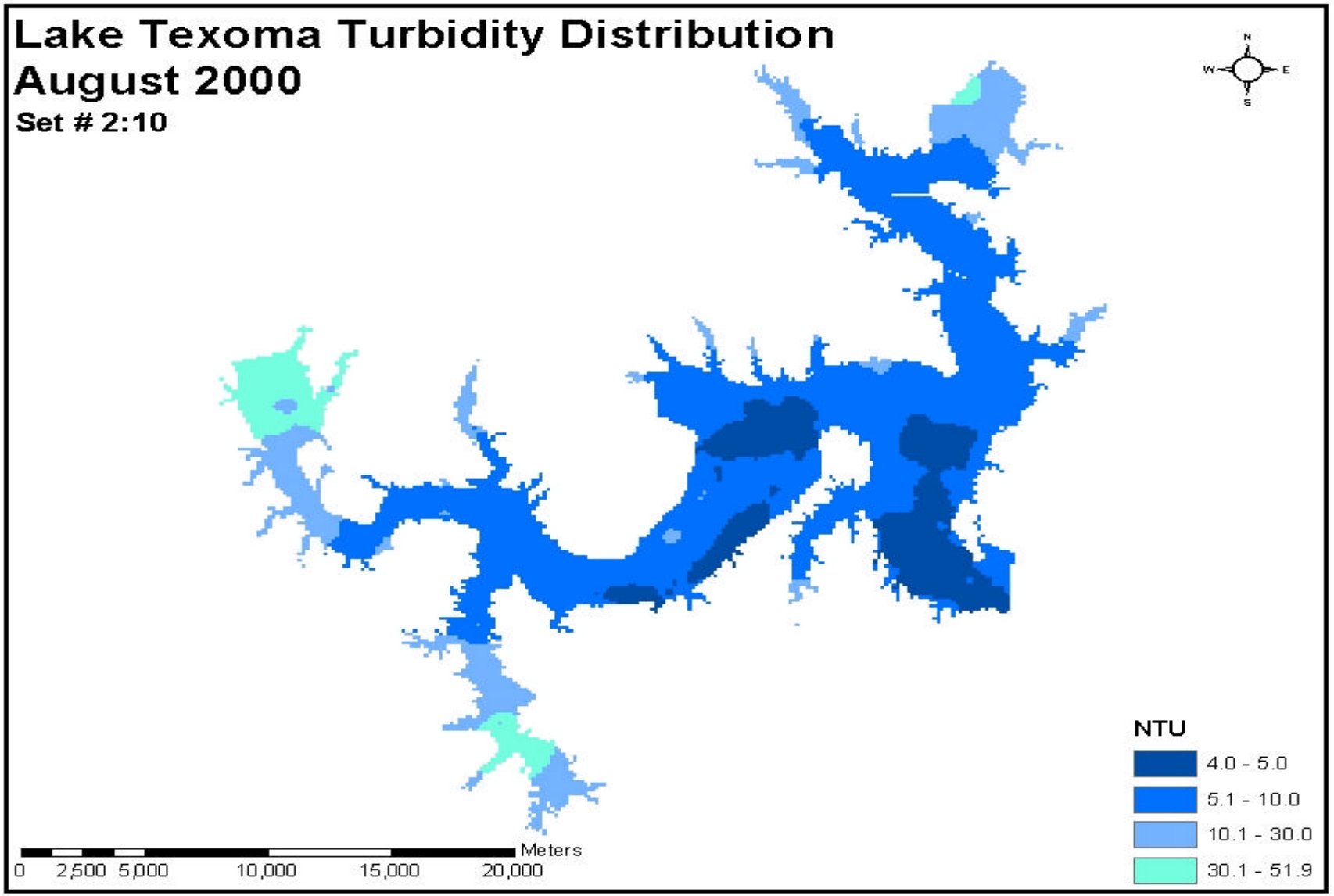
Lake Texoma Turbidity Distribution
August 2000
Set # 2:10
N
W
E
S
NTU
4.0 - 5.0
5.1 - 10.0
10.1 - 30.0
30.1 - 51.9
Meters
0
2,500
5,000
10,000
15,000
20,000

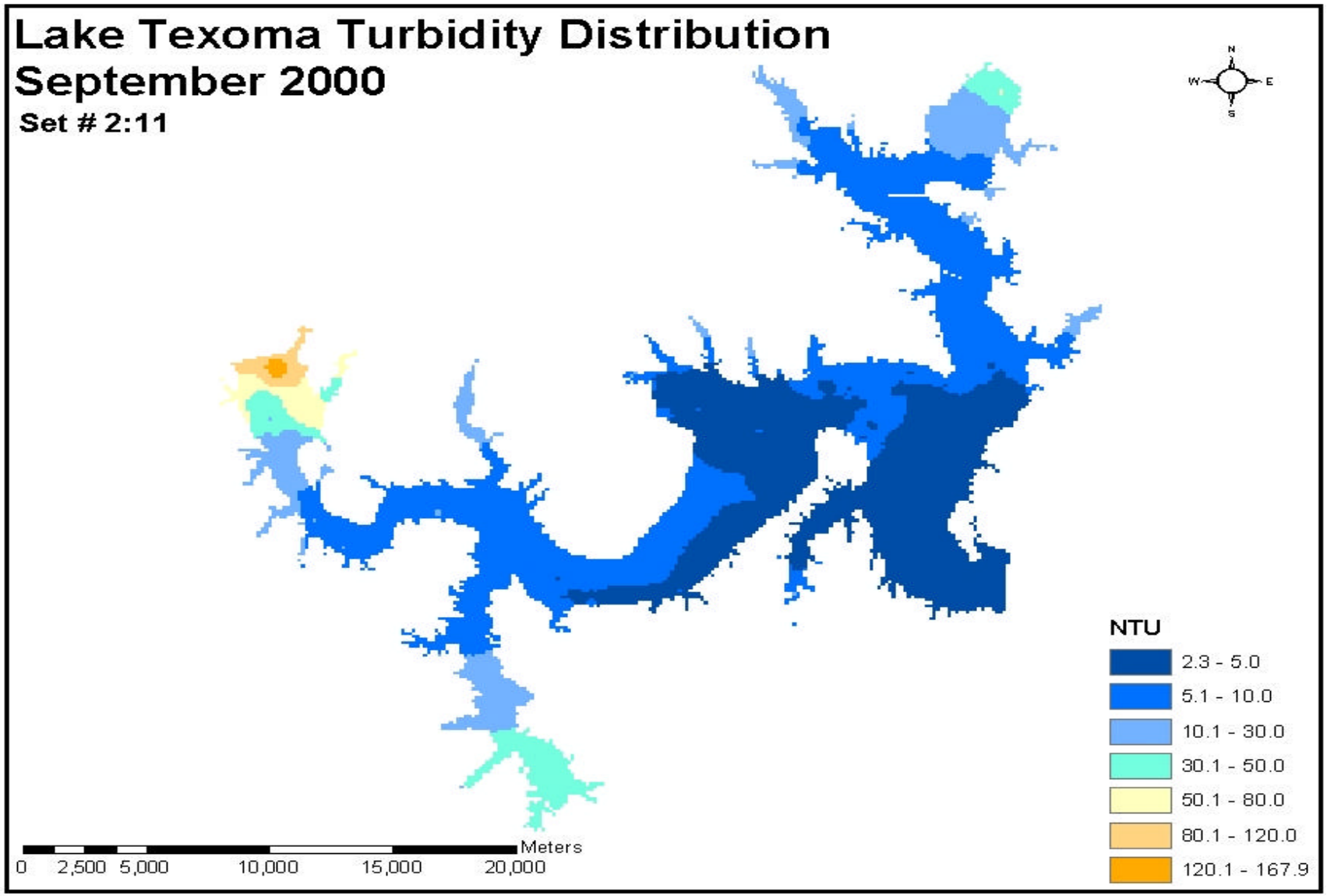
Lake Texoma Turbidity Distribution
September 2000
Set # 2:11
N
W
E
S
NTU
2.3 - 5.0
5.1 - 10.0
10.1 - 30.0
30.1 - 50.0
50.1 - 80.0
80.1 - 120.0
120.1 - 167.9
Meters
0
2,500
5,000
10,000
15,000
20,000

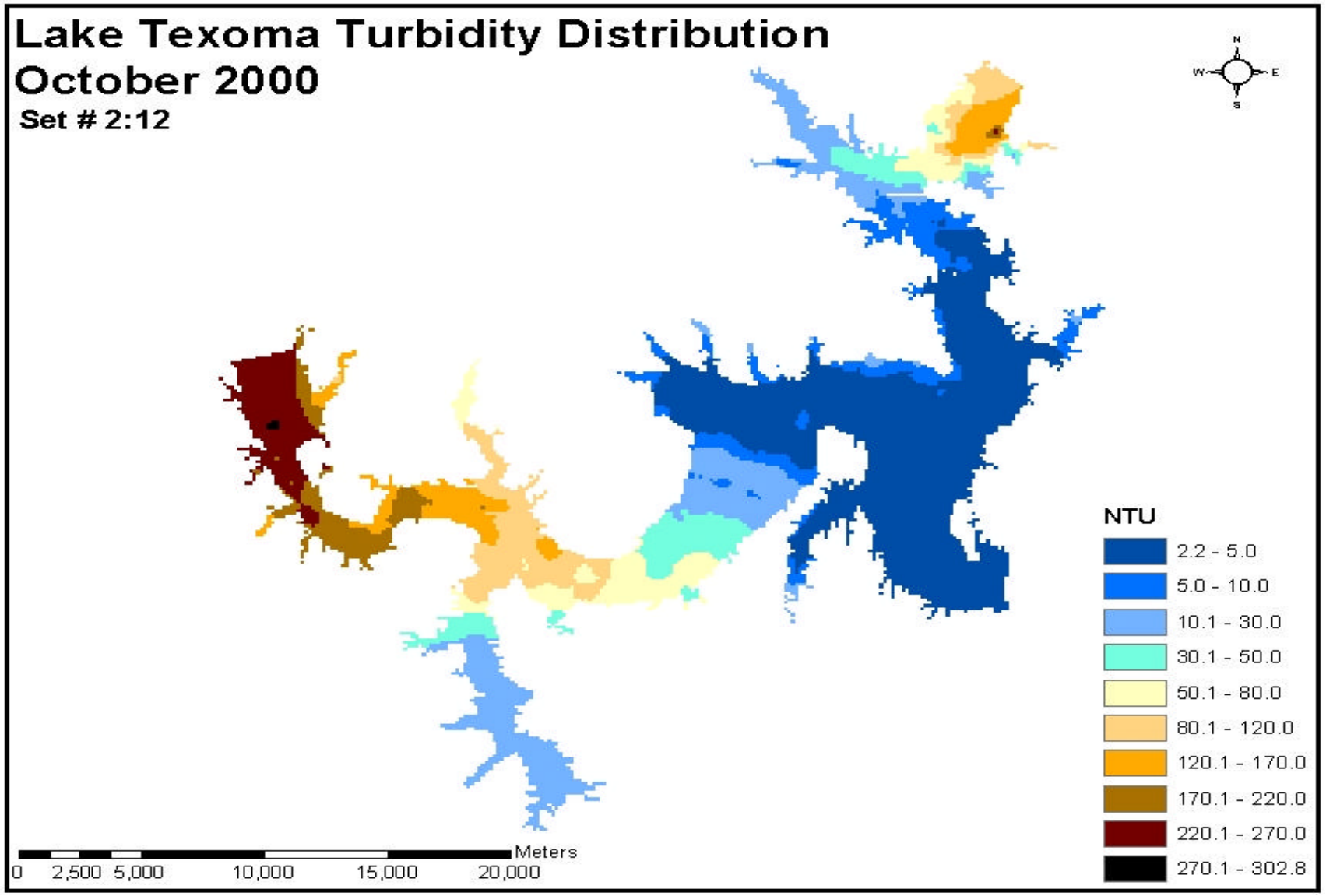
Lake Texoma Turbidity Distribution
October 2000
Set # 2:12
N
W
E
S
NTU
2.2 - 5.0
5.0 - 10.0
10.1 - 30.0
30.1 - 50.0
50.1 - 80.0
80.1 - 120.0
120.1 - 170.0
170.1 - 220.0
220.1 - 270.0
270.1 - 302.8
Meters
0 2,500 5,000 10,000 15,000 20,000

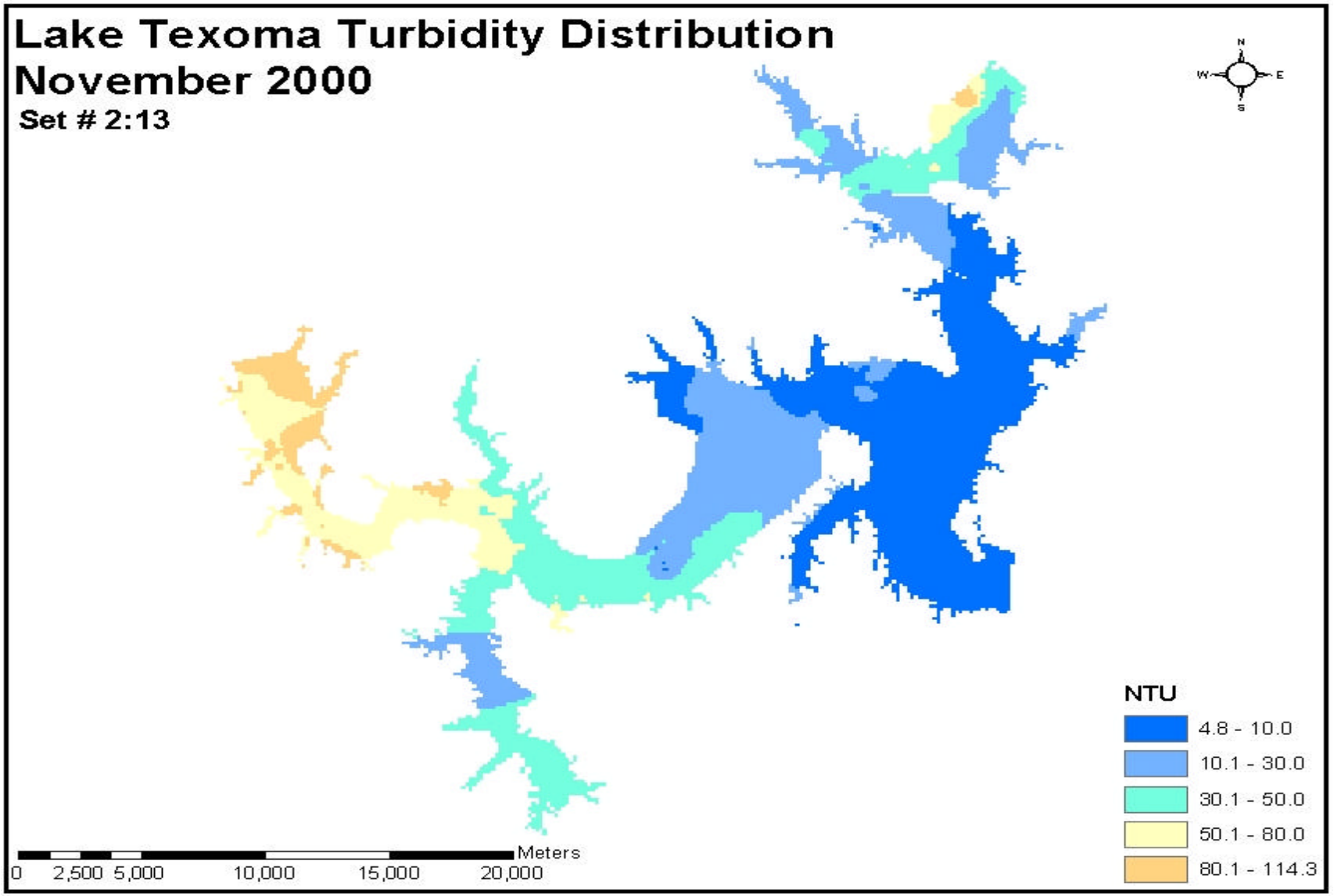
Lake Texoma Turbidity Distribution
November 2000
Set # 2:13
N
W
E
S
NTU
4.8 - 10.0
10.1 - 30.0
30.1 - 50.0
50.1 - 80.0
80.1 - 114.3
Meters
0
2,500
5,000
10,000
15,000
20,000

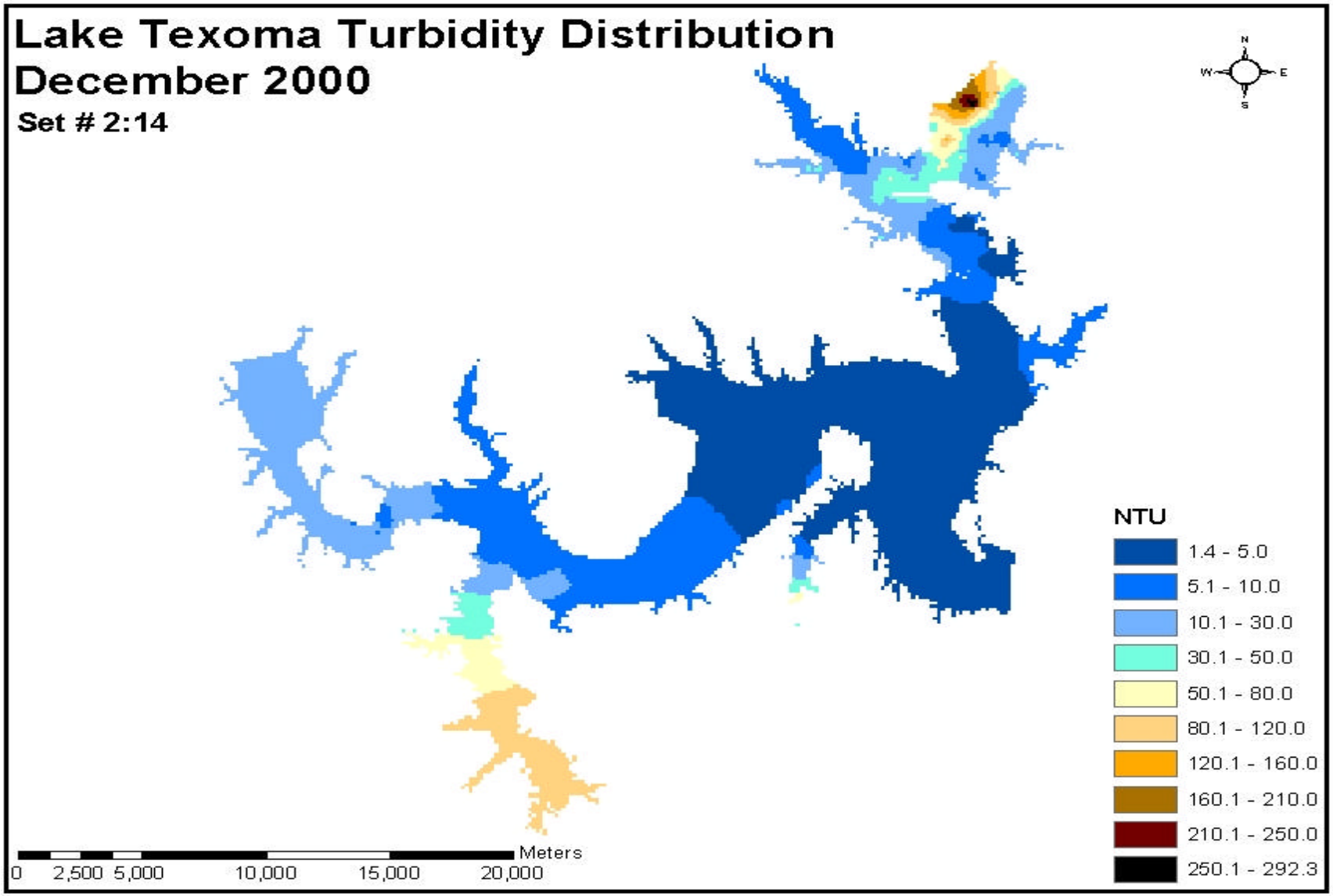
Lake Texoma Turbidity Distribution
December 2000
Set # 2:14
N
W
E
S
NTU
1.4 - 5.0
5.1 - 10.0
10.1 - 30.0
30.1 - 50.0
50.1 - 80.0
80.1 - 120.0
120.1 - 160.0
160.1 - 210.0
210.1 - 250.0
250.1 - 292.3
Meters
0 2,500 5,000 10,000 15,000 20,000

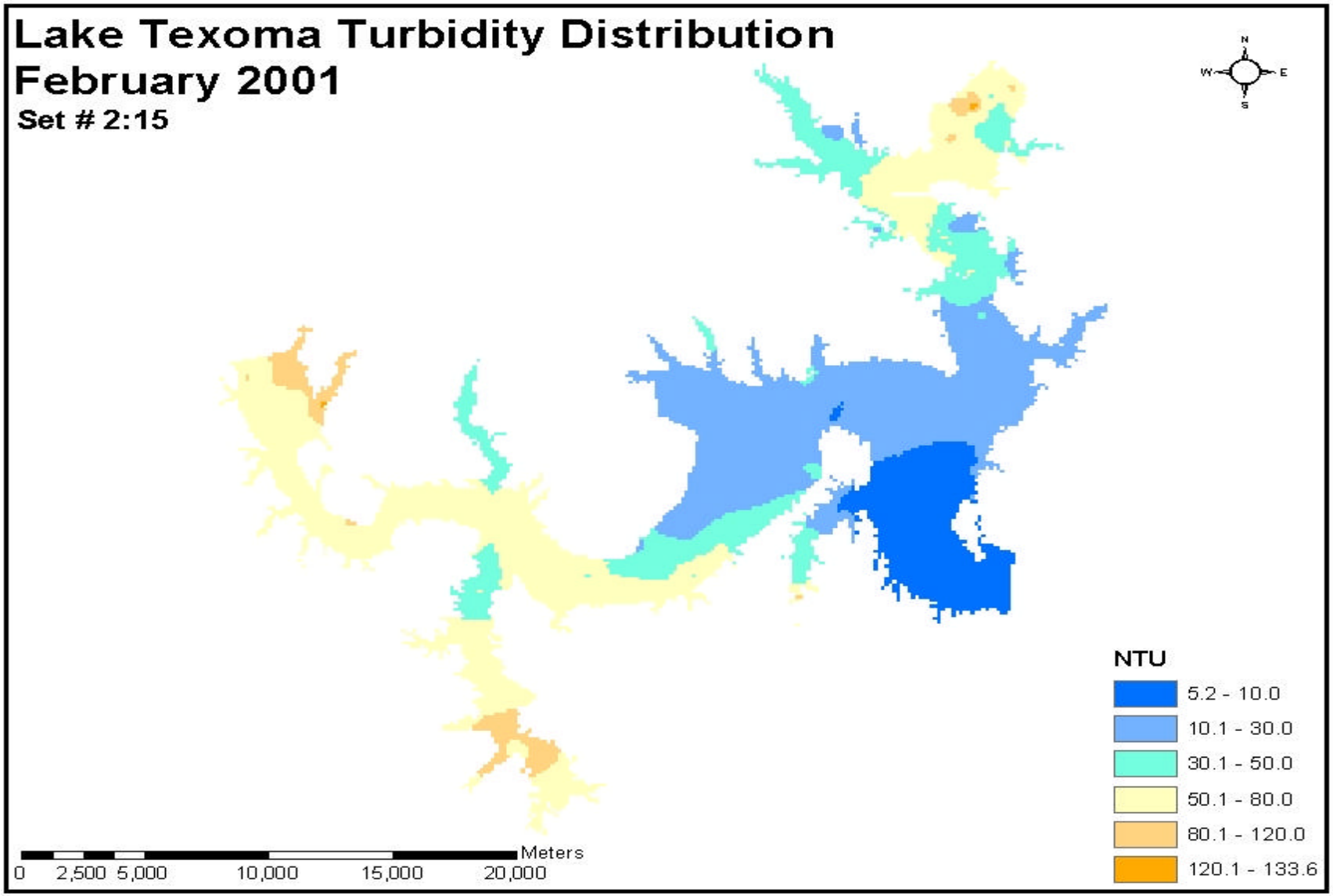
Lake Texoma Turbidity Distribution
February 2001
Set # 2:15
N
W
E
S
NTU
5.2 - 10.0
10.1 - 30.0
30.1 - 50.0
50.1 - 80.0
80.1 - 120.0
120.1 - 133.6
Meters
0 2,500 5,000 10,000 15,000 20,000

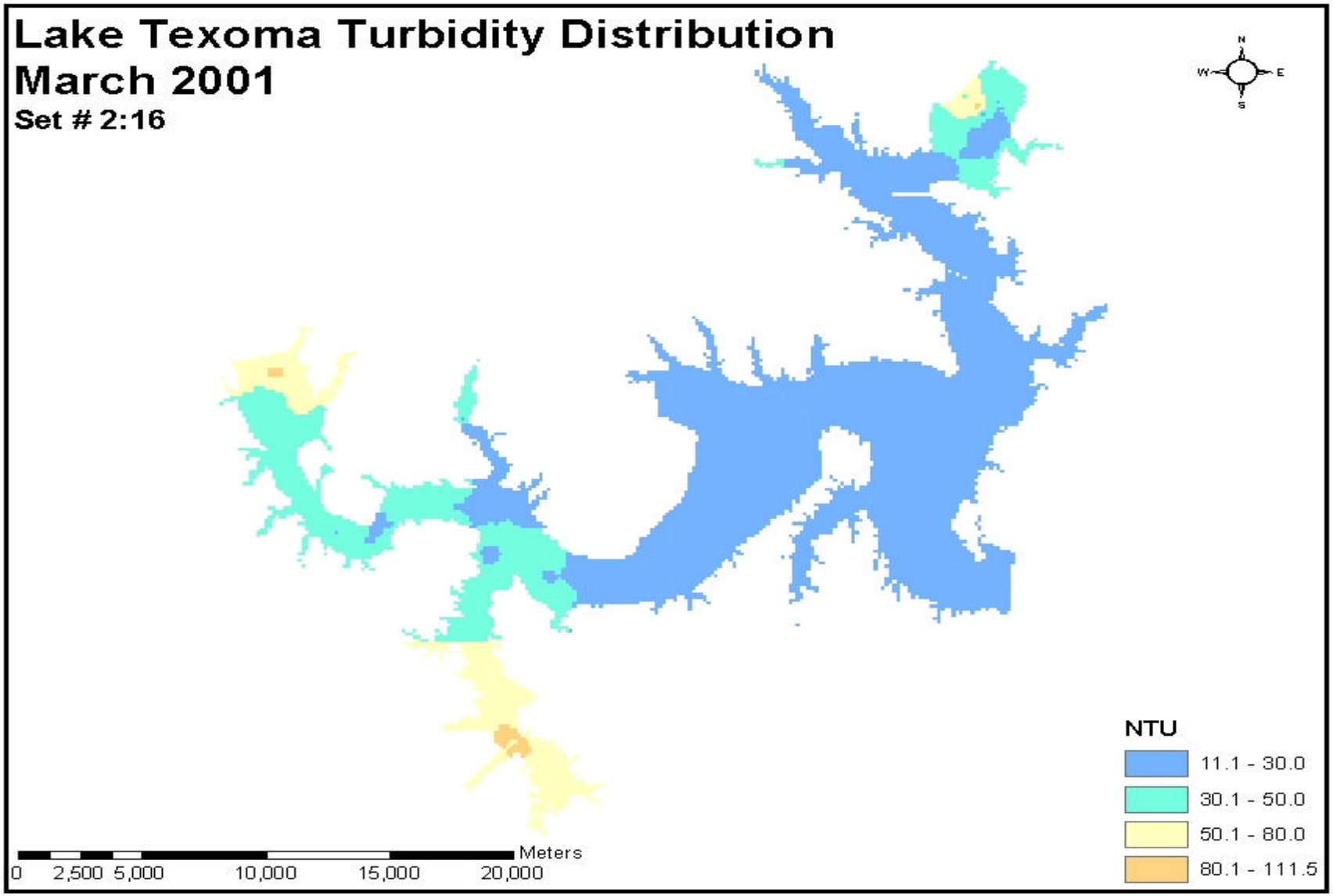
Lake Texoma Turbidity Distribution
March 2001
Set # 2:16
N
W
E
S
NTU
11.1 - 30.0
30.1 - 50.0
50.1 - 80.0
80.1 - 111.5
Meters
0
2,500
5,000
10,000
15,000
20,000

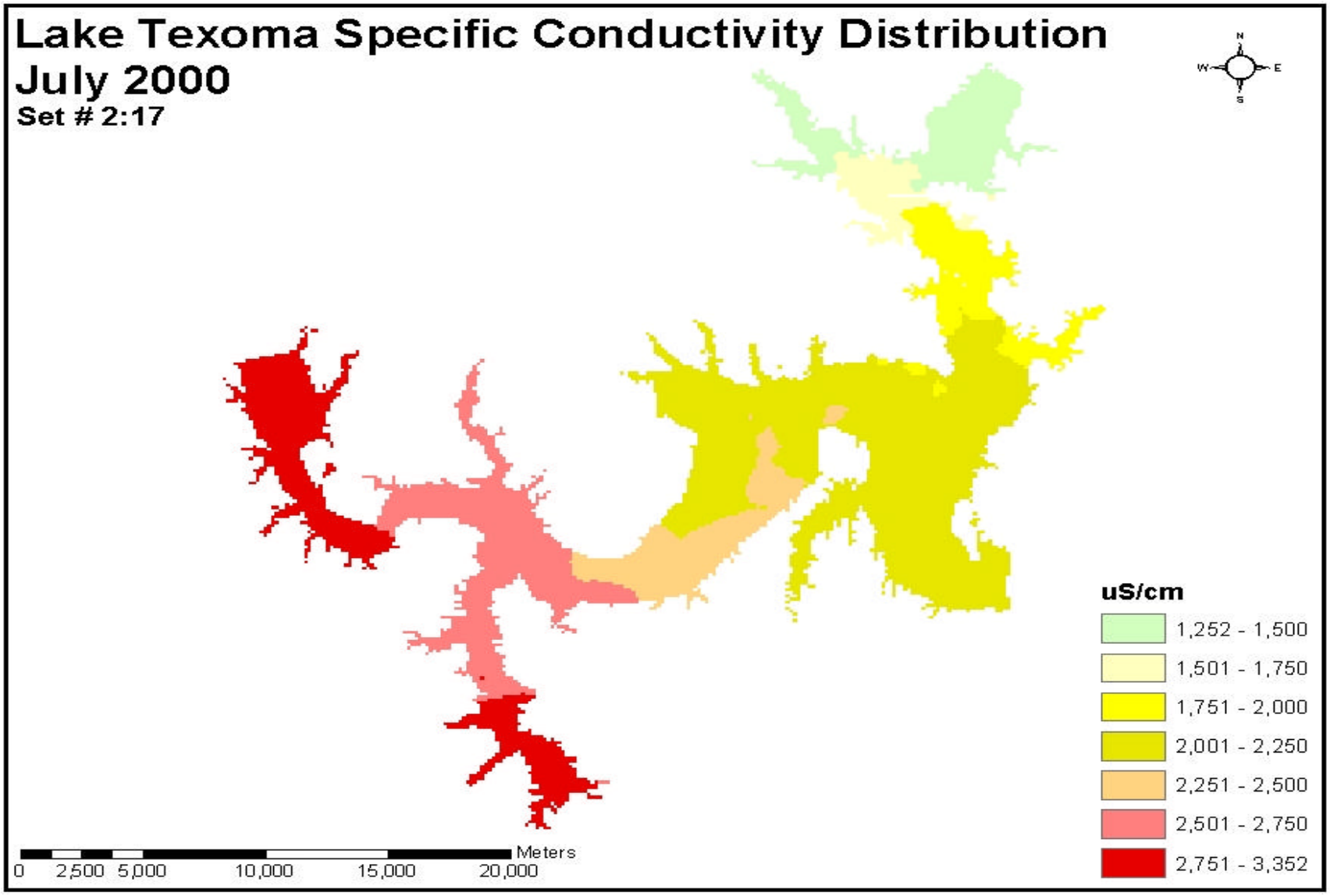
Lake Texoma Specific Conductivity Distribution
July 2000
Set # 2:17
N
W
E
S
uS/cm
1,252 - 1,500
1,501 - 1,750
1,751 - 2,000
2,001 - 2,250
2,251 - 2,500
2,501 - 2,750
2,751 - 3,352
Meters
0 2,500 5,000 10,000 15,000 20,000

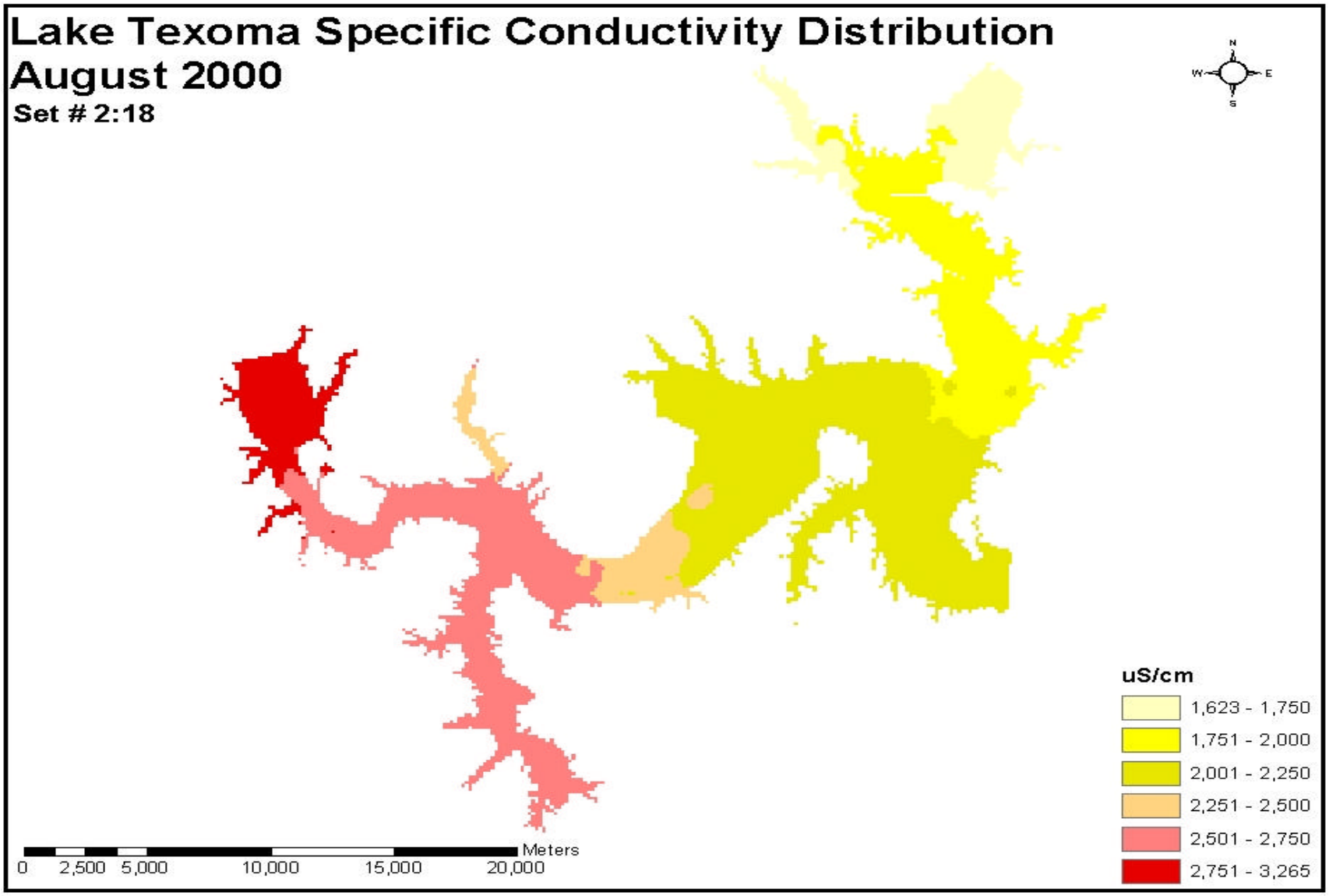
Lake Texoma Specific Conductivity Distribution
August 2000
Set # 2:18
N
W
E
S
uS/cm
1,623 - 1,750
1,751 - 2,000
2,001 - 2,250
2,251 - 2,500
2,501 - 2,750
2,751 - 3,265
Meters
0
2,500
5,000
10,000
15,000
20,000

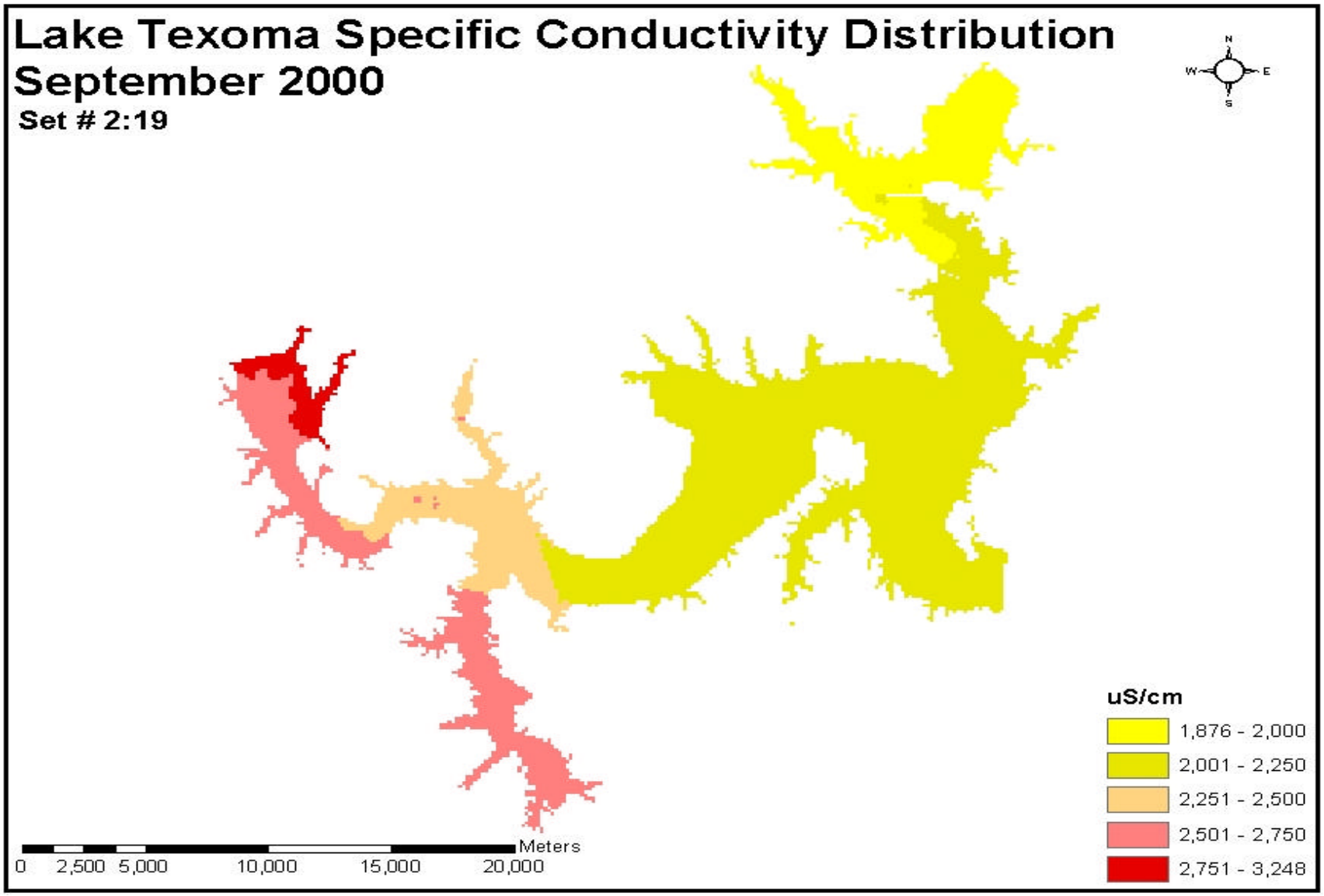
Lake Texoma Specific Conductivity Distribution
September 2000
Set # 2:19
N
W
E
S
uS/cm
1,876 - 2,000
2,001 - 2,250
2,251 - 2,500
2,501 - 2,750
2,751 - 3,248
Meters
0
2,500
5,000
10,000
15,000
20,000

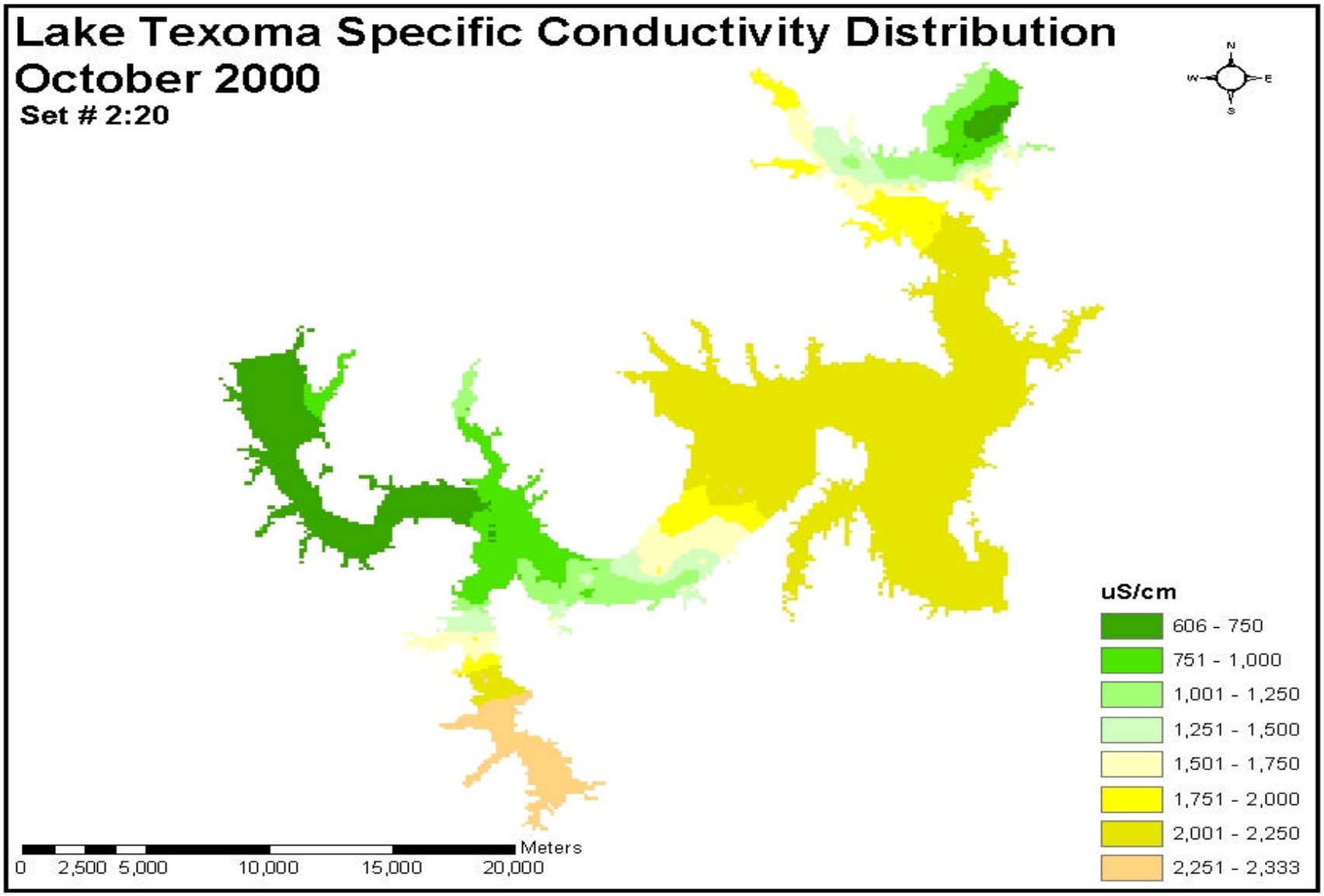
Lake Texoma Specific Conductivity Distribution
October 2000
Set # 2:20
N
W
E
S
uS/cm
606 - 750
751 - 1,000
1,001 - 1,250
1,251 - 1,500
1,501 - 1,750
1,751 - 2,000
2,001 - 2,250
2,251 - 2,333
Meters
0 2,500 5,000 10,000 15,000 20,000

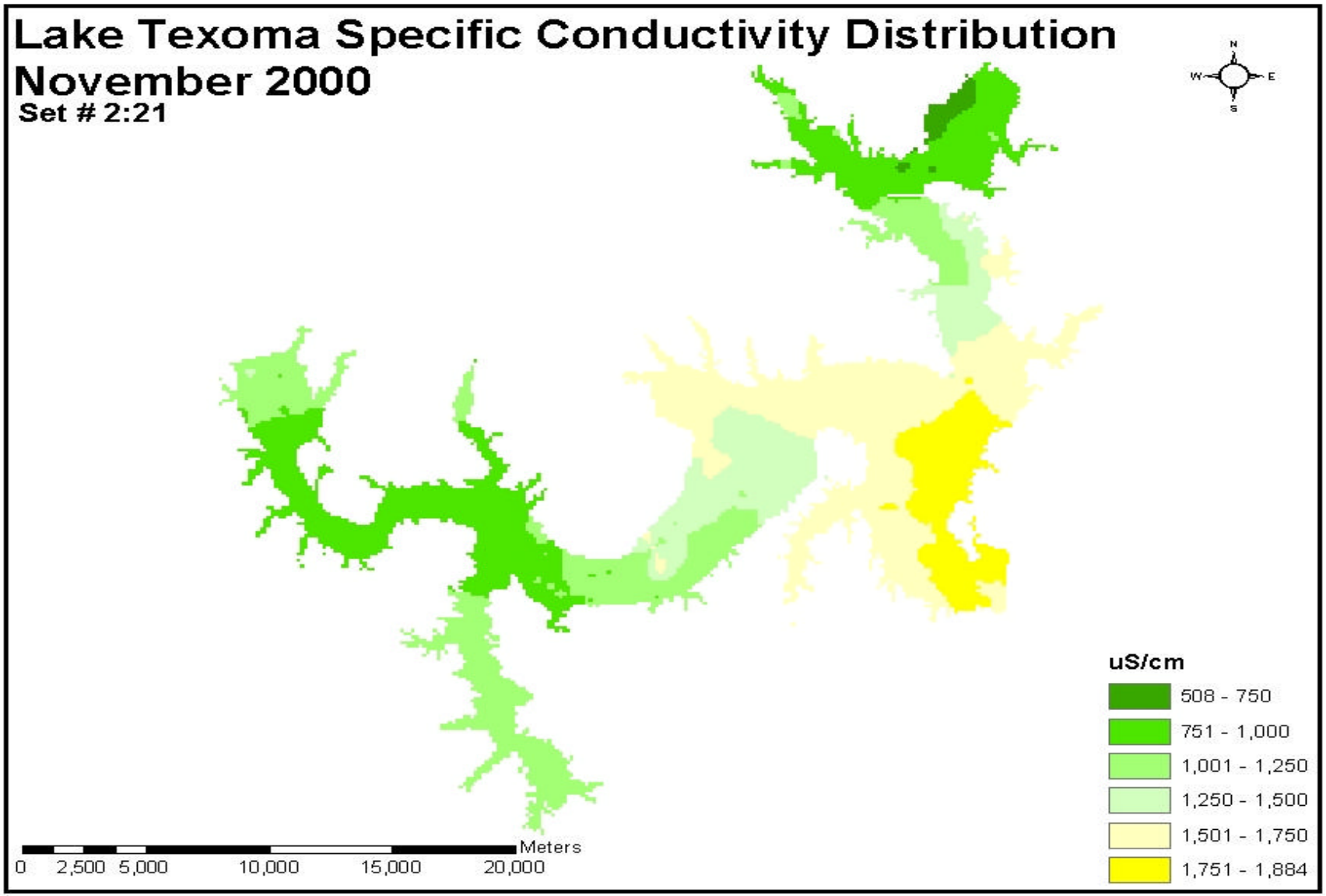
Lake Texoma Specific Conductivity Distribution
November 2000
Set # 2:21
N
W
E
S
uS/cm
508 - 750
751 - 1,000
1,001 - 1,250
1,250 - 1,500
1,501 - 1,750
1,751 - 1,884
Meters
0
2,500
5,000
10,000
15,000
20,000

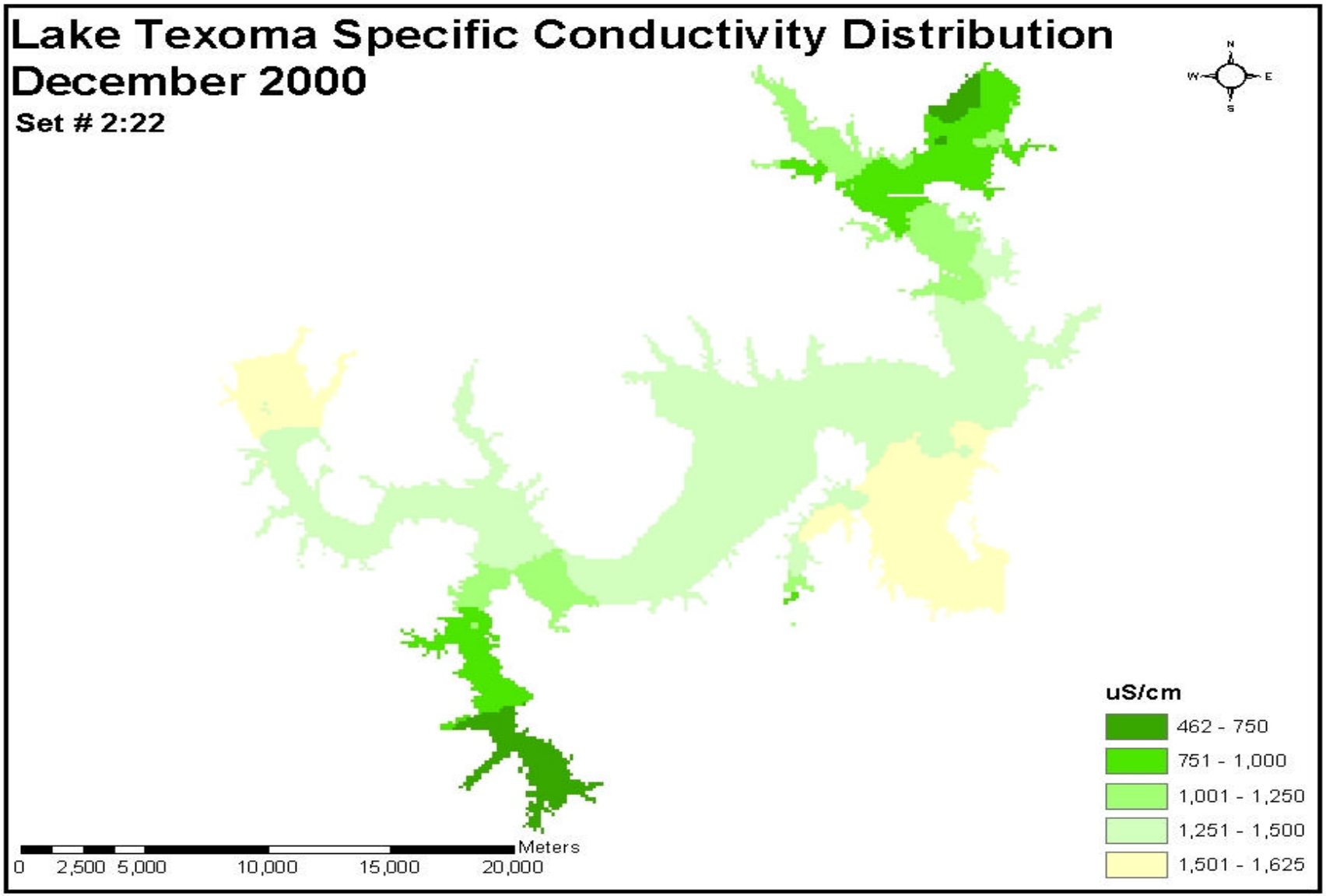
Lake Texoma Specific Conductivity Distribution
December 2000
Set # 2:22
N
W
E
S
uS/cm
462 - 750
751 - 1,000
1,001 - 1,250
1,251 - 1,500
1,501 - 1,625
Meters
0
2,500
5,000
10,000
15,000
20,000

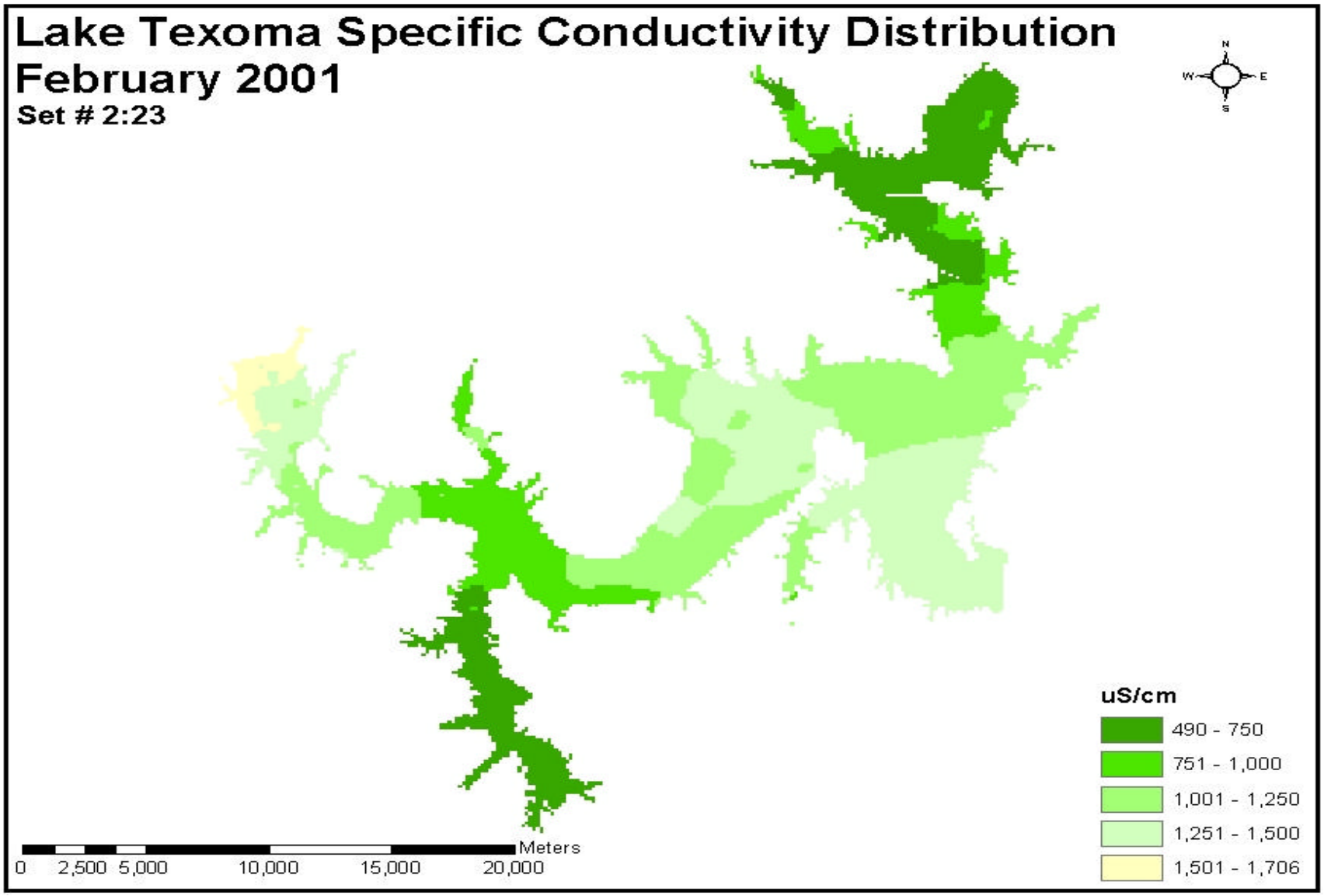
Lake Texoma Specific Conductivity Distribution
February 2001
Set # 2:23
N
W
E
S
uS/cm
490 - 750
751 - 1,000
1,001 - 1,250
1,251 - 1,500
1,501 - 1,706
Meters
0
2,500
5,000
10,000
15,000
20,000

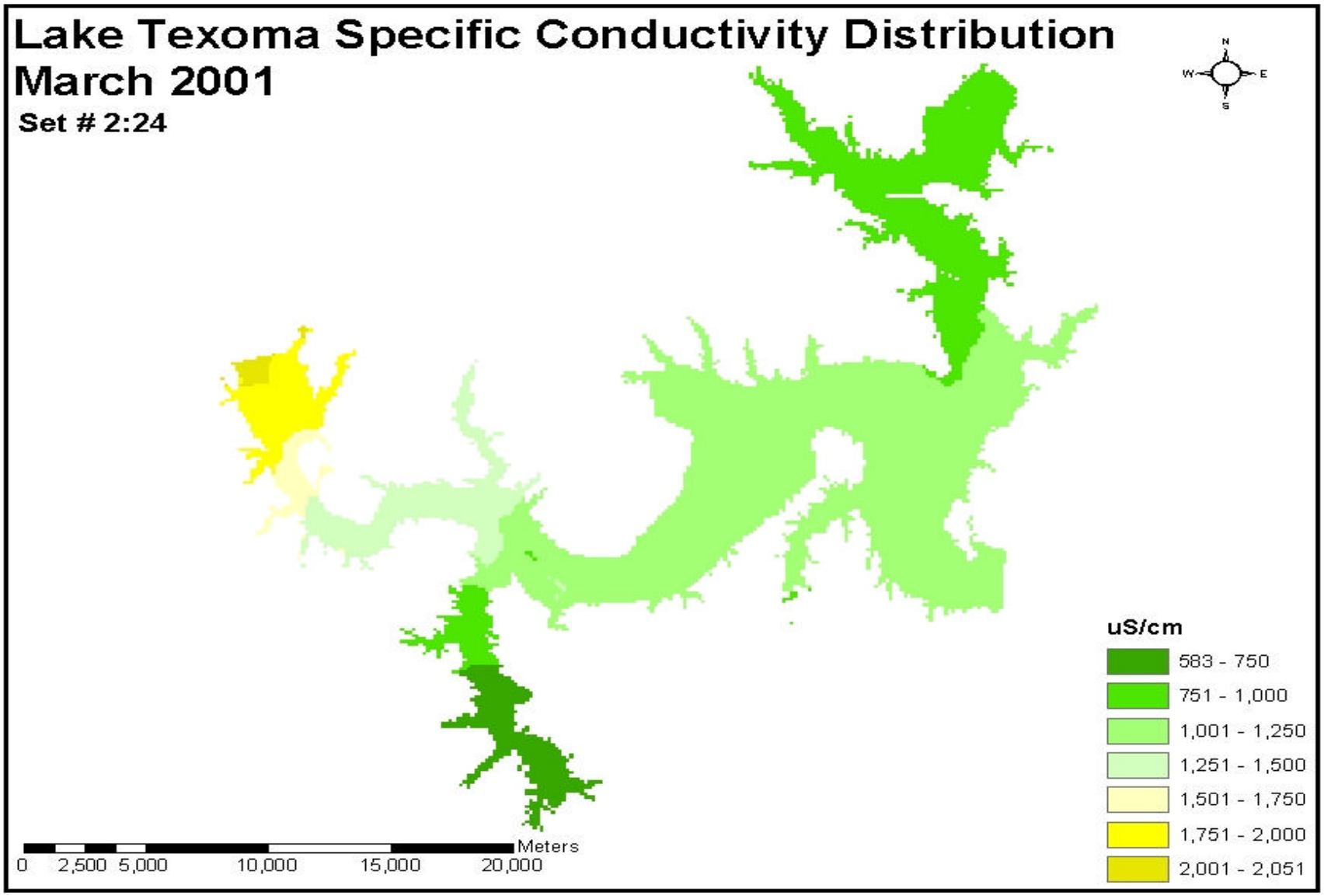
Lake Texoma Specific Conductivity Distribution
March 2001
Set # 2:24
N
W
E
S
uS/cm
583 - 750
751 - 1,000
1,001 - 1,250
1,251 - 1,500
1,501 - 1,750
1,751 - 2,000
2,001 - 2,051
Meters
0 2,500 5,000 10,000 15,000 20,000

APPENDIX C

Table of All Statistically Significant Regression Models
Alpha Level = 0.05

Lake Zone Abbreviations

RRZ = Red River Zone, RRTZ = Red River Transition Zone, MLZ = Main Lake Zone, WRTZ = Washita River Transition Zone, WRZ = Washita River Zone, BMA = Big Mineral Arm,

Model Abbreviations

Chl-a = Chlorophyll-a, Turb = Turbidity, SpC = Specific Conductivity, NSS = Not Statistically Significant

Lake Zone	Model					
RRZ	**Turb = SpC**	intercept	slope	R^2	probability	
	All Data	151.1	-0.052	0.45	p < 0.0001	
	Summer	-45	0.023	0.05	0.0002	
	Winter	244.6	-0.138	0.59	p < 0.0001	
	Chl-a = Turb					
	All Data	22.1	-0.112	0.26	p < 0.0001	
	Summer	31.9	0.052	0.03	0.0092	
	Winter	7.3	-0.024	0.15	p < 0.0001	
	Chl-a = SpC					
	All Data	-13.4	0.016	0.9	p < 0.0001	
	Summer	-22.1	0.02	0.41	p < 0.0001	
	Winter	-5.5	0.009	0.69	p < 0.0001	
	Chl-a = Turb & SpC	intercept	slope T	slope SpC	R^2	probability
	All Data	-21.2	0.052	0.019	0.94	p < 0.0001
	Summer	-21.9	0.005	0.02	0.41	p < 0.0001
	Winter	-14.5	0.037	0.014	0.83	p < 0.0001
RRTZ	**Turb = SpC**	intercept	slope	R^2	probability	
	All Data	75.2	-0.031	0.45	p < 0.0001	
	Summer	-0.6	0.003	0.08	p < 0.0001	
	Winter	115.4	-0.065	0.36	p < 0.0001	
	Chl-a = Turb					
	All Data	14.3	-0.15	0.21	p < 0.0001	
	Summer	10.3	1.91	0.37	p < 0.0001	
	Winter	NSS	NSS	NSS	NSS	
	Chl-a = SpC					
	All Data	-11.9	0.014	0.84	p < 0.0001	
	Summer	-8.2	0.012	0.18	p < 0.0001	
	Winter	-4.7	0.008	0.39	p < 0.0001	
	Chl-a = Turb & SpC	intercept	slope T	slope SpC	R^2	probability
	All Data	-18.6	0.09	0.016	0.88	p < 0.0001
	Summer	-7.3	1.67	0.008	0.44	p < 0.0001
	Winter	-13.3	0.074	0.012	0.68	p < 0.0001
MLZ	**Turb = SpC**	intercept	slope	R^2	probability	
	All Data	19.4	-0.007	0.45	p < 0.0001	

	Summer	22.1	-0.008	0.18	p < 0.0001	
	Winter	21.2	-0.009	0.39	p < 0.0001	
	Chl-a = Turb					
	All Data	10	-0.406	0.09	p < 0.0001	
	Summer	7.7	1.51	0.21	p < 0.0001	
	Winter	NSS	NSS	NSS	NSS	
	Chl-a = SpC					
	All Data	-9.5	0.01	0.43	p < 0.0001	
	Summer	45.8	-0.015	0.05	p < 0.0001	
	Winter	0.9	0.002	0.14	p < 0.0001	
	Chl-a = Turb & SpC	intercept	slope T	slope SpC	R^2	probability
	All Data	-16.1	0.341	0.012	0.46	p < 0.0001
	Summer	13.7	1.45	-0.003	0.21	p < 0.0001
	Winter	-0.95	0.086	0.002	0.19	p < 0.0001
WRTZ	**Turb = SpC**	intercept	slope	R^2	probability	
	All Data	45.2	-0.021	0.54	p < 0.0001	
	Summer	18.4	-0.006	0.17	p < 0.0001	
	Winter	49.6	-0.025	0.47	p < 0.0001	
	Chl-a = Turb					
	All Data	12.3	-0.21	0.16	p < 0.0001	
	Summer	16.3	0.208	0.02	0.0043	
	Winter	NSS	NSS	NSS	NSS	
	Chl-a = SpC					
	All Data	-5.5	0.01	0.47	p < 0.0001	
	Summer	NSS	NSS	NSS	NSS	
	Winter	2.3	0.001	0.09	p < 0.0001	
	Chl-a = Turb & SpC	intercept	slope T	slope SpC	R^2	probability
	All Data	-10.7	0.115	0.013	0.49	p < 0.0001
	Summer	8.3	0.315	0.004	0.05	p < 0.0001
	Winter	-0.6	0.058	0.003	0.19	p < 0.0001
WRZ	**Turb = SpC**	intercept	slope	R^2	probability	
	All Data	109.4	-0.058	0.33	p < 0.0001	
	Summer	NSS	NSS	NSS	NSS	
	Winter	162.5	-0.123	0.27	p < 0.0001	

	Chl-a = Turb					
	All Data	15.7	-0.089	0.16	p < 0.0001	
	Summer	NSS	NSS	NSS	NSS	
	Winter	NSS	NSS	NSS	NSS	
	Chl-a = SpC					
	All Data	-10	0.019	0.7	p < 0.0001	
	Summer	31.1	-0.004	0.06	0.0096	
	Winter	0.3	0.005	0.08	p < 0.0001	
	Chl-a = Turb & SpC	intercept	slope T	slope SpC	R^2	probability
	All Data	-13.1	0.028	0.021	0.71	p < 0.0001
	Summer	31	0.006	-0.004	0.06	0.0295
	Winter	-3.4	0.023	0.008	0.14	p < 0.0001
BMA	**Turb = SpC**	intercept	slope	R^2	probability	
	All Data	81	-0.026	0.64	p < 0.0001	
	Summer	NSS	NSS	NSS	NSS	
	Winter	92.9	-0.039	0.49	p < 0.0001	
	Chl-a = Turb					
	All Data	30.3	-0.334	0.4	p < 0.0001	
	Summer	22.7	0.619	0.65	p < 0.0001	
	Winter	19.6	-0.203	0.22	p < 0.0001	
	Chl-a = SpC					
	All Data	-8	0.016	0.81	p < 0.0001	
	Summer	NSS	NSS	NSS	NSS	
	Winter	-13.6	0.022	0.81	p < 0.0001	
	Chl-a = Turb & SpC	intercept	slope T	slope SpC	R^2	probability
	All Data	-18.9	0.135	0.019	0.84	p < 0.0001
	Summer	-7.1	0.608	0.011	0.66	p < 0.0001
	Winter	-26.3	0.137	0.027	0.86	p < 0.0001

REFERENCES

Alpine, A.A., S.M. Wienke, J.E. Cloern, and B.E. Cole. 1988. *Plankton Studies in San Francisco Bay, IX, Chlorophyll Distribution and Hydrographic Properties of South San Francisco Bay, 1984-1986*. U.S. Geological Survey, Open File Report 88-319.

American Public Health Association. 1995. *Standard Methods for the Examination of Water and Wastewater, 19th Edition*. APHA, Washington, DC.

Atkinson, S.F., K.L. Dickson, J. Franks, D.C. Garret, B.A. Hunter, W.T. Waller, and S. Burks. 1996. *An Evaluation of U.S. Army Corps of Engineers Provided Historical Water Quality Data from Lake Texoma: Implications for a Water Quality Monitoring Program*. Report to the U.S. Army Corps of Engineers, Tulsa District.

Atkinson, S.F., K.L. Dickson, W.T. Waller, L. Ammann, J. Franks, T. Clyde, J. Gibbs, and D. Rolbiecki. 1999. *A Chemical, Physical and Biological Water Quality Survey of Lake Texoma: August 1996 – September 1997 Final Report*. Report to the U.S. Army Corps of Engineers, Tulsa District.

Beitinger, T. 1999. Personal communication, University of North Texas.

Berman, T. 1972. Profiles of Chlorophyll Concentrations by in vivo fluorescence: Some Limnological Applications. Limnology and Oceanography. 17:616-618.

Brooks, R. A., and R. E. Ferrell, Jr. 1970. The Lateral Distribution of Clay Minerals in Lakes Ponchartrain and Maurepas, Louisiana. Journal of Sediment Petrology. 40:855-863.

Carlson, R. E., and J. Shapiro. 1981. Dissolved Humic Substances: A Major Source of Error in Fluorometric Analyses Involving Lake Waters. Limnology and Oceanography. 26:785-790.

Fee, E. J. 1976. The Vertical and Seasonal Distribution of Chlorophyll in Lakes of the Experimental Lakes Area, Northwestern Ontario: Implications for Primary Production Estimates. Limnology and Oceanography. 21:767-783.

Flemer, D. A. 1969. Continuous Measurement of in vivo Chlorophyll of a Dinoflagellate Bloom in Chesapeake Bay. Chesapeake Science. 10:99-103.

Gade, D., S. L. Burks, and A. V. Zale. 1992. *An Evaluation of the Effect of Decreased Chloride Concentration in the Red River Basin on Primary Production and Sport Fish Abundance in Lake Texoma*. Report to the U.S. Army Corps of Engineers, Tulsa District.

George, D. G., and S. I. Heaney. 1978. Factors Affecting the Spatial Distribution of Phytoplankton in a Small Productive Lake. Journal Ecology.

Gibbs, J.S. 1998. *Environmental Factors Influencing Chlorophyll-a Concentrations in Lake Texoma*. Masters Thesis, University of North Texas, Denton, TX.

Ground, T. A., and A. W. Groeger. 1994. Chemical Classification and Trophic Characteristics of Texas Reservoirs. Lake and Reservoir Management. 10:189-201.

Harrel, R. C. 1966. *Stream Order and Community Structure of Benthic Macroinvertebrates and Fishes in an Intermittent Stream*. Doctoral Dissertation, Oklahoma State University, Stillwater, OK.

Harris, G. P. 1980. The Relationship Between Chlorophyll-a Fluorescence, Diffuse Attenuation Changes and Photosynthesis in Natural Phytoplankton Populations. Journal of Plankton Research. 2:109-127.

Heaney, S. I. 1978. Some Observations on the Use of the In Vivo Fluorescence Technique to Determine Chlorophyll-a in Natural Populations and Cultures of Freshwater Phytoplankton. Freshwater Biology. 8:115-126.

Herman, A. W., and K. L. Denman. 1977. Rapid Underwater Profiling of Chlorophyll with an In Situ Fluorometer Mounted on a 'Batfish' Vehicle. Deep-Sea Research. 24:385-397.

Hulse, G. 1975. *A Shipboard Monitoring System*. Technical Report 22. Marine Science Research Center, State University of New York, Stony Brook.

Keeton, D. 1959. *Limnological Effects of Introducing Oil Field Brines into Farm Fish Ponds to Reduce the Turbidity.* Oklahoma Fishery Research Laboratory Report 72, Norman, Ok.

Kiefer, D. A. 1973a. Fluorescence Properties of Natural Phytoplankton Populations. Marine Biology. 22:263-269.

___. 1973b. Chlorophyll-a Fluorescence in Marine Centric Diatoms: Response of Chloroplasts to Light and Nutrient Stress. Marine Biology. 23:39-46.

Labaugh, J. W. 1995. Relation of Algal Biovolume to Chlorophyll-a in Selected Lakes and Wetlands in the North-Central United States. Canadian Journal of Fisheries and Aquatic Science. 52:416-424.

Likens, G. E. 1975. *Primary Productivity of Inland Aquatic Ecosystems. In:* Primary Productivity of the Biosphere, H. Lieth and E. H. Whittaker (Editors). Springer-Verlag, New York, NY, pp. 185-202.

Lorenzen, C. J. 1966. A Method for the Continuous Measurement of in vivo Chlorophyll Concentration. Deep-Sea Research. 13:223-227.

Madden, C. J., and J. W. Day Jr. 1992. An Instrument System for High-Speed Mapping of Chlorophyll-a and Physico-Chemical Variables in Surface Waters. Estuaries. 15:421-427.

Marshall, C. T., and R. H. Peters. 1989. General Patterns in the Seasonal Development of Chlorophyll-a for Temperate Lakes. Limnology and Oceanography. 34:856-867

Mathis, B. J. 1965. *Community Structure of Benthic Macroinvertebrates in an Intermittent Stream Receiving Oil Field Brines*. Doctoral Dissertation, Oklahoma State University, Stillwater, OK.

McCabe, R. 1989. *Striped Bass and Striped Bass Hybrid in Texas*. Texas Parks and Wildlife Department document PWD-BK-3200-21-6/89.

Persson, G. 1990. *Utilization of Phosphorus in Suspended Particulate Matter as Tested by Algal Bioassays. In*: Proceedings of International Association of Theoretical and Applied Limnology, Munich 1989. Volume 24, Part 1, V. Sládecek and A. Sládeckevá (Editors).

Rolbiecki, D.A. 1998. *Underwater Optical Properties of Lake Texoma (Oklahoma-Texas) Using Secchi Disk, Submarine Photometer, and High-Resolution Spectroscopy*. Masters Thesis, University of North Texas, Denton, TX

Setser, P. J., N. L. Guinasso, Jr., N. L. Condra, D. A. Weisenburg, and D. R. Schink, 1983. A Deep-Towed Pumping System for Continuous Underwater Sampling. Environmental Science and Technology. 17:47-49.

Sieburth, J. M., and D. R. Kester, 1999. Real-Time Environmental Monitoring. Sea Technology. 10:2-5.

Stauffer, R. E., 1988. Sampling Strategies and Associated Errors in Estimating Epilimnetic Chlorophyll in Eutrophic Lakes. Water Resources Research. 24:1459-1469.

Strickland, J. D., 1968. Continuous Measurement of in vivo Chlorophyll: A Precautionary Note. Deep-Sea Research. 15:225-227.

Stumm, W., and J. J. Morgan. 1970. *Aquatic Chemistry: An Introduction Emphasizing Chemical Equilibria in Natural Waters*. Wiley – Interscience, New York, NY.

Taylor, M. J., and B. T. Yost, 1989. *Description of Salinity, Temperature, Chlorophyll, Suspended Sediment, and Velocity Data, South San Francisco Bay, California, Feb-April: 1987*. U.S. Geological Survey, Open File Report 89-619.

Toro, E., P. R. Schroeder, E. Fleming, and S. Nolen. 1996. *Evaluation of the Potential Effect of Chloride Reduction on Turbidity in Lake Texoma for the Red River Chloride Reduction Project, Tulsa District, Oklahoma*. Miscellaneous Paper EL-96-draft, U.S. Army Engineer Waterways Experiment Station, Vicksburg, MS.

YSI, 1999. *Environmental Monitoring Systems Operation Manual*. Yellow Springs Instruments, Yellow Springs, OH.

Zar, J. H., 1996. *Biostatistical Analysis, Third Edition*. Prentice-Hall, Upper Saddle River, NJ.